# Subsea PLEM & PLET

## Theory and Application

### Third Edition

March, 2018

J. Koto

Published By
Ocean & Aerospace Research Institute,
Indonesia

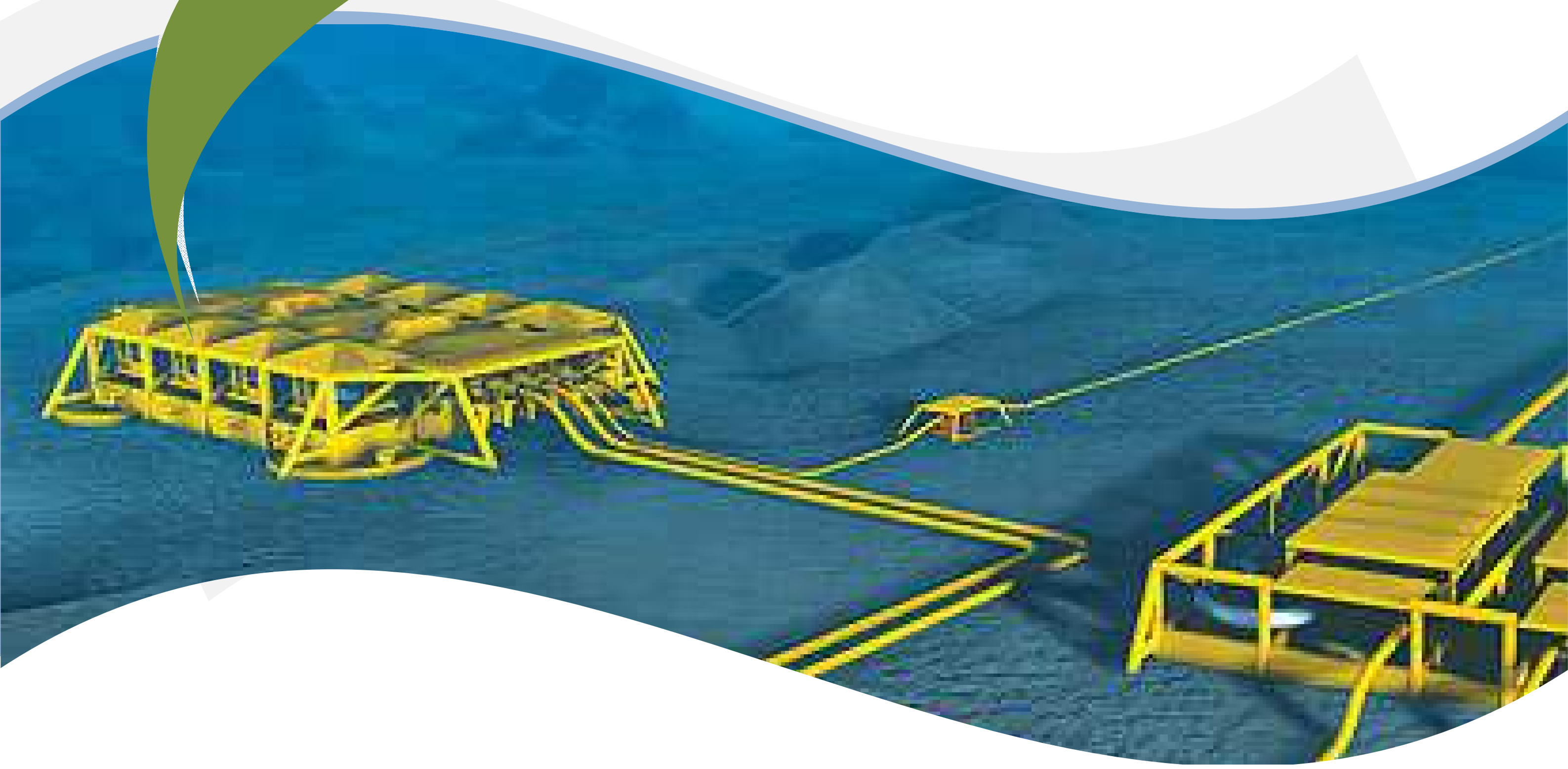

# Preface

بسم الله الرحمن الرحيم

This book introduces subsea Pipeline End Termination and Manifold (PLET/PLEM) which consists of six chapters. The First chapter discusses on overview of subsea PLET/PLEM. In the second chapter, PLET/PLEM design code and regulation and design steps are explained in detailed. The Third chapter discusses on structure and strength analysis, The Four chapter discusses on mudmat sizing and design. The fifth chapter discusses on installation and its challenges. The last chapter comes up with examples as real cases of PLEM installation in shallow and deep water.

In the book, many pictures and illustrations are enclosed in this book to assist the readers' understanding. It should be noted that some pictures and contents are borrowed from other companies' websites and brochures, without written permit. Even though the exact sources are quoted and listed in the references, please use this book for education purposes only.

2017 (Second Edition)
Book No: 2017060102.

*Published by* OCEAN & AEROSPACE Research Institute

# Authors

**Jaswar KOTO, Dr.Eng, C.Eng, C.Mar.Eng**

**Professor** on Offshore Engineering

**President** of Ocean & Aerospace Research Institute, Indonesia

**President** of International Society of Ocean, Mechanical & Aerospace -scientists & engineers- (ISOMAse)

**Contract** at Mechanical Engineering, Universiti Teknologi Malaysia.

**Email:** jaswar.koto@gmail.com, jaswar@isomase.org & jaswar@utm.my

# Acknowledgements

Alhamdulillahhirobbilalamin, first and foremost, all praises and syukur are only to Allah (S.W.T) to give us strength and ability to complete this book.

We would like to take this opportunity to express our highest appreciation to our colleagues and friends in the Ocean and Aerospace Research Institute, Indonesia, Universiti Teknologi Malaysia (UTM) and Institut Teknologi Sepuluh Nopember (ITS), Indonesia to provide proper guidance, full support, encouragement, invaluable ideas, comment, recommendation, critics, suggestions and advice that to assist us for the successful completion of this book.

To our families that always pray for our successful, all this things cannot pay for all what they all have done. Our special thanks also to our postgraduate students.

Above this all, our highest praises, thanks and syukur to Almighty Allah Subhanahu Wa'Talla, the most gracious the most merciful, who gave us the knowledge, courage and patience to accomplish this project. May the peace and blessings of Allah be upon Prophet Muhammad Sallallahu Alaihi Wasallam.

The authors are grateful to all friends, institutions and parties for supporting this book.

# Table of Contents

# List of Figures

# List of Tables

# List of Symbols

| | | |
|---|---|---|
| $\nabla$ | – | Displaced Volume of Water |
| $A$ | – | Nominal Cross Sectional Area of A Cable |
| $A_x$ | – | Projected Area of Lifted Object, X-Direction |
| $A_{33}$ | – | Hydrodynamic Added Mass |
| $C_A$ | – | Added Mass Coefficient |
| $C_D$ | – | Drag Coefficient |
| $C_M$ | – | Hydrodynamic Inertia Coefficient |
| $C_{dn}$ | – | Drag Coefficient for Normal Flow past Lifting Line |
| $C_{dx}$ | – | Drag Coefficient for Flow past Lifted Object, X-Direction |
| $D_c$ | – | Lifting Line Diameter |
| $E$ | – | Modulus Elasticity of The Cable |
| $F_B$ | – | Buoyancy Force |
| $F_{D0}$ | – | Drag Force on Lifted Object |
| $F_{dyn}$ | – | Dynamic Force in Lifting Line |
| $F_{dyn,Max}$ | – | Maximum Allowable Dynamic Force |
| $F_G$ | – | Gravity Force |
| $F_{stat}$ | – | Static Force in the Lifting Line |
| $G$ | – | Acceleration Of Gravity |
| $H_S$ | – | Significant Wave Height |
| $k$ | – | Ratio between Weight of Lifted Object and Weight of Cable |
| $K_E$ | – | Stiffness of Lifting System |
| $L$ | – | Length of Lifting Line |
| $Ls$ | – | Stretched Length of Cable |
| $M$ | – | Weight of Object in Air per Unit Length |
| $M`$ | – | Weight of Lifted Object in Air + Hydrodynamic Added Mass Z- Direction |
| $M_{sub}$ | – | Submerged Weight of Object per Unit Length |
| $q$ | – | Drag Force on Lifting Line per Unit Length |
| $RAO_{heave}$ | – | Vertical Displacement Amplitude in Heave |
| $RAO_{roll}$ | – | Roll Angle Amplitude |
| $T_o$ | – | Natural Period |

| | | |
|---|---|---|
| $T_p$ | – | Wave Peak Period |
| $T_Z$ | – | Wave Zero Up-Crossing Period |
| $U$ | – | Current Velocity |
| $W$ | – | Fully Submerged Weight of the Lifted Object |
| $w$ | – | Fully Submerged Weight per Unit Length of the Cable |
| $x$ | – | Distance From the Amid Ship Point for Roll Motion to Location Of Crane Tip |
| $\Lambda$ | – | Ratio between the Drag on the Lifted Object and Weight Of The Lifting Line |
| $\xi_l$ | – | Is the Horizontal Offset of the Lifted Object |
| $\rho_{sw}$ | – | Is the Density of Seawater |

# List of Abbreviations

| | | |
|---|---|---|
| AHTS | – | Anchor Handling Tug Supply |
| BOB | – | Braid Optimized for Bending |
| CTCU | – | Cable Traction Control Unit |
| DNV | – | Det Norske Veritas |
| DOF | – | Degree of Freedom |
| DSIM | – | Drill String Installation Method |
| FID | – | Floating Installation Device |
| FRDS | – | Fiber Rope Deployment System |
| GoM | – | Gulf of Mexico |
| HCLS | – | Heave Compensated Landing System |
| PBM | – | Pencil Buoy Method |
| PIM | – | Pendulous Installation Method |
| PLEM | – | Pipeline End Manifold |
| PLET | – | Pipeline End Termination |
| RAO | – | Response Amplitude Operator |
| SIM | – | Sheave Installation Method |
| SPS | – | Subsea Production System |
| SWL | – | Safe Working Load |
| WWIM | – | Winch Wire Installation Method |

# Chapter.1

# 1.0 Pipeline End Structure

## *1.1 Subsea Structure*

A typical subsea production can include the following particulars:

1. Manifold
2. Templates
3. Foundations
4. PLEMs
5. PLETs
6. Jumpers and flying leads
7. Subsea wellheads and trees (vertical and horizontal)
8. Riser bases
9. Subsea power supply and control system

According to Wang et.al (2012), subsea structure come in different size, shape and weight. It can be ranging into weight of thousand tons. Table 2.1 below illustrates the typical range of weights and dimensions for various subsea structures and equipment modules. Stated particular are only indicating approximation.

**Table 1.1**: Weight and Dimension of Subsea Hardware (Wang et.al, 2012)

| Hardware | Weight | Dimension |
|---|---|---|
| **Unit** | [Te] | [LxBxH/(ø×H) [m] |
| **Processing Modules** | 200 – 400 | Up to (15x15x8) |
| **Manifolds** | 50-400 | (5x5x4)-(25x20x8) |
| **PLEMs** | 50-400 | (5x5x4)-(25x20x8) |
| **Template** | 100-400 | (10x10x6)-(30x20x7) |
| **Riser Base** | 50-200 | Up to (20x20x10) |
| **PLETs** | 30-100 | (5x4x3)-(10x8x6) |
| **SDAs** | 50-100 | (5x4x3)-(10x10x8) |
| **SUTAs** | 5-50 | Up to (5x5x6) |
| **Pumping Modules** | 5-50 | (1x1x1.5)-(5x5x6) |
| **Vertical Jumpers** | 5-50 | Up to (50x6) (LxH) |

| | | |
|---|---|---|
| **Horizontal Jumpers** | 5-50 | Up to (50x15) (LxB) |
| **Suction Pile** | 40-200 | (ø4.5×15) - (ø10×30) |
| **Drag Anchor** | 50-75 | Up to (15x5) |
| **Subsea Tree** | 10-70 | Up to (5x5x6) |
| **Mid-water arch** | 5-100 | (10x6x4) – (20x9x5) |

## *1.2 PLEM & PLET*

At the moment, oil and gas fields move from shallow marine structures to deep seas, it would be very advantageous to consider the subsea tie-ins of the export system with existing in-built pipeline systems offering future more complex transportation system. In order to do that this is necessary to incorporate with the Pipeline End Manifold (PLEM) to tie in the complex pipeline system.

The PLEM is a simple subsea structure set at the end of pipeline that is used to connect a rigid pipeline with other subsea structures, such as manifolds or trees, through a jumper. It is also called a Pipeline End Termination (PLET) when serving as a support for one pipeline valve and one vertical connector, while the PLEM is supporting two or more pipeline connections. The PLEM and PLET systems are typically used in new construction where a pipeline terminates or needs to be jumper to another location, such as an FPSO, refinery and holding tank. PLETs, PLEMs, and tees can incorporate one or multiple tie-in points, vertical or horizontal, with other components such as isolation gate or ball valves, diverter valves, pig-launcher facilities, an array of sensors, or wyes.

Figure 1-1 shows PLEM and PLET used in Gorgon field, which located on Barrow Island, around 60 km off the northwest coast of Western Australia. The in-line structure is a simple manifold set at the middle of the pipeline, which is connected in line with the pipeline and used as a tee connector to divide or combine pipelines.

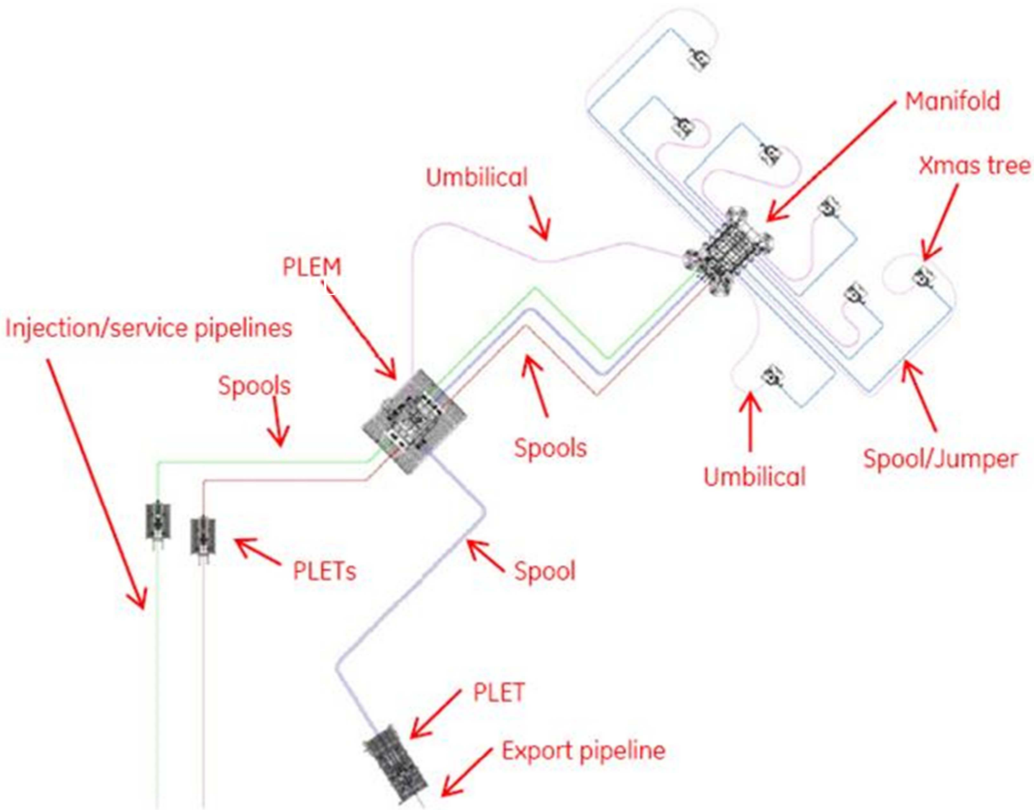


**Figure 1.1**: PLET and PLEM used in Gorgon field [GE Oil]


**Figure 1.2**: Gorgon field is located on Barrow Island, around 60 kilometres off the northwest coast of Western Australia [GE Oil].

The deep-water PLEM with its mudmat and up-looking hub was designed as an economical and reliable method for terminating pipelines of all sizes. The mudmat is favored for economy and position compliance. The PLEM must be remotely installable and designed to support ROV execution. PLEMs are installed with the pipeline end from the installation barge and are lowered into their final position. A PLEM can also be a platform for a range of optional components such as valves, taps, and instrumentation. After installation, the PLEM can be accessed for repair or maintenance by removing the pipeline connection jumper and recovering the PLEM to the surface.

### 1.2.1. General Layout

The purpose of the PLEM is to provide an installation structure to attach these piping components and then lower them to the seafloor in the desired orientation The PLEM serves as a manifold to split the product flow into multiple routes that may feed into an FPSO, refinery and holding tanks concurrently. The PLEM will contain such components as hubs, wyes, ball valves, ROV-interface panels and jumper systems that may include collet connectors, remote inline or articulating connectors (RIC/RAC), male end closures The PLEM structure must not only withstand the installation loads while being lowered to the seafloor, but also retrieval to the surface should a failure occur. Figure.1.3 shows a typical configuration for a PLEM. The PLEM can be any configuration, but generally is made up of the following assemblies: piping, frames, foundation and yoke as shown in Figure 1.4.

The PLEM foundation provides support for the structural frame of the piping system. In addition to their normal functions, PLEMs are designed to accommodate reasonable thermal expansion of the pipeline during operation. To accommodate for this movement, the design is based on a stationary mudmat foundation that supports a moving pipe support frame, which allows the pipeline end to slide on the frame. The preliminary foundation center section for a foldable mudmat is selected with a width and length that is based on the nominated installation vessel-handling capabilities. The foundation section geometry is further developed by providing folding wings on each side of the center section to obtain the required foundation area to support the anticipated loads on the PLEM.

| PLEM configuration | |
|---|---|
| Piping | • System of piping aand its components |
| Structural Frame | • Frame is to supports the piping and its components such as wye, valves and hubs |
| Foundation | • Foundation or mudmat is functioned to distributes the loads to the seabed while minimizing settlement |
| Yoke | • The yoke is installed which is hinged to the structural frame, to minimize torsion-related rotation of the PLEM pipeline assembly during installation and laydown of the PLEM onto the seabed |

**Figure 1.3**: PLEM configuration

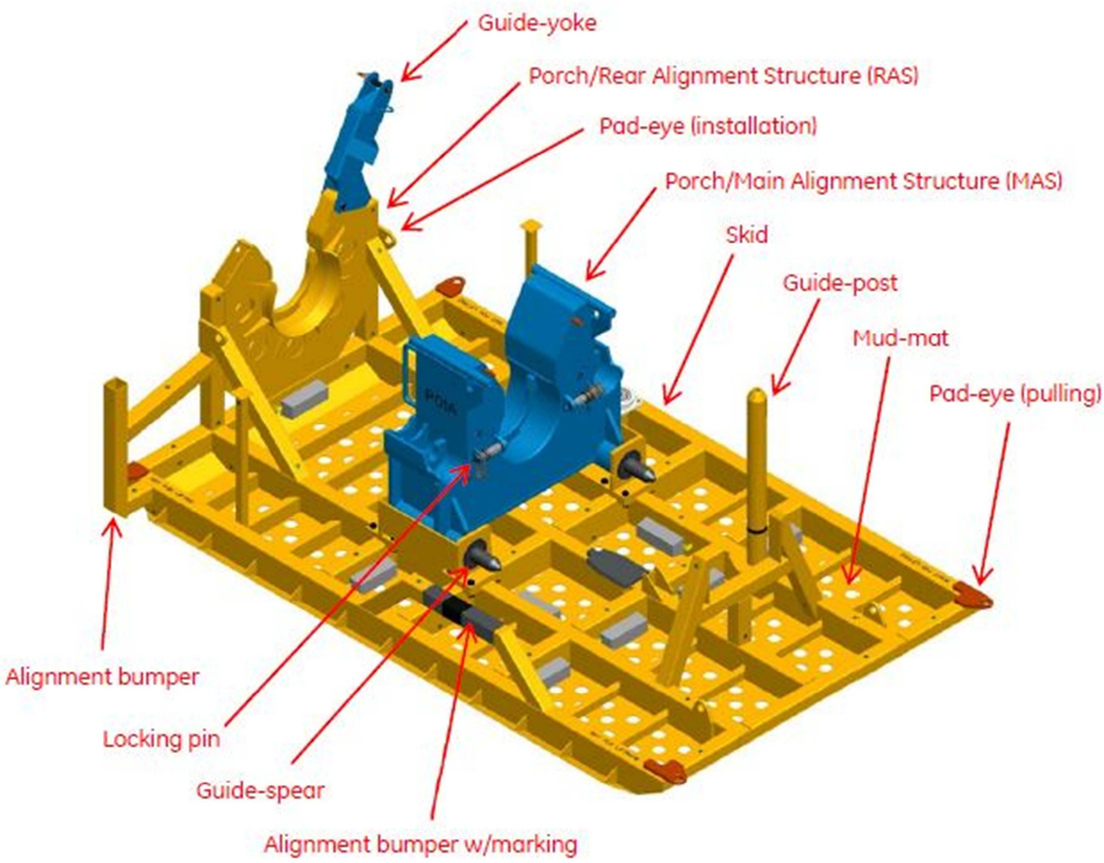


**Figure 1.4:** Typical Configuration of an open PLET [Thorsen].

### 1.2.2. Components of PLEMs

Figure.1.5 shows a 304.8-mm. pipeline that transports gas to a 406.4-mm pipeline via two PLEMs. Collet connectors are used for both PLEMs and connected by a rigid jumper [G. Corbetta]. The PLEMs provide the supporting structure for the piping systems and collet connectors.

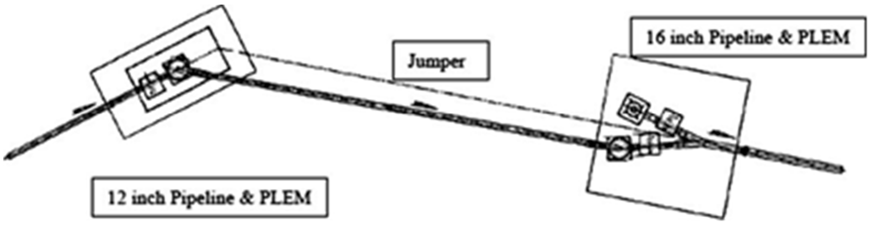


**Figure 1.5:** Pipeline Connection via Two PLEMs and One Rigid Jumper [J.K. Antani].

Detailed configurations for both PLEMs are illustrated in Figure.1-4. In the following sections, the 304.8-mm and 406.4-mm PLEMs shown in the figure are used to explain the components of a PLEM

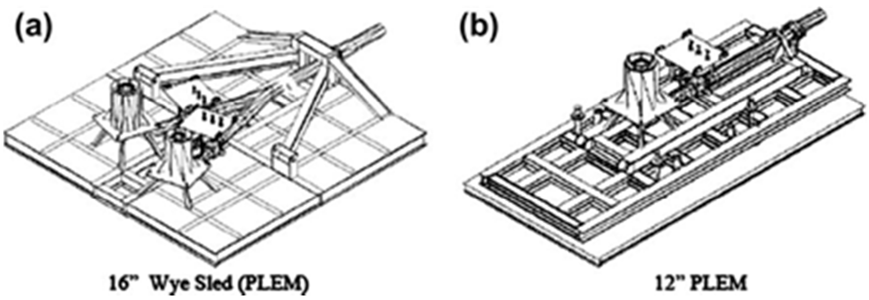


**Figure 1.6:** An example of 16 in Wye Sled and 12 in PLEMs [J.K. Antani]

# Chapter.2

# 2.0 Standard of Design Practice

## *2.1. Steps PLEM Design*

The PLET and PLEM have facilities for multiphase flowmeters and pig launching and/or receiving equipment. The PLET and PLEM should incorporate one or multiple tie-in points, vertical or horizontal, with other components such as isolation gate or ball valves, diverter valves, pig-launcher facilities, an array of sensors, or wyes. The standard interface and components such as hubs and flange outlets are provided for oil & gas production and well service lines according to client's specific requirements. The PLEM and PLET vary in size and complexity and can include a variety of features and facilities.

Similar to other subsea equipment, the design steps for a PLEM/PLET may be divided into four which is specification, initial design, drafting model and stress and fatigue analysis as shown in Figure 2.1. The design may incorporate features to suit any installation methods or vessels for installation purposes.

| Design Steps of PLEM | |
|---|---|
| Specification | • Specification of design includes geometry and piping configuration, foundation selection may by pile or mudmat, installation requirement such as yoke and hinges, and fabrication and installation limitations |
| Initial Design | • Initial design includes sizing which is determining the principal load path, configuring the primary structural components such as forging, yoke, etc. and the layout of structure frames and supports to support valves and pressure/temperature components that facilitate installation and maintenance, and sizing the mudmat based on loads, structure dead weight, and soil data |
| Drafting Model | • Drafting a model for analysis includes developing a 3D PLEM system with AutoCAD 3D software and saving the 3D model in a SAT format file for finite element detailed analysis; meanwhile a SACS/ StruCAD model is developed to determine the structure steel frame member's sizes |
| Stress and Fatique | • Stress and fatique analysis includes importing the SAT file into ABAQUS/ ANSYS finite element software, meshing the 3D model, applying the loads in the operating and installation conditions, then applying a stress analysis and checking stress to satisfy the design criteria |

**Figure 2.1**: Design steps of PLEM/PLET

## *2.3. Information for Design and Analysis*

In order to keep up with the times, PLEM designs need to be based on data. In the offshore engineering field where analytics rules, design is becoming data-driven. Data forms the cornerstone of PLEM development process. It can quickly inform development priorities for enhanced user experience, improved user satisfaction and increased adoption rates.

Some information is usually required before design of PLEM and PLET. The specifications of PLEM and thermal load are given by the clients. The following data are required for the PLEM and PLET design and analysis:

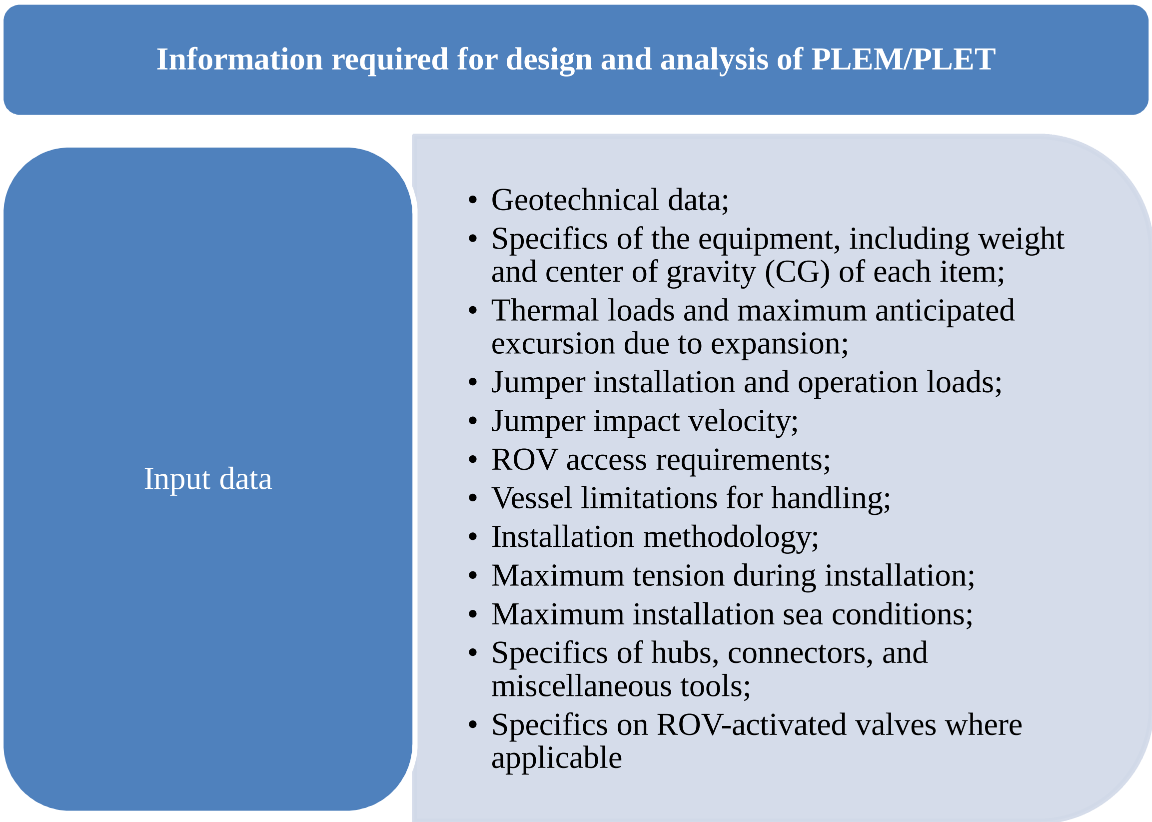


**Figure 2.2**: Information required for design and analysis of PLEM/PLET

## *2.1. Practiced Design Codes*

Standards are documents that describe the important features of a product, service or system. By applying standards, designers and manufactures can help to ensure that their products and services are consistent, compatible, safe and effective. Subsea equipment is assembled from components made in different countries, so standards are more important than ever. Codes are collections of laws and rules which provide correct procedures to maintain uniformity and safety.

The design codes and regulations used for PLEM design should be approved by clients depending on the project's requirements. The following specifications are used for the reference:

| Design Codes for PLEM Design and Analysis | |
|---|---|
| DNV RP B401 | • Cathodic Protection Designs |
| API RP2A (WSD) | • Foundations, for the design of the mudmat |
| NACE RP 0176 | • Corrosion Control of Steel Fixed Platforms Associated with Petroleum Production |
| NACE TM 0190 | • Impressed Current Test Method for Laboratory Testing of Aluminum Anodes |
| NACE No.2 ISSSP-SP10 | • Near-White Metal Blast Cleaning |
| NACE RP0387 | • Metallurgical and Inspection Requirements for Cast Sacrificial Anodes for Offshore Applications |
| NACE 7L198 | • Design of Galvanic Anode Cathodic Protection System for Offshore Structure |
| API 1104 | • Pipeline and Pipe Welding, 18th ed |
| AWS D1.1-02 | • Structural Welding Coded Steel |
| ISP 8501-1 | • Preparation of Steel Substrates before Application of Paints and Related Products |

**Figure 2.3**: Practical design codes used for design and analysis of PLEM/PLET

However, deepwater Gulf of Mexico fields compete very favorably with oil producing provinces around the world, owing to the high rate of geologic success and relatively more favorable royalty and fiscal regime, but exploration of oil and gas is driven by technology rather than traditional geology approaches, drilling activity in the Gulf of

Mexico could be constrained by the lack of available rigs and the structures in question are elusive to conventional seismic imaging, obscured by vast salt canopies.

The following codes and regulations are often used by the designer for structural analysis of PLEM in the deep-water of Gulf of Mexico.

| Design Codes for PLEM Design and Analysis at Gulf of Mexico | |
|---|---|
| AISC | • Steel Construction Manual, Allowable Stress Design (ASD) |
| API RP 2A-WSD | • Recommended Practice for Planning, Designing and Construction: Fixed Offshore Platform Working Stress Design (WSD) |
| API 2RD | • Design of Risers for Floating Production Systems (FPSs) and Tension-Leg Platforms (TLPs) |
| API 5L | • Specification for Line Pipe |
| ASME B31.8 | • Gas Transmission and Distribution Piping Systems |

**Figure 2.4**: Practical design codes used for design and analysis of PLEM/PLET at Gulf of Mexico

# Chapter.3

# 3.0 Structure and Strength Analysis

## *3.1. Design Analysis*

The PLEM should be designed to facilitate installation and allow them to land properly. If the PLEM is designed with a yoke to support the installation, the yoke may be designed based on the forces obtained from pipelay analysis for the pipeline in a flooded condition. The yoke design also considers the irretrievability loads. Designs of the yoke and PLEM are coordinated with the installation contractor for adaptability with the installation vessel capability. The PLEM analysis for structural integrity should include the following design conditions:

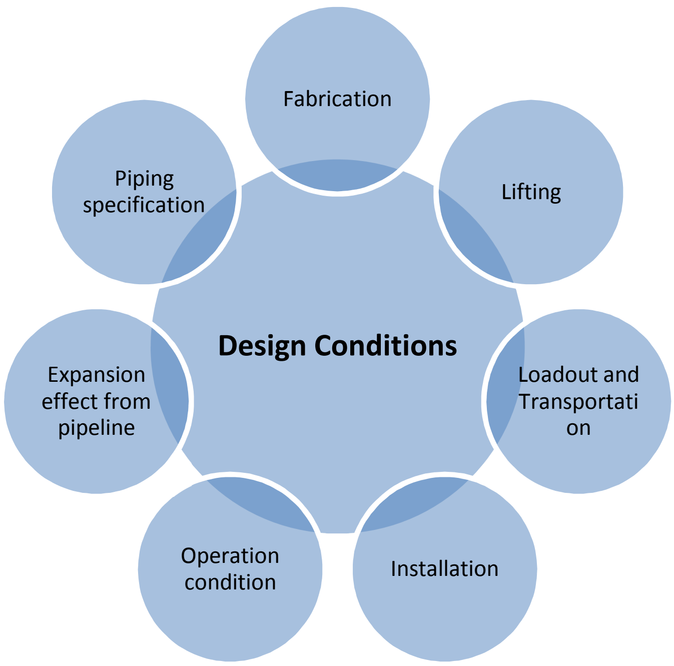


**Figure 3.1:** Environmental condition should be considered during PLEM design and analysis

In-place operating conditions, structural loads, and fatigue damage should be included. The thermal and pressure-induced expansion of pipelines in the operating condition will give effect to the PLEM. Piping requirements, including bends, tees, reducers, and valves should be considered.

The PLEM is designed with padeyes and miscellaneous installation aids as required and has a sufficient number of padeyes for handling during various phases of installation. The design should ensure that the CG of the PLEM assembly, including the yoke, is near the geometric center of the mudmat, in line with the center of the pipeline (or slightly below) and below the pivot point of the yoke and slightly to the rear of the yoke pivot to ensure that the PLEM will stabilize with the correct orientation for landing. The center of the yoke pin will be located in line with the flow-line as shown in Figure.3-2. The pivot is the local coordinate origin on the PLEM for dimensions and calculations. The offsets epipe and ePLEM are negative numbers. The PLEM is welded to the pipeline to minimize the cost and potential leak paths.

The equipment size and location for a PLEM should take into consideration the need for ROV operability and visibility. The structural frame and mudmat for the PLEM are coated and cathodically protected for the design field life. The cathodic protection design and analysis may be carried out based on DNV RP B401 [DNV], "Cathodic Protection Design."

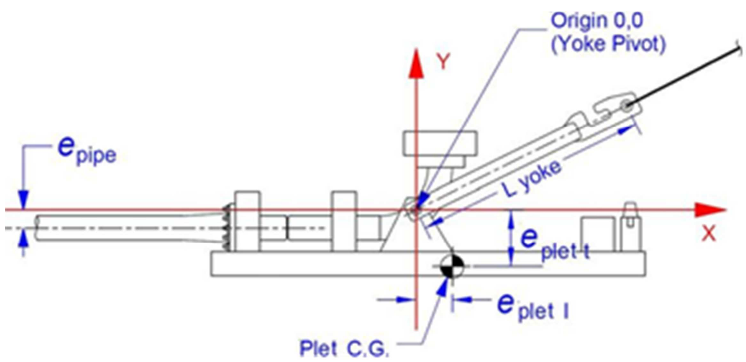


**Figure 3.2:** Coordinates and CG Position of Second-End PLEM [Y. Bai]

## *3.1. Structure Analysis*

The PLEM should be designed to facilitate installation and allow them to land properly on the seabed. Figure 3.3 shows circle should be performed during PLEM design and analysis which includes such as selection criteria for structural members and design criteria, material selection and specific analysis including bolts and flange connections where applicable, structural analysis of the frame, piping and support location, foundation analysis including installation (suction caisson, mudmat, pin piles etc.) and settlement, expansion and thermal analysis of final manifold design by Finite Element and seismic load assessment covering structural frame, piping, foundations and support location design.

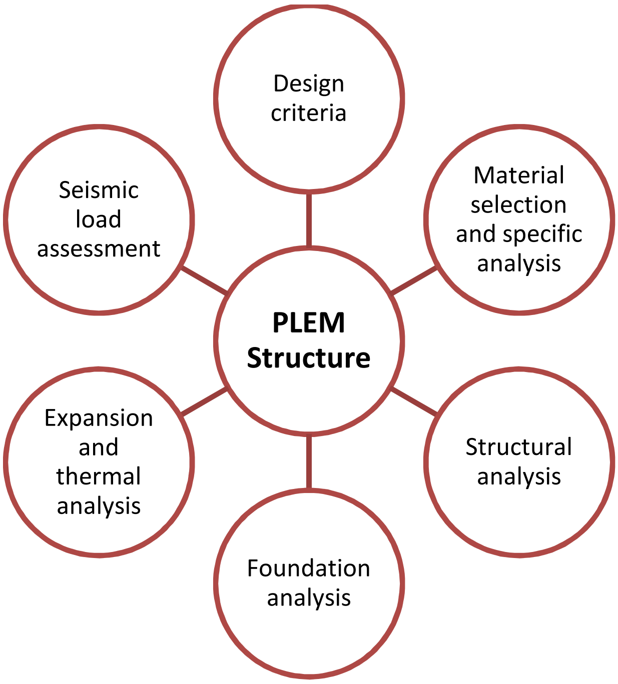


**Figure 3.3:** Circle of PLEM design and analysis

The structural analysis software SACS/StruCAD, which is widely used in the analysis of subsea steel structures, is one of the most useful tools for the analysis of a PLEM's steel frame structure. The SACS/StruCAD analysis provides loads, stresses, and deflections for all structural members of the PLEMs in various load conditions. The structural design of a PLEM should be performed in accordance with the latest editions of API-RP-2A and AISC's Steel Construction Manual, Allowable Stress Design (ASD) [AISC].

The structural analyses for a PLEM should be carried out for lifting, installation, and in-place load conditions. Under installation conditions, the controlling design load on the PLEM is the tension load from the pipeline. The tension load includes the weight of the PLEM plus the tension in the pipeline with a dynamic factor of 1.5.

## *3.3. Strength Analysis*

A preliminary mudmat area for the PLEM is estimated based on the soil bearing capacity and the estimated weights of the hubs, valves, piping, jumper loads, and mat. The soil shear strength profiles are developed based on site-specific soil data obtained from drop cores. The design shear strength is obtained as the depth-averaged value over the shear strength profile at a depth equal to half the PLEM width.

The foundation bearing stresses are calculated for the following anticipated jumper loading conditions [K.H. Andersen]:

- Jumper installation;
- Jumper operating;
- Jumper operating, future jumper installation;
- Future jumper operating.

The mudmat has a shallow foundation and may be designed to cover the following issues per API-RP2A WSD or DNV Classification Notes No. 30.4, “Foundations” [DNV]:

- Settlement;
- Eccentric loading;
- Overturning and cyclic effects;
- Safety factors for bearing, sliding, torsional, and overturn failures.

Mudmats with skirts are designed to keep the PLEM stability and to reduce settlement and movement on the seabed when in clay soil. However, PLEMs without skirts are often used in shallow water on sandy soil so it can move about on the seabed, because the penetration on sand is very small.

# Chapter.4

# 4.0 The Foundation

## *4.1. Introduction*

The PLEMs foundation provides a support for the PLEM structure. A preliminary mudmat area or dimensions for the PLEM are estimated based on the soil bearing capacity and the estimated weights of the hubs, valves, piping, jumper loads, and mudmat. The mudmat may be designed with skirts for stability and to reduce settlement and movement on the seabed. The dimensions will be adjusted with consideration given to the limitations imposed by the installation vessel, fabrication shop, and overland and sea transportation situations. The design should be analyzed for structural integrity in terms of:

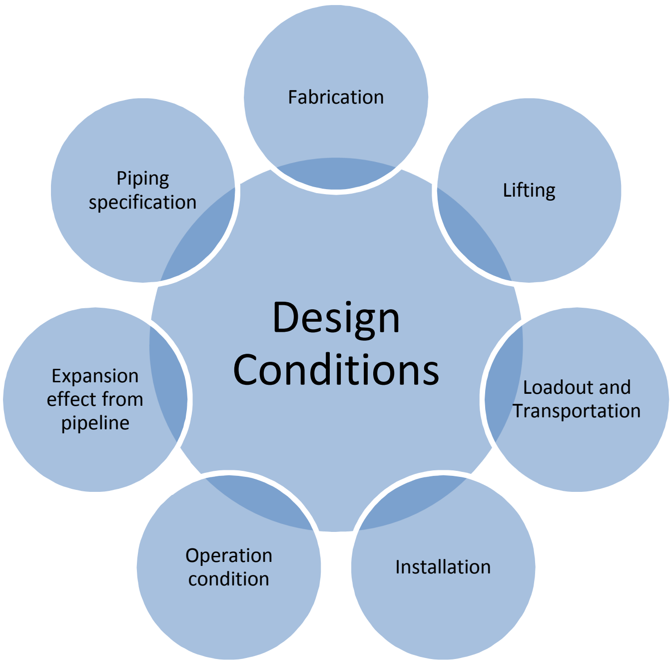


**Figure 4.1:** Environmental condition should be considered during PLEM design and analysis.

Knowledge of the soil properties at the PLEM target area is required to properly size the mudmat, to determine stability, and to estimate short-term and long-term settlement.

These soil data are more important for a mudmat than the deep soil sample required for pile design.

## *4.2. Load Conditions*

The foundations should be designed to support the PLEMs with the design loads as indicated, within limits of the required safety factors in accordance with API RP2A (WSD) and a minimum factor of safety for soil bearing of 2.0. General load conditions for mudmat sizing are as follows:

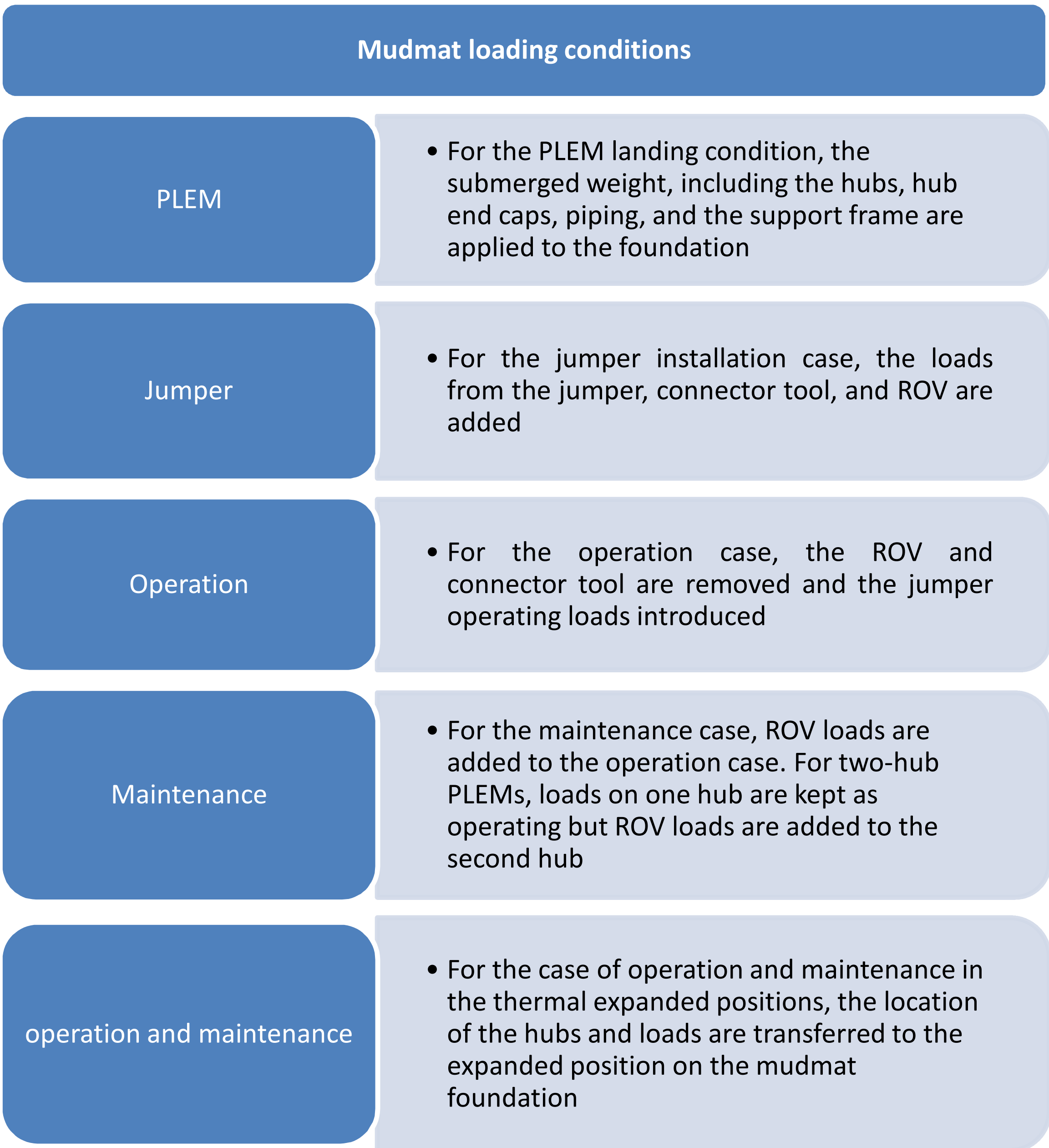


**Figure 4.2:** General load for Mudmat

## *4.3. Mudmat Analysis*

When seabed soil is too soft to bear the load of subsea structures such as PLET and PLEM, mudmats are designed and installed to provide additional support. The commonly used plate mudmats, often made with carbon steel, consist of a top plate and a number of perpendicular vertical stiffeners that function as load-bearing beams. But the simplicity of the design belies their importance.

Mudmats are just as vital as the subsea equipment resting on them. The Mudmat must be designed to have sufficient strength, particularly buckling strength, and that requires considerable design analysis. Since most mudmats are custom-designed for individual load performances, subsea soil properties, and installation requirements, nearly every mudmat requires its own unique stress and buckling analysis. The analysis process used to be largely manual, time-consuming, and unwieldy. The design of mudmat foundations should include the following issues per API RP 2A-WSD:

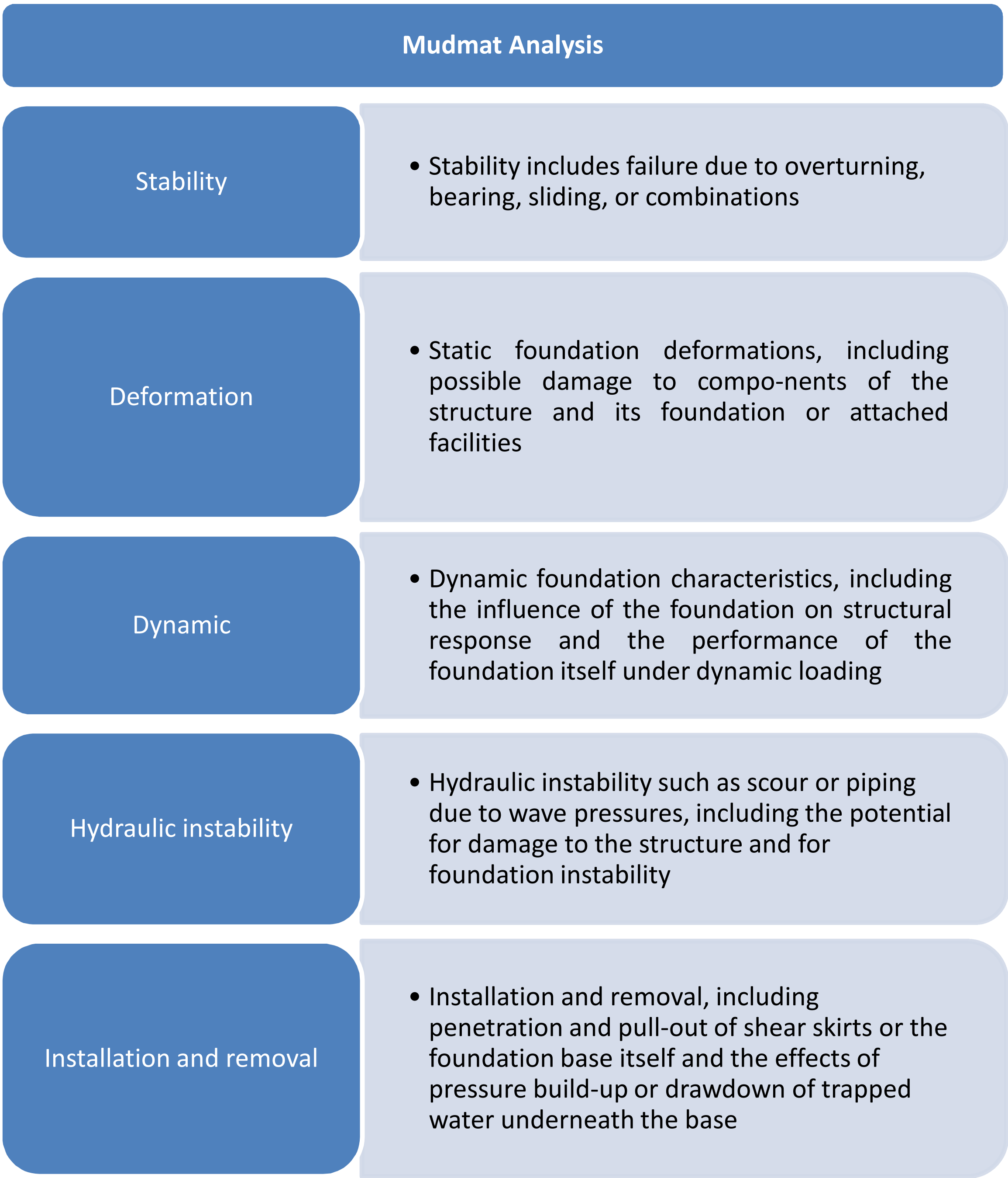


**Figure 4.3:** Issues during Mudmat analysis

### 4.3.1. Overturning Capacity

The objective of checking the overturning capacity for a shallow foundation is to ensure that, under the applied loads, the foundation will be stable if placed on a hard surface. Overturning could take place either around the longitudinal edge or the transverse edge of the foundation. The governing overturning direction will yield the lowest safety factor.

The following formula is used to calculate the overturning safety factor of the shallow foundation around one of its edges:

$$sefty\ factor_{overturning} = \frac{F_z L}{M} \tag{4-1}$$

in which $M$ is the resultant overturning moment in the overturning direction, $F_z$ is the resultant vertical force acting at the geometric center of the mudmat, and $L$ is the distance from the geometric center to the rotating axis.

Load eccentricity decreases the ultimate vertical load that a footing can withstand. This effect is accounted for in bearing capacity analysis by reducing the effective area of the footing according to empirical guidelines. The calculation method of effective area is detailed in the section title "C6.13 Stability of Shallow Foundations" of API-RP-2A [API].

The recommendations pertaining to the design issues for a shallow foundation are given in Sections 6.13 through 6.17 of API-RP-2A [API] and include:

- Stability of shallow foundations;
- Static deformation of shallow foundations (short-term and long-term deformation);
- Dynamic behavior of shallow foundations;
- Hydraulic instability of shallow foundations;
- Installation and removal of shall foundations.

The following sections provide a detailed design example for a mudmat based on DNV Classification Notes No. 30.4, "Foundations" [M. Faulk].

### 4.3.2. Penetration Resistance of Skirts

The height of the skirts is designed to guarantee that with the occurrence of the maximum estimated consolidation settlement, the structures will retain their ability to be displaced freely through the mudline.

The skirt penetration resistance in sand, $Q_P$, is estimated according to DNV code [DNV]:

$$Q_P = q_t A_t + \tau_w A_w \tag{4-2}$$

Where; $q_t$ is skirt tip pressure, $q_t = k_p q_{c,CPT}$, $\tau_w$ is skirt wall friction, $\tau_w = k_f q_{c,CPT}$; $A_t$ and $A_w$ is skirt tip and skirt wall area, respectively; $q_{c,CPT}$ is point resistance from CPT boring according to [DNV]; $k_p$ is 0.6 and $k_f$ is 0.003 for highest expected penetration resistance; $k_p$ is ¼ 0.3 and $k_f$ is 0.001 for most probable penetration resistance.

The following relationship is an example of soil survey results at the PLEM location:

$$q_{c,CPT} = 40\ x\ z\ [MPa], for\ z < 0.5\ m$$

### 4.3.3. Bearing Capacity during Installation

The mudmat minimum dimensions required to keep the structure supported at the mudline are a function of the ultimate vertical capacity of the soil, considering the effect of the resultant load eccentricities (related to its length and width), as a reduction of the mudmat area (effective area concept).

Assuming that the subsoil contains sand, the vertical bearing capacity is checked according to:

$$Q_v = 0.5 N_\gamma \gamma' B A + N_q p' A \tag{4-3}$$

Where; $N_\gamma$ and $N_q$ are load bearing factors; $\gamma'$ is effective unit weight of sand; $B$ is width of mudmat; $A$ is mudmat foundation area; $p'$is effective vertical stress.

For the case of clayey soil, the vertical bearing capacity may in principle be found by:

$$Q_v = N_c S_u A \tag{4-4}$$

Where; $N_c$ is load bearing factor (function of several factors); $S_u$ is average undrained shear strength along slip surface.

### 4.3.4. Bearing Capacity during Operation

Potential soil failure modes due to trawler loading and thermal expansion loading include failure from lateral sliding and deep-seated failure. A short description of calculation principles for the different failure modes is given below.

**Lateral Sliding**

The lateral soil resistance against pure sliding of the foundation may be calculated by:

$$Q_h = r\tan(\varphi)\,W \qquad (4\text{-}5)$$

Where, $r\tan(\varphi)$ is the friction between foundation and seabed and $W$ is the vertical load on the mudmat.

If a rock berm is placed on the mudmat, additional lateral capacity (earth pressure) is obtained according to:

$$Q_v = p_p - p_a \qquad (4\text{-}6)$$

Where; $p_p - p_a = (\chi_p + \chi_a)^{1/2}\gamma' H_r B$, and $\chi_p + \chi_a$ is earth pressure coefficients; $\gamma'$is effective unit weight of rock; $H_r$is height of rock dump; $B$ is equivalent width of mudmat.

**Deep-Seated Vertical Failure**

A foundation's stability is based on the limiting equilibrium methods ensuring equilibrium between the driving and the resisting forces, according to Janbu et al. [N. Janbu]. The foundation base has been idealized to account for load eccentricity according to the principle of plastic stress distribution over an effective base area.

In addition, a verification of the final rotation (loss of horizontality) of the structures should be done, considering the overturning moment envelope that will act during the entire life of the structure.

### 4.3.5. Settlement Analyses

The settlement of the structures is analyzed according to Janbu's method [N. Janbu]. The soil strains 3 are calculated by:

$$\varepsilon = \Delta^{\sigma_v'}/_{M} \qquad (4\text{-}7)$$

where $\Delta\sigma_v'$ is the vertical effective stress increase, and $M$ is the deformation modulus. Distribution of additional vertical soil stress with depth is based on the recommendation given by Janbu [N. Janbu].

The vertical consolidation settlement $\delta$ is then found by:

$$\delta = \int_0^H \varepsilon dz \tag{4-8}$$

where H is soil layer thickness.

# Chapter.5

# 5.0 PLEM Installation

## *5.1. Introduction*

The installation of pipeline-end manifold (PLEM) as part of a deepwater flow line system must closely integrate design. The installation procedures are to ensure the equipment running smoothly, predictably, and safely. Pipeline tensions are high in deep water and installation vessels costly. Therefore, design of the PLEM and the corresponding installation procedure must be as simple as possible. The installation analysis for a pipeline system with a PLEM should check the following items as follows tensile of pipeline, bending & shear stress and hoop stress:

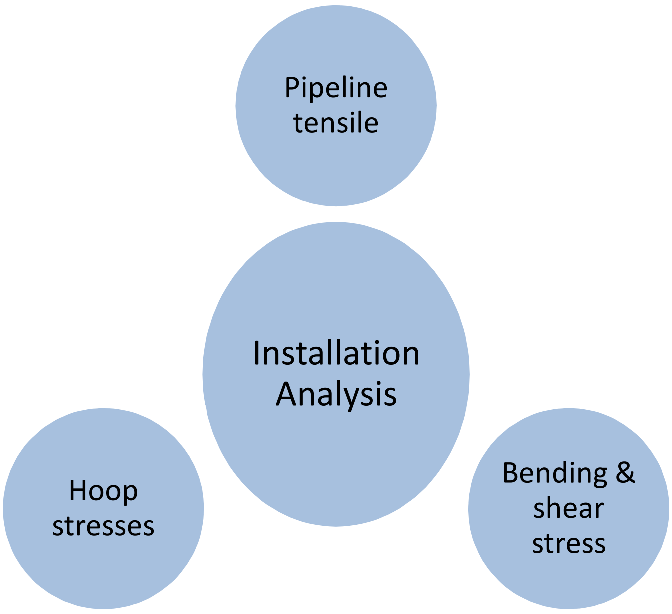


**Figure 5.1:** Installation Sequence for a PLEM

The installation operations can be divided into the following main steps:

| | |
|---|---|
| Start | • First-End PLEM from going overboard through the splash zone |
| Initiation | • Initiation of first-end PLEM |
| Pipeline laying | • Normal pipe laying (including installation of buoyancy) |
| Abandonment | • Abandonment of second-end PLEM |
| Recovery | • Abandonment and Recovery (contingency operations) |

**Figure 5.2:** Steps of installation operations

The following analyses should be executed to ensure pipeline integrity during operations which static, dynamic and buckling analysis as show below:

**Static Analysis**

- The main objectives of static analysis is to determine the requirements for each step during the installation due to vessel movement, pipe payout, etc.

**Dynamic Analysis**

- Dynamic motion in regular and iiregullar waves for both empty and flooded conditions are required. The most critical steps of the installation defined by the static analysis should also be subjected to regular and iiregular waves dynamic analysis. The main objective of this dynamic motion analysis is to define the critical environmental conditions for the installation window. In the anallysis firstly, if regular wave results are found to be too conservative, an irregular wave analysis may be considered as an alternative

**Buckling Analysis**

- A local buckling check should be used to verify that the pipeline will resist combined loads for axial force, bending moment, external and internal pressures
- No local buckling will occur along the catenary for each of the steps

**Installation Analysis**

- The critical steps for fatigue occurring during installation are whenever the pipe is clamped for several hours to weld the PLEM

**Figure 5.3:** Pipeline integrity during operations

OFFPIPE and Orcaflex are popular tools for the analysis of offshore pipeline and PLEM installations. OFFPIPE offers a recognized pipeline installation simulation that is simple, fast, and gives results with reasonable accuracy. However, it was developed based on the DOS operating system without a Windows interphase to illustrate the installation procedure. Compared with OFFPIPE, Orcaflex is widely utilized for subsea installation analyses because of its friendly interface. Orcaflex is a fully 3D, nonlinear, time-domain finite element program capable of dealing with arbitrarily large deflections of the pipe from the initial configuration. A simple lumped mass element is used, which greatly simplifies the mathematical formulation and allows for quick and efficient development of the program to include additional force terms and constraints on the system in response to new engineering requirements. The program is designed for the static and dynamic analysis of subsea structures, pipeline, and cable systems in an offshore environment.

During the design phase of a PLEM, there is not usually enough information and data available for the installation analysis using the software just described. Some simplified methods have been developed based on Math-CAD or Excel worksheets. One of the typical methods described below is mainly based on a paper by Gilchrist [R.T. Gilchrist], where further details are given.

## *5.2. Challenges in Ultra-Deep Water*

According to Penati et.al (2015), subsea structures and other systems are having different approach when depth in ultra-deep water (more than 1500m). The technologies in drilling and installation in water depth greater than 3000m is not common. The engineering and installation capabilities have to perform difficult offshore operations, where specific vessels and special purpose equipment are needed. Due to increasing water depth, the limitation of technologies is capped, where the structures weight that required to be hold is not enough.

The pipeline in a PLEM must not be overstressed at any time during different load conditions. The PLEM must be stable during installation and configured to land on the seabed in the correct orientation. The PLEM used to initiate pipelay is termed a first-end PLEM. A PLEM installed on completion of the pipelay is termed a second-end PLEM. The second-end PLEM has a yoke that pivots near the pipe centerline and the PLEM center of gravity. The following problems could occur during installation and should be considered during the design procedure:

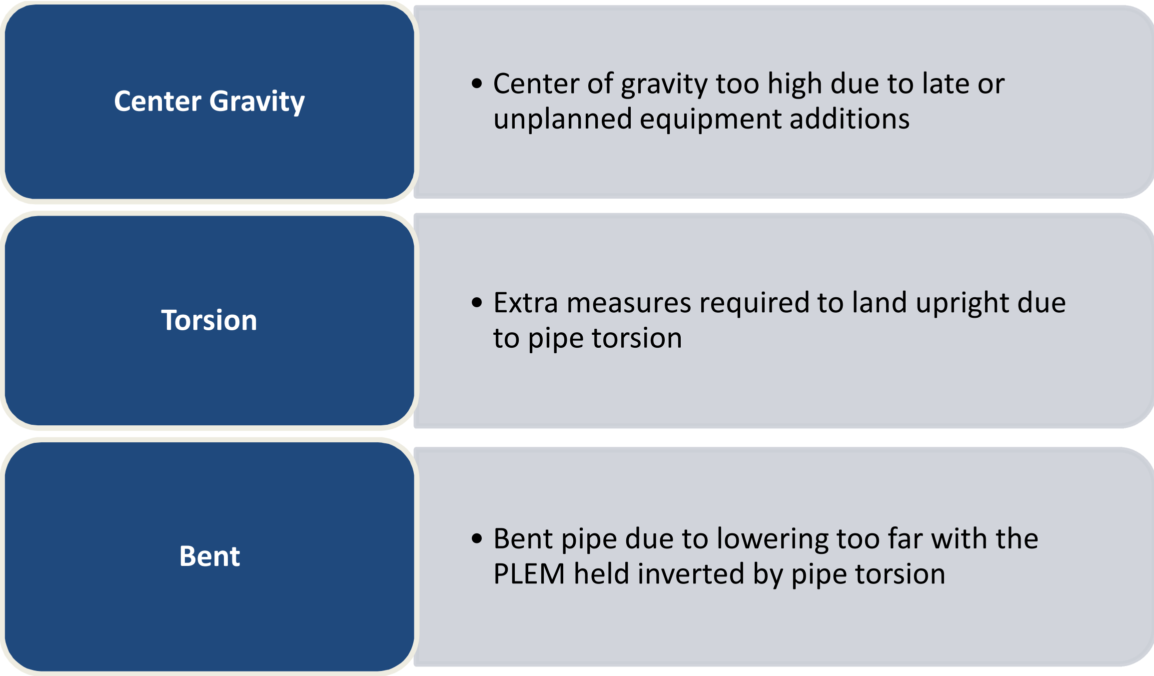


**Figure 5.4:** Challenges of PLEM installation

The installation of a second-end PLEM starts with the abandonment configuration of the pipeline. The pipeline can be laid by using an S-lay or J-lay process. On completion of pipe laying, the pipeline is fitted with an Abandonment and Recovery (A&R) head to prevent flooding and for attachment of the A&R wire. There are two reasons for not attaching the PLEM at this point:

- It is not practical to attach and maneuver the PLEM structure through the pipelay stinger or J-lay tower.
- It is prudent to lay the end of the pipe on the bottom and assess the unconstrained top-of-pipe orientation before attaching the PLEM.

The PLEM weight, balance, and geometry are all optimized during design to ensure that the PLEM has an intrinsic tendency to land in the correct orientation. Nevertheless, experience has shown that it is essential to attach the PLEM according to the observed natural top-of-pipe.

Figure.3-2 shows the installation sequence for a second-end PLEM. In the Figure.3-2a, the pipeline is lowered to the seabed with an A&R wire. The cut length and top-of-pipe are assessed with an ROV inspection. In Figure.3-2b, the pipeline is recovered to the vessel in a J-mode (pipeline is suspended without an over-bend in this configuration) and set in a hang-off receptacle or slips so that the A&R head can be removed from the pipeline end to the attached PLEM. In Figure.3-2c, with the PLEM welded, the entire assembly is lifted from the support and lowered to the seabed. If all goes well, the PLEM sled gently lands upright on the seabed

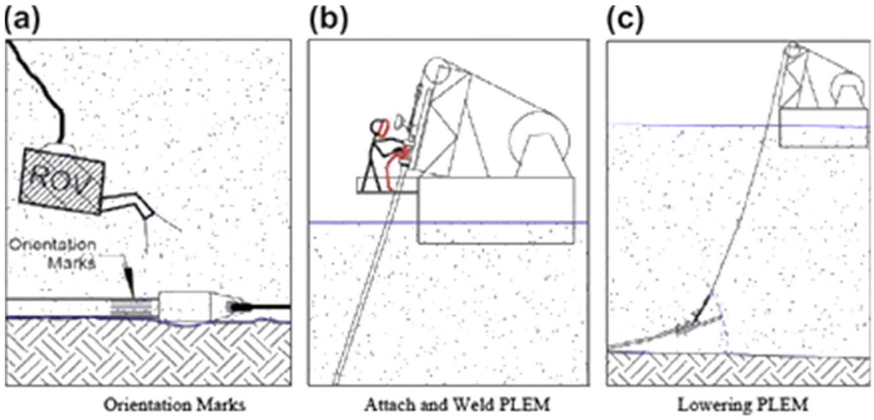


**Figure 5.5:** Installation Sequence for a Second-End PLEM [N. Janbu]

The rigging to lower the PLEM is connected to a yoke that applies a lift force to a pivot near the centerline of the pipe and above the CG of the PLEM. The pivot is located so as to:

- Control bending load on the pipeline throughout the installation sequence.
- Direct the force to correct the orientation of the PLEM as the PLEM approaches the seabed.

## *5.3. Installation Method for PLEM/PLET*

Referring to Rebeiro (2006), there are conventional and non-conventional methods in deploying manifold. The conventional methods include the traditional installation by wire cable using AHTS or Crane Barge and installation by drilling riser. The non-conventional methods are sheave installation method (SIM) and pendulous installation method (PIM). In the recent years, the methods of installing has increase in numbers, Cao (2016) stated the mainstream installation methods for SPS include drill-string installation method (DSIM), the method is the same as by drilling riser method. Next, other method stated is winch-wire installation method (WWIM) which also is the same as method using wire cable mention earlier. Then, the followings method also included such as SIM, PIM, pencil buoy method (PBM), the heave compensated landing system (HCLS) and Floating installation device (FID) with its installation method. Above mentioned methods have its own capabilities and limitations when performing in different water depth.

### 5.3.1 Installation by Wire Cable Using AHTS or Crane Barge, WWIM

According to EOSP (2007), for project Bualang Field with water depth 60m, the method to install PLEM is by using wire cable operated from pipe lay barge with installed crane with lifting load of 120 tonnes. The method uses crane barge, the crane lift the PLEM and put it into the splash zone. After it has submerged, PLEM will be lowered to the seabed and set down using USBL beacons and ROV to monitor position and orientation. A spreader is used to control the orientation of the PLEM. This method has its limitation in performing installation more than 1000m water depth as the weight of the wire is the same with the manifold, creating higher resonance value.


**Figure 2.1:** Lifting of subsea hardware on Lewek Champion

### 5.3.2 Installation by Drilling Riser, DSIM

According to Hampton (1981), the usage of semi-submersible is not only for drilling purposes but can also be used to deploy subsea hardware. In accordance to Wang et.al (2012), the day rate of using MODU such as semi-submersible has become obsolete as it has an expensive operating cost. The use of semi-submersible in installing manifold is also a rare occurrence. It also has limited capability of installing 300tonnes subsea hardware in 1000m of water depth.


**Figure 2.2**: Installing Manifold Using Semi-Submersible

### 5.3.3 Sheave Installation Method

According to Wang et.al (2012), the Sheave Installation Method (SIM) was develop to deploy 175Te Manifold into 1885m water depth. It is a conventional deployment system with two point configuration. The method uses three vessel to install the manifold. A semisubmersible (SS) and two AHTS Tug is needed. The semisubmersible act as drilling vessel which uses the crane to lift the manifold and deploy into the splash zone while providing heave motion compensation during lowering through splash zone and landing on the seabed. The configuration is as shown in figure below:

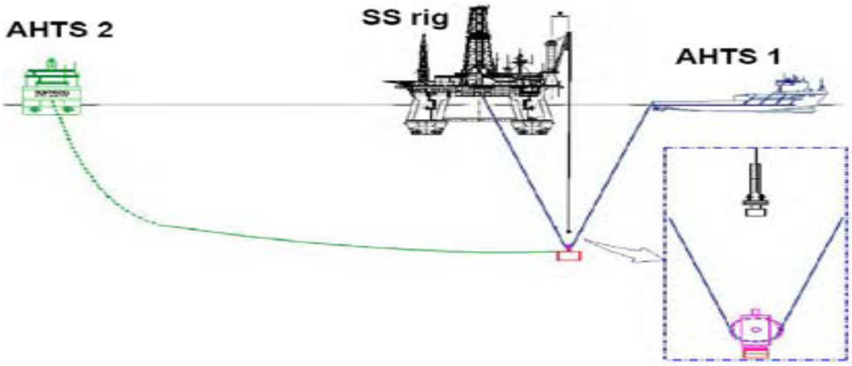


**Figure 2.3**: Sheave Installation Method

### 5.3.4 Pendulous Installation Method

According to Wang et.al (2013), the Pendulous Installation Method (PIM) is a non-conventional method to install structures in deep and ultra-deep water. It was develop by Petrobras to install a 280Te large manifold in water depth of 1900m. The PIM uses two small installation vessel from using deep water construction vessels and heavy lifts vessels. The PIM uses conventional steel wire winch system as a launch line to the structure in a pendulous motion and uses a conventional synthetic fibre rope to deploy the structure into bed. The method is illustrates as of the figure below:

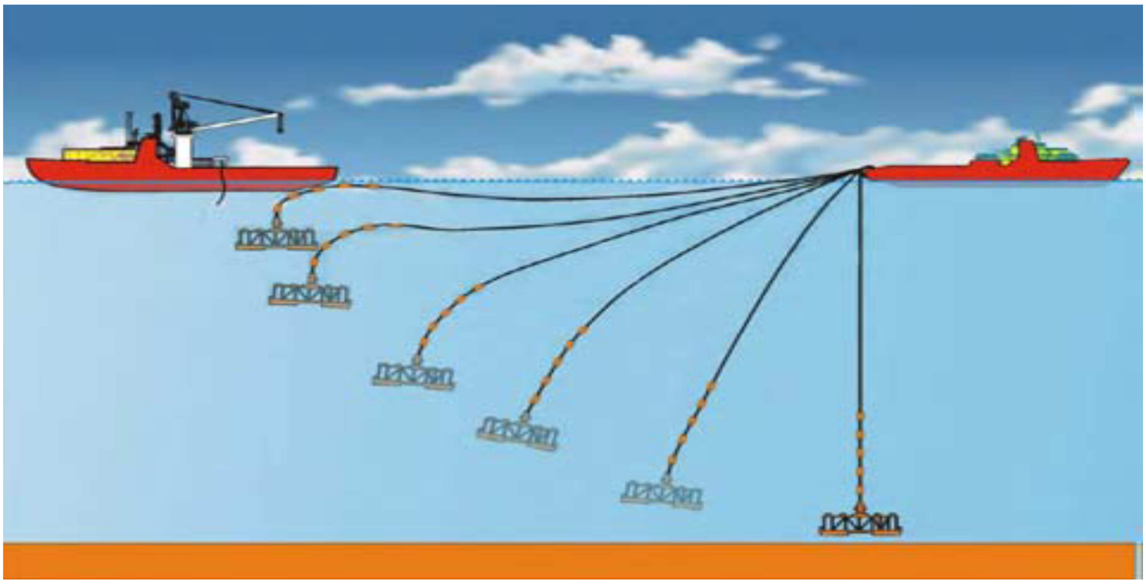

**Figure 2.4**: Pendulous Installation Method

### 5.3.5 Pencil Buoy Method (PBM)

Risoey (2007) state that the PBM is subsurface transportation and installation method that is developed by Aker Solutions. The manifold is suspended from a pencil-shape buoy during wet tow process from onshore or lifting site. Upon reaching the installation site, the towing wire is winched in and the pencil buoy is detached. After that, the method is similar to WWIM, where the deployment under water has the standard offshore operation. This method is suitable for installation in harsh-environment and long distance site location. The method only requires standard equipment on board AHTS tugs, custom made special pencil buoy, and a passive heave compensator. Below illustrates the setup of the PBM.

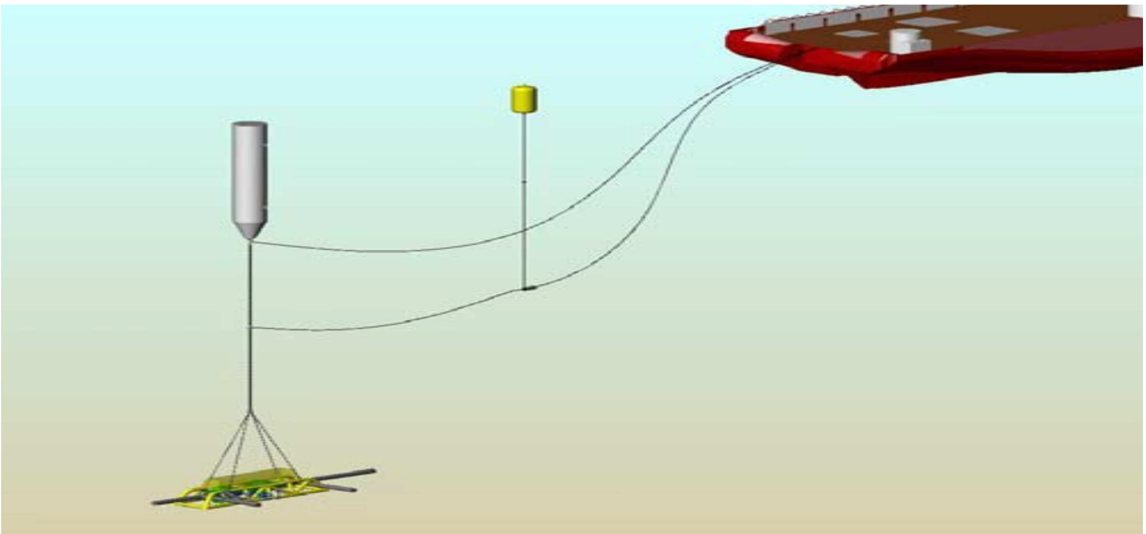

**Figure 2.5**: The Pencil Buoy Method setup

### 5.3.6 Heave Compensated Loading System (HCLS)

The Heave Compensated Loading System (HCLS) is a similar method as PBM that use specific chain and buoy system. The difference is that the buoy is used in the installation process rather than detached from the PBM. The manifold is not supported directly by the vessel, but is supported by the buoy under the wave zone. Thus, the needs of large, stable vessel such as semi-submersible can be avoided in term of offloading the payload from deck, but require large deck to transport the SDS because of the dimension. (Nelson, 1997).

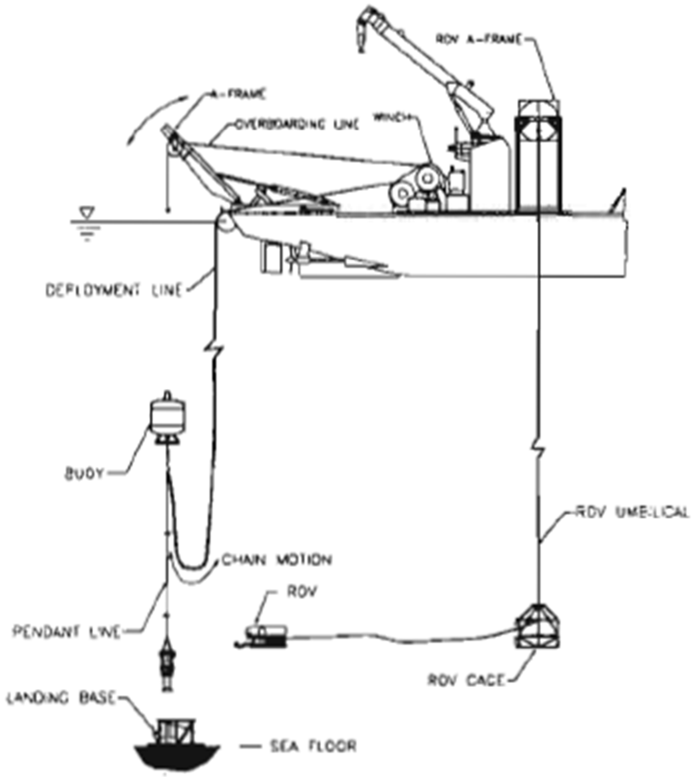


**Figure 2.6**: Heave Compensated Loading System configuration

### 5.3.7 Floating Installation Device (FID) with its Installation Method

Cao (2016) stated that the FID was to design to tackle three major challenges in various deep-water installations which are environmental conditions due to dynamic responses, crane lifting capacity and installation cost. The main concept of the FID is originated from the PBM. Instead of using pencil-shaped buoy, this method utilizes the FID to support the SPS in transportation and installation process. The FID use a low-cost lifting vessel, which reduce the expensive cost of specific vessel such as HCV.

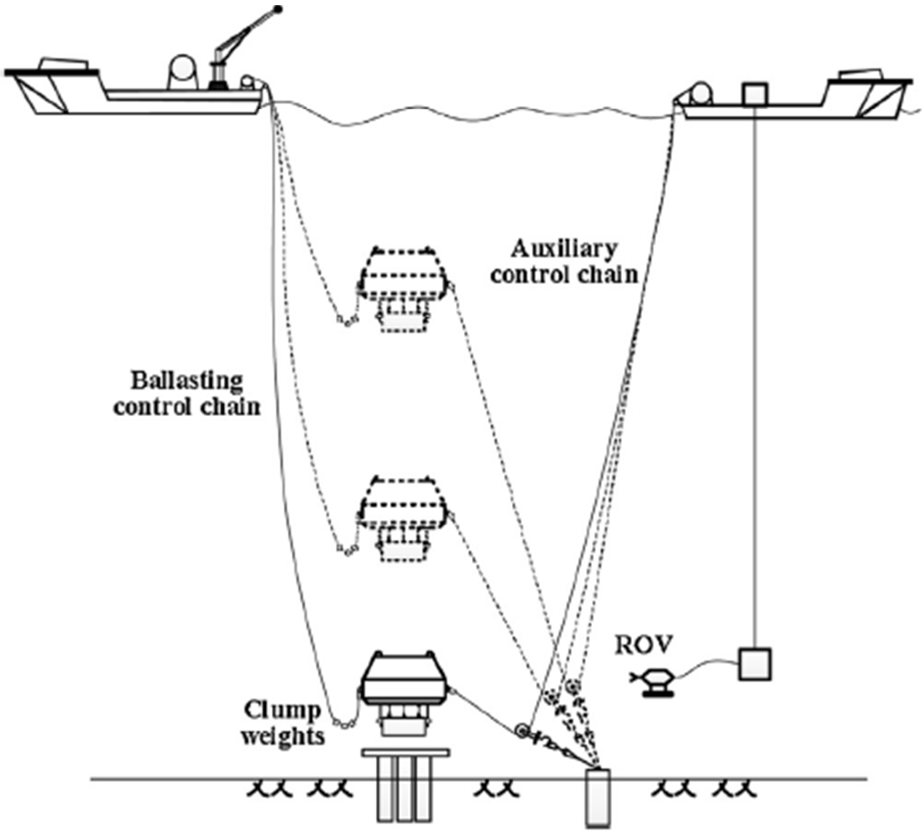


**Figure 2.7**: Lowering Process Of Subsea Hardware Using Floating Installation Device (FID)

### 5.3.8 Utilization of Fiber Rope Deployment System

The company ODIM, developed a new deployment system which utilized the technology on fiber rope deployment system. It is the conventional ways of vertical deployment, but use the fiber rope instead of steel wire. The traditional use of steel wire has its limitation when conquering deep water installation. According to Sverre et.al (2007), the self-weight of the steel wire reduce the payload capacity in lowering operation in deep water situation. To enable the use of steel wire, it needed a larger diameter which then requires larger drum and larger installation vessel due to its heavy weight. The largest FRDS developed has the capability of installing subsea structure up to 125t at 3000m water depth.

### 5.3.9 Summary

In order to assess methods in installation of the PLEM/PLET, for condition of ultra-deep water, the methods as above are summarized as follows:

**Table 2.2**: The Summary of Different Installation Method at 1450m, 250tonnes Manifold

| Category | FID | Drilling Riser | Wire Cable | SIM | PIM | PBM |
|---|---|---|---|---|---|---|
| **Maximum Water Depth [m]** | >2000 | ~1000 | ~1000 | >2000 | >2000 | ~2000 |
| **Special Vessel needed** | No | Yes | No | Yes | No | No |
| **Maximum lateral displacement [m]** | 26.7 | 16.2 | 8.7 | 12.1 | 6.7 | 9.3 |
| **Vibration amplitude [kN]** | 38.7 | 107.5 | 186.4 | 129.5 | 163.2 | 178.9 |
| **Maximum axial tension [kN]** | 1035.7 | 2369.9 | 2489.9 | 1391.9 | 2017.5 | 2478.4 |

From the table above, the maximum lateral displacement has small range of different in value and the maximum axial tension also has small range of different in value. The significant different is the ability to perform in ultra-deep water where most of the installation method only applicable up to 2000m. For the thesis purposes, the installation method has to able to perform in water depth up to 3000m.

The Floating Installation Device (FID) is considered to be the most applicable method in deploying and installing PLEM/PLET in ultra-deep water. The system is then taken to further study. The technology is already been study by Cao (2016) and compared, thus a different parameters for deeper water depth should be study.

## *5.4. Fiber Rope Deployment System*

In tackling ultra-deep water installation problem, the fiber rope deployment system is considered to be most suitable as it is able to install up to 3000m.

### 5.4.1. Deployment System and Rope Management Process

According to Sverre et.al (2010), the use of fiber rope solve the problem of self-weight of the steel wire when in deep water. The increasing weight of the lifting cable reduces the payload capacity of the lifting line, and increasing the dimension of lifting cable needed, thus increase the force required for the handling system. The solution of using fiber rope which have high strength and relatively small weight in air. The fiber rope is naturally buoyant in water, and the payload capacity only decreases significantly smaller as the water depth increases. The use of small installation vessel as the handling system is small. However, the behavior of the fiber rope is different than steel wire. The fiber rope can be repaired offshore by cutting and splicing new sections. Due to the different behavior of the rope, conventional rope handling system are not applicable for the fiber rope.

### 5.4.2. Handling System

According to Sverre et.al (2010), for the FRDS, the traction unit that is used is Cable Traction Control Unit (CTCU) patented by company ODIN. The CTCU has a traction unit that able to control the tension of the rope on the storage drum. This enable the avoidance of creep and the rope from squeezed into softly spooled layers. The CTCU system has active heave compensation, which reduces the resonant motion of the installation vessel.

There are inboard damping device use to smoothen the tension of the CTCU and storage winch. Upon leaving the CTCU, the rope is guided through the outboard damping device to control the tension and pull limit.

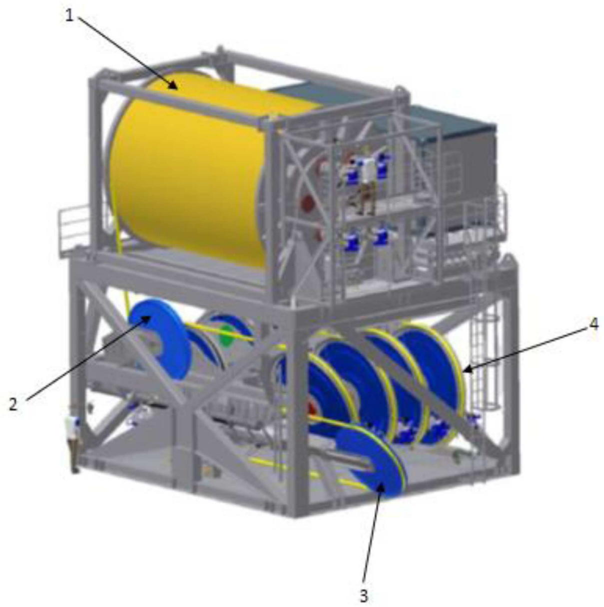


**Figure 2.8:** Fiber Rope Deployment System

Where number 1 is storage drum, number 2 is spooling device, number 3 is inboard damping device and number 4 is cable traction control unit.

## *5.3. Second-End PLEM*

Flow lines and pipelines that end in deepwater must be terminated with hardware that permits connection to other facilities, such as a PLEM to permit connection to other facilities. If the PLEM is installed upon completion of pipelay, the PLEM is termed a "second end" PLEM then the pipeline can be initiated with a first-end PLEM.

### 5.3.1. Static Force Balance of a PLEM

To assess the design of a PLEM, the static force balance of the PLEM is evaluated to predict the behavior of the PLEM during different steps of the installation procedure. For static force analysis, the following simplifications are assumed:

- Dynamic forces due to vessel motions and PLEM lowering movements are negligible.
- Pipe and cable shear loads are negligible. The suspended pipe and cable are modeled as catenaries. This assumption tends to slightly over-predict pipe touchdown bending strain and slightly under-predict pipe top tension.
- The PLEM is always aligned with the centerline of the top of the suspended pipeline.
- Wave and current loads to the PLEM and pipeline are ignored.

When the PLEM mudmat is at the water surface through the splash zone, wave and current loads will cause high flowline stresses at the PLEM bulkhead. Even through the maximum stress is in general below the allowable value, the installation contractor should consider reducing the installation sea state and avoiding pipeline welding or other activities when the PLEM is at the water surface to avoid a girth weld fatigue failure. As the PLEM is positioned deeper, the wave-induced velocity dissipates and steady current becomes the dominant contributor to the hydraulic load. The dynamic effects are negligible.

The relationship of free body forces at the second-end PLEM with a cable in the top and pipe in the bottom during installation is shown in Figure.5-1, Where, $W_s$ is submerged weight of PLEM; $T_{oc}$ is bottom tension of cable; $T_p$ is top tension of pipeline; $\theta_{oc}$ is bottom angle of cable; $\theta_p$ is top angle of pipe.

Summations of forces in the x and y directions are:

$$\sum F_x = T_{oc} \cdot \cos(\theta_{oc}) - T_p \cdot \cos(\theta_p) = 0$$

$$T_{oc} = T_p \frac{\cos(\theta_p)}{\cos(\theta_{oc})} \quad (5\text{-}1)$$

$$\sum F_y = T_{oc} \cdot \sin(\theta_{oc}) - T_p \cdot \sin(\theta_p) = W_s$$

Substitute Eq.5-1 into Eq.5-2, then top tension of pipe is written as follows:

$$T_p = {W_s}\Big/\left[\frac{\cos(\theta_p)}{\cos(\theta_{oc})} \cdot \sin(\theta_{oc}) - \sin(\theta_p)\right] \quad (5\text{-}2)$$

The force vector diagram in Figure.5-1 is a graphical representation of Equations (5-1) and (5-2).

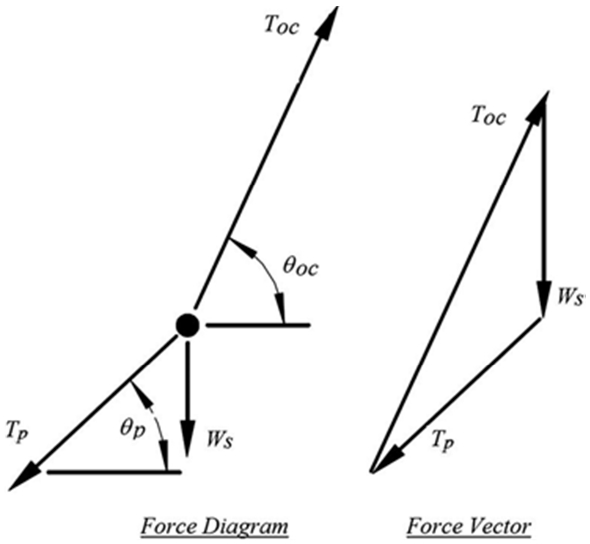


**Figure 5.6:** Static Force Balance of Second-End PLEM [Y. Bai].

### 5.3.2. Bending Load on a Pipe with the PLEM Correctly Oriented

Figure.5-2 shows the forces and moment balances at the pivot point of the second-end PLEM, in which the summary of moments due to forces is resisted by a balancing moment in the suspended pipe, Mpipe. The pipe must be capable of providing the reaction moment without overstressing during the installation procedures.

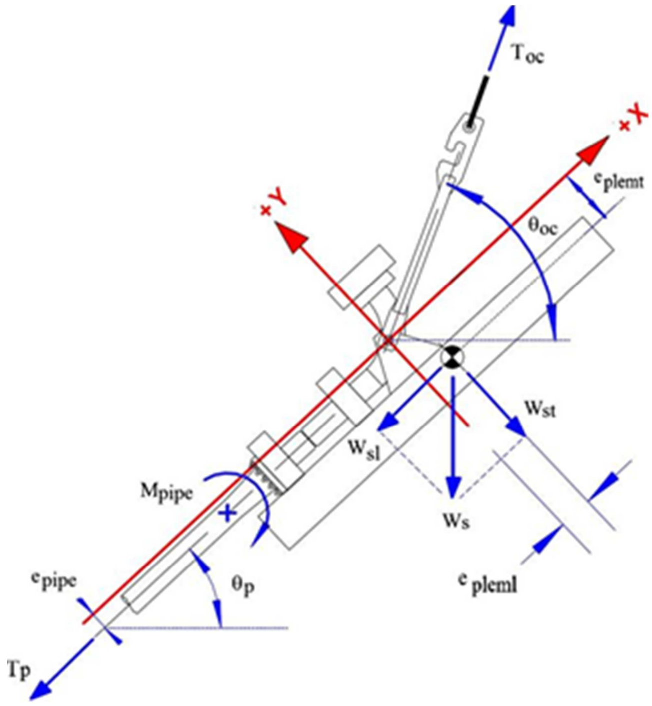


**Figure 5.7:** Forces and Moments Balance at Pivot Point of Second-End PLEM [Y. Bai]

The sum of moments in the PLEM is zero because the only loads considered are vector forces acting through the PLEM pivot. The moments occurring due to eccentricity of forces between the pivot, pipe axis, and PLEM center of gravity are calculated in the following equations:

Moment about the pivot due to pipe top tension is expressed as:

$$M_{tp} = -T_p \cdot e_{pipe} \tag{5-3}$$

Where; $e_{pipe}$ is the pipe eccentricity from the pivot, and is negative here.

Moment about the pivot due to PLEM weight is broken down into two components as follows:

1. Moment due to the transverse weight component times the longitudinal eccentricity:

$$W_{st} = W_s \cdot \cos(\theta_p) \tag{5-4}$$

$$M_{pleml} = W_{st} \cdot e_{pleml} \tag{5-5}$$

Where; $e_{pleml}$ is the PLEM CG longitudinal eccentricity from the pivot, and $W_{st}$ is the transverse component of the submerged weight of the PLEM.

2. Moment due to the longitudinal weight component times transverse eccentricity:

$$W_{sl} = W_s \cdot \sin(\theta_p) \quad (5\text{-}6)$$

$$M_{plemt} = W_{sl} \cdot e_{plemt} \quad (5\text{-}7)$$

Where; $e_{plemt}$ is the PLEM CG transverse eccentricity from the pivot, and $W_{sl}$ is the longitudinal component of the submerged weight of the PLEM.

The reaction at the pivot is a force vector only; a pivot has no moment capacity. There is no moment due to cable tension because it is a vector that never has any eccentricity with respect to the pivot. The total moment about the pivot must sum to zero. Therefore,

$$M_{pipe} = M_{tp} + M_{pleml} + M_{plemt} \quad (5\text{-}8)$$

Pipe bending moments arise from the eccentricity of the pivot from the centerline of the pipe (pipe tension is applied in line with the pipe) and eccentricity of the PLEM CG from the pivot. The bending load on the pipe to balance the moment load about the pivot should be evaluated through the running sequence. The pivot and CG of the PLEM must be located to avoid exceeding the moment capacity of the pipe. To keep the stress of pipe in the allowable range, the pivot should be located above and aft of the PLEM CG and above the centerline of the pipe. At the beginning, the pipe bending moment is dominated by the moment arising from the eccentricity of the pipe centerline from the pivot. At the end, the pipe reaction moment is dominated by the moment arising from the longitudinal eccentricity of the PLEM CG from the pivot.

The durability of the system can be increased by fitting the PLEM with a tailpiece of heavy wall pipe (one or two joints), which will have greater moment capacity either to increase the safety factor or to allow greater eccentricity of the pivot. The moment force on the pipe from Equation (20-18) is conservative because deflection of the pipe due to the moment force tends to reduce the pipe eccentricity and that in turn reduces the moment load on the pipe.

### 5.3.3. Righting Torsion with the PLEM Misoriented by 90 Degrees

It is essential for the PLEM to land in the correct orientation, which is ensured by designing a PLEM with a righting torsion to force the unit upright as it approaches the seabed if it does not land in the correct orientation. Righting torsion is zero when the PLEM is correctly oriented and a maximum when the PLEM is misoriented by 90 degrees. In this section, the PLEM is assumed to be out of orientation a full 90 degrees to calculate the maximum righting torsion.

Figure 5-3 illustrates the PLEM rotated 90 degrees out of correct orientation in which the righting torsion is applied. Two forces act to rotate the PLEM upright:

- The transverse component $W_{st}$ of the PLEM's submerged weight, $W_s$. The yoke weight should be included in the PLEM submerged weight and the CG calculations.
- The transverse component $T_{oct}$ of A&R cable bottom tension $T_{oc}$, an upward force applied at the yoke lift eye.

The axis for the righting torsion is the centerline of the pipe. Only transverse load components $W_{st}$ and Toc time their eccentricities to contribute to the righting torsion. Longitudinal loads do not contribute to the righting torsion. The value of $W_{st}$, the transverse component of PLEM submerged weight, is taken from Equation (5-1).

The transverse component of cable tension is:

$$T_{oct} = T_{oct} \cdot \sin(\theta_{oc} - \vartheta_p) \qquad (5\text{-}9)$$

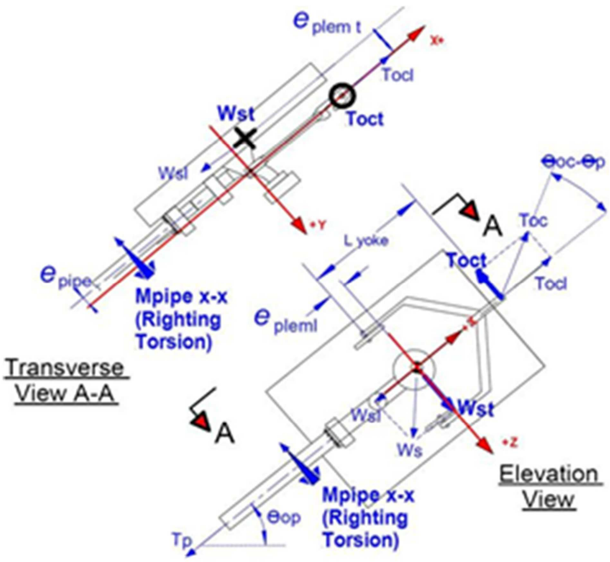


**Figure 5.8:** Righting Torsion for PLEM that is disoriented by 90 degrees [Y. Bai]

The righting torsions about the pipe axis are:

$$M_{pipe\ x-x\ plem} = W_{st} \cdot (e_{plemt} - e_{pipe}) \quad (5\text{-}10)$$

$$M_{pipe\ x-x\ cable} = T_{oct} \cdot e_{pipe} \quad (5\text{-}11)$$

$$M_{pipe\ x-x} = M_{pipe\ x-x\ plem} + M_{pipe\ x-x\ cable} \quad (5\text{-}12)$$

where $T_{oct}$ is the cable bottom tension, transverse component, and $M_{x-x}$ is the pipe torsional moment. Note that the transverse loads and consequently the righting torsion are small when the pipe end is near vertical. It is not unusual for a PLEM to rotate one or more times during the descent. The x-x subscript indicates that the axis of the moment is parallel to the x axis of the PLEM.

Righting torsion can be increased by increasing the PLEM weight and increasing the transverse eccentricityof the CG. The most efficient wayof doing this is to add the thickness of the mudmat. To adjust the longitudinal location of the PLEM CG, the fore and aft plates can be of different thicknesses. Increasing the pivot eccentricity from the pipe centerline is usually not an option because pipe bending stress at the start of the installation is dominated by the contri-bution of Tp. epipe as shown in Equation (5-13). In deep-water situations, the PLEM's submerged weight is always much lower than initial top-of-pipe tension, so there is more scope to change the eccentricity of the PLEM CG.

The yoke's lateral load is also at a maximum when the PLEM is misoriented by 90 degrees. The lateral design load for the yoke and pivots is expressed as:

$$F_{yoke-lateral} = T_{oct} \quad (5\text{-}13)$$

### 5.3.4. Bending Load on a Pipe with PLEM Misoriented by 90 Degrees

Figure 5-4 illustrates the 90-degree misoriented case, in which the moment in the pipe is different from that in the correctly oriented running case.

The bending moment due to cable eccentricity is:

$$M_{pipe\ \gamma-\gamma\ (90\ degree\ out\ oof\ orientation)} = W_{st} \cdot (L_{yoke} - e_{pleml}) \quad (5\text{-}14)$$

Shortening the yoke length can reduce this moment load. However, a long yoke is beneficial at the end of the lowering sequence when the yoke lifts.

Force couples due to pipe eccentricity, and PLEM CG eccentricity from the yoke still exists in the x-y plane. The moment z-z due to pipe eccen-tricity from the yoke pivot is the same as previously noted in Equation (5-12):

$$M_{pipe\ z-z\ (top\ tension)} = -T_p \cdot e_{pipe} \tag{5-15}$$

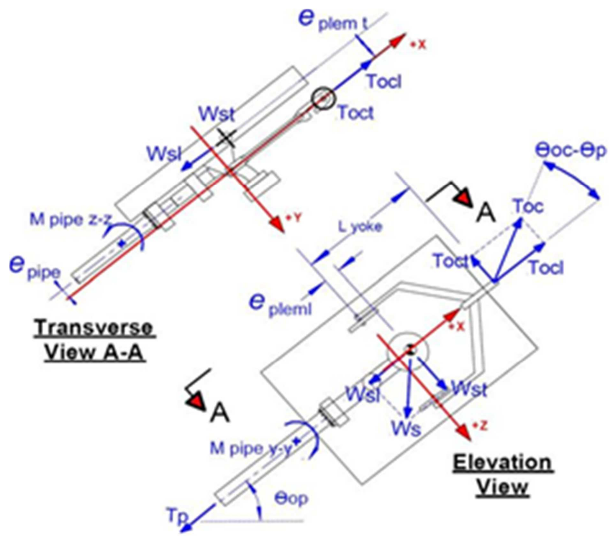


**Figure 5.9:** Pipe moments for PLEM which is disoriented by 90 degrees

The moment z-z due to the longitudinal component of sled weight is:

$$M_{pipe\ z-z\ (plem)} = -W_{st} \cdot e_{plemt} \tag{5-16}$$

The total moment z-z is:

$$M_{pipe\ z-z} = M_{pipe\ z-z\ (top\ tension)} + M_{pipe\ z-z\ (plem)} \tag{5-17}$$

The combined pipe moment with the PLEM running 90 degrees misor-iented is the vector sum of the z-z and y-y moments:

$$M_{pipe\ (90^0 misoriented)} = \sqrt{M_{Z-z}^2 + M_{Y-Y}^2} \tag{5-18}$$

This equation can be used to determine when the lowering should be stopped if the PLEM is out of orientation and the yoke has failed to lift. If the PLEM does not right, the situation must be reviewed with particular attention paid to actual CG location, uprighting torsion calculations, and pipe torque. If pipe torque is the problem, the PLEM is best recovered and the PLEM reoriented about the pipe.

### 5.4. First-End PLEMs

Figure 5.10 illustrates a first end PLEM, which can be recognized as a variant of a second-end PLEM in that the yoke and mudmat functions are combined.

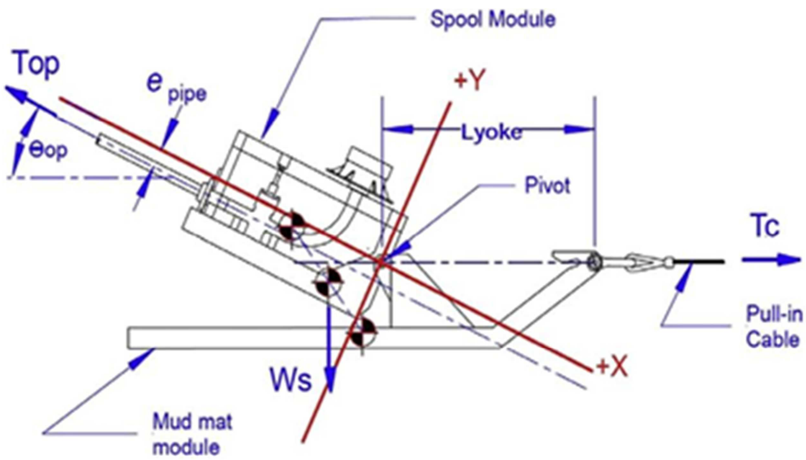


**Figure 5.10:** First End PLEM [Y. Bai]

A typical installation procedure for the first-end PLEM is:

- Preinstall pull-in pile and lay cable out to an accessible stand-off location.
- At the standoff location, lower the PLEM on the pipe.
- Connect the pull-in cable to the PLEM.
- Pull the PLEM into position while adding pipe and maintaining the PLEM clearance from the seabed.

With the pull-in cable pulling horizontally, the static forces acting at the PLEM are as shown in Figure 5-5. The forces in Figure 5-5 are analogous to Figure 5-6 for the second-end PLEM except the pipe and cable have swapped positions. The equations are:

$$\sum F_x = T_{oc} - T_p \cdot \cos(\theta_p) = 0 \quad (5\text{-}19)$$

$$\sum F_y = W_s - T_p \cdot \sin(\theta_p) = 0 \quad (5\text{-}20)$$

The force vector polygon in Figure 5-6 is a graphical representation of Equation.5-19 and

Equation.5-20. There is only one solution for pipe bottom tension and pipe bottom angle in this state of equilibrium. The equations for pipe bottom tension and pipe bottom angle are expressed as follows:

$$T_{op} = \sqrt{T_{oc}^2 + W_s^2} \quad (5\text{-}21)$$

$$\theta_p = arctan\left(\frac{W_s}{T_{oc}}\right) \quad (5\text{-}22)$$

Fixing these two variables in turn defines the suspended pipe span. The suspended pipe span can be solved using catenary equations. The analysis is carried to the conclusion of the pull-in by decreasing the PLEM submerged weight Ws in steps once the PLEM is over the target location. When the cable bottom tension is equal to the pipe bottom tension, then normal pipelay has been achieved.

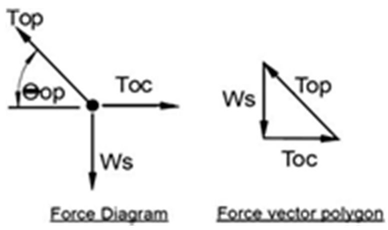


**Figure 5.11:** First-End PLEM Static Forces [Y. Bai]

## *5.5. Stress Analysis Of PLEM*

Pipe outer surface stresses due to the bending moment loads can be calculated using the following formula:

$$\sigma_{bending} = \frac{M \cdot D}{2L} \quad (5\text{-}23)$$

where $M$ is the moment, $L$ is the moment of inertia for pipe section, and $D$ is the pipe outer diameter.

Pipe stress resulting from pipe-top tension is shown as:

$$\sigma_{tension} = \frac{T}{A_s} \quad (5\text{-}24)$$

Pipe stress due to hydrostatic pressure is compressive:

$$\sigma_{hydrostatic} = \frac{P_e \cdot A_e}{A_s} \quad (5\text{-}25)$$

Where; $P_e$ is the pipe external pressure (hydrostatic pressure); $A_e$ is the external area of the pipeline, $A_e = \frac{\pi D^2}{4}$; and $A_s$ is the pipeline cross-section area of steel.

The maximum pipe outer surface stress in the pipe is the sum of all three of the above stresses:

$$\sigma_{pipe} = \sigma_{bending} + \sigma_{tension} + \sigma_{hydrostatic} \quad (5\text{-}26)$$

## *5.6. Crane Analysis*

Static equilibrium of crane can be defined with the following two equations:

$$\vec{F}_{net} = \vec{0}$$

$$\vec{\tau}_{net-0} = \vec{0} \quad (5\text{-}27)$$

Equation 5-27 can be written as zero vectors in x, y and z directions as follows:

$$F_{net-x} = 0,\ F_{net-y} = 0,\ F_{net-z} = 0 \quad (5.28)$$

Now we have three scalar equations. These essentially say that for an object in equilibrium, the forces in all three directions must each add up to zero Newtons. Technically, it could still be moving at a constant speed, but we call that equilibrium.

Torque also is a vector (technically). However, 3-D torque is a bit complicated so introductory physics textbooks usually stick to cases that are two-dimensional with the torque about some fixed axis (labeled "o"). In this case, torque can be calculated as (the scalar torque):

$$\tau_o = \tau\, F\ \sin\theta \quad (5.29)$$

In this definition, r is the distance from the point "$o$" to the location that a force is applied to some rigid object. F is the magnitude of this force and $\theta$ is the angle between the force and r. If a torque would make the object rotate counter clockwise be positive torque and the clockwise torques would then be negative.

So, in two dimensions we really just have the three following equations:

$$F_{net-x} = 0, \ F_{net-y} = 0, \ \tau_{net-o} = 0 \tag{5.30}$$

It's important to notice that for an object in equilibrium, it doesn't matter where the point "$o$" is for the net torques.

**Force on the Piston**

In order to look at forces are acting on this arm, therefore sketch of the crane arm with all the forces on it should be explained as shown below.

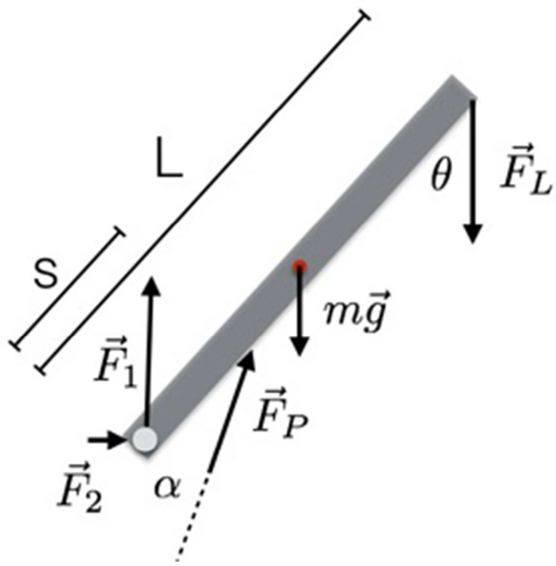


**Figure 5.12:** Forces are acting on crane's arm

Here are some notes:

- It is assumed the location of the center of mass is at $L/2$.
- The distance from the point where the piston pushes to the pivot point (at the bottom) is labeled "$s$".
- The pivot point can push both vertically and horizontally.

- $\alpha$ is the angle between the piston and the arm and $\theta$ is the angle between the vertical forces and the arm. θ is also the angle that the arm is tilted.

Now It can be written down two force equilibrium equations in the horizontal direction "$x$" and the vertical "$y$".

$$F_{net-x} = F_2 + F_p \sin(\alpha + \theta) = 0$$
$$F_{net-y} = F_1 + F_p \cos(\alpha + \theta) - mg - F_L = 0 \quad (5.31)$$

The direction of force $F_2$ is the right in which will be negative value for $F_2$. For the net torque equation, it is needed to first pick a point about which to calculate the torque. Any point should work, but the easiest thing is to choose the pivot point at the bottom of the crane. With this as my torque point, both $F_1$ and $F_2$ contribute zero torque since the distance from the force to the point is zero. This gives the following torque equation.

$$\tau_{net-o} = F_p s \sin\alpha - mg\left(\frac{L}{2}\right)\sin\theta - F_L L \sin\theta = 0 \quad (5.32)$$

Here we can see why the piston is so important. There are three forces that exert a torque about point o, but only one of them is in the counter clockwise direction—that from the piston. So this force has to create a torque to balance both the torque due to the weight of the arm and due to the load. This torque equation for the force from the piston (maybe piston isn't the correct technical term, but now it's too late).

$$F_p = \frac{mg(L/2)\sin\theta + F_L L \sin\theta}{s \sin\alpha} \quad (5.33)$$

# Chapter.6

# 6.0 Shallow-water PLEM Installation

## *6.1. Installation of PLEM and Mooring Base*

The Bualuang Field lies approximately 120km northeast of the town of Songkhla, Thailand at block B8/38 which lies 60km west of the Chevron-operated gas/condensate and oil fields. The water depth is approximately 60m. The Bualuang field was discovered in 1992 and subsequently appraised by two further wells in 1997. The initial development wells, Bualuang 05 and 01, were drilled and logged to true vertical depths of 1,220m and 1,270m, respectively

The jackets for the the Bualuang field were engineered by WorleyParsons [Offshore]

The jackets, topside (pictured), pipelines and moorings for the Bualuang field's FPSO were installed by Lewek Champion [Offshore]

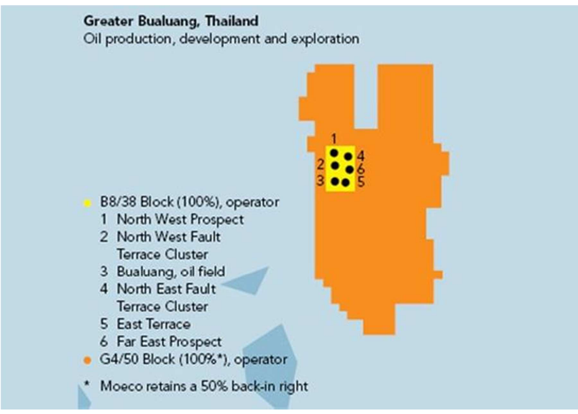


The Bualuang installed platform [Offshore]

**Figure 6.1:** Bualuang Field Development

The first stage Bualuang Field Development Project intends to install a single four leg platform (BLWPA) producing to a FPSO via 10” subsea pipeline. Expected crude oil production when wellhead platform is online is approximately 15,000 BOPD. Target first oil production is early 2008. Figure 6.2 shows the installation procedure of PLEM and Mooring base.

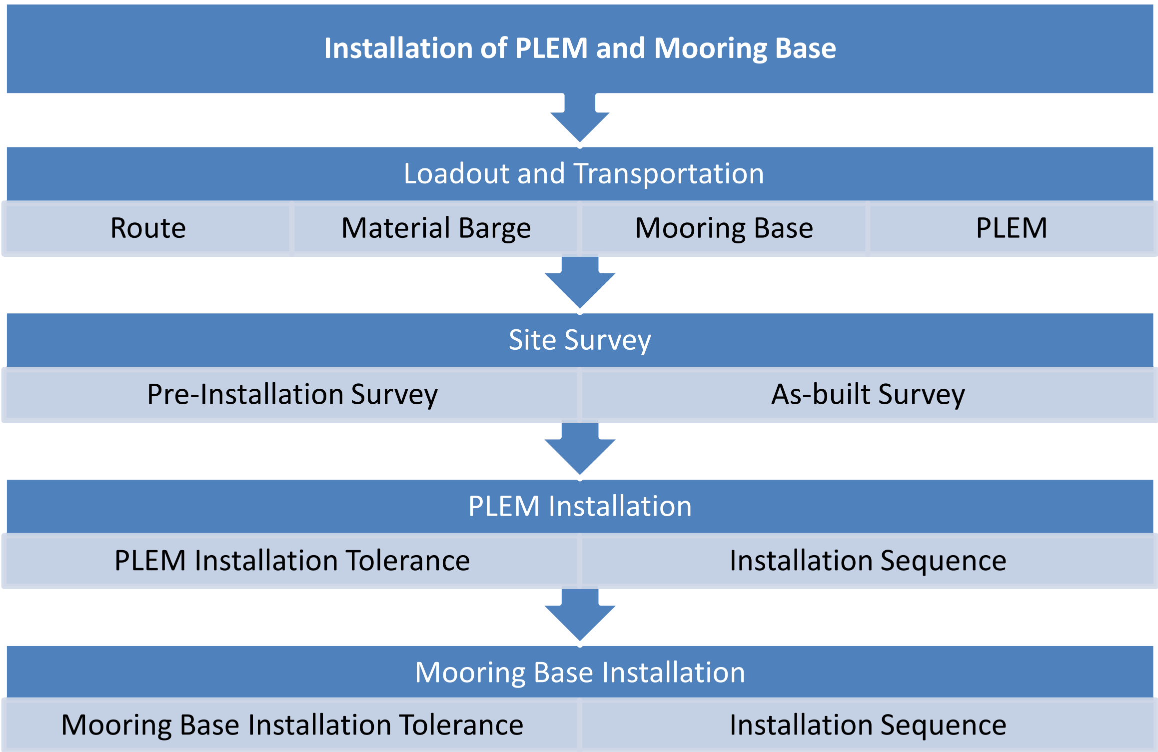


**Figure 6.2:** Installation Procedure of PLEM and Mooring Base

## 6.1.1. Loadout and Transportation

The loadout and transportation consist of route, material barge, mooring base and PLEM analysis. Three lifting slings shall be preinstalled onshore to lifting points on the Suction Pump Unit (SPU). A single 55m long 82m dia IWRC sling shall be rigged to the three slings preinstalled onto the SPU offshore. This arrangement will avoid wetting the crane block during PLEM installation. The spool installation rigging shall double as the installation for the PLEM. This rigging shall be rigged up just prior to PLEM installation. The lift rigging shall be approx 65 m long to avoid wetting the crane whip block. For stability of the towing condition and ease of offshore installation the Mooring Base will be loaded out on the bow port side of the Maritime Might.

### 6.1.2. Site Specific Survey

#### 6.1.2.1. Pre-Installation Survey

A pre-engineering survey has been conducted by GFI and is available for use. The survey has shown that there are no obstructions on the seabed that will affect the work. Upon setup of Lewek Champion, an ROV video tape pre-installation debris (50mx50m) survey shall be conducted to ensure installation site is free of debris & that there are no obstructions

#### 6.1.2.2. As-Built Survey

Subsequent to completion of the Mooring Base and PLEM a level and dimensional survey (where applicable) will be undertaken by the surveyors. The final measurements, dimensions and level will be presented to the client in the as-built dossier. The following as-built surveys are to be conducted:

##### *6.1.2.2.1. Mooring Base Survey*

The important data for the jacket are;

1. Mooring Base Level
2. Mooring Base Position & Orientation
3. Elevation of Mooring Base with respect to seabed

##### *6.1.2.2.2. PLEM Survey*

The important data for the topside are;

1. PLEM Level
2. PLEM Position and Orientation
3. Eleation of PLEM with respect to seabed

##### *6.1.2.2.3. Seabed Debris Survey By Rov Post Installation.*

Upon completion of the Mooring Base and PLEM, an ROV debris survey will be conducted to ensure that the area has been covered and no major items have been left at the vicinity of the respective installation site.

### 6.1.3. PLEM Installation

The PLEM will be lifted off the Maritime Might moored on the Port side of the Lewek Champion and slewed across the pipe tunnel and placed into the water on the starboard side. The piping of the PLEM and all uncapped tubing shall be allowed to free flood as they are lowered into the water. Once submerged, the PLEM will be lowered to the seabed and set down using USBL beacons and ROV to monitor position and orientation. A spreader located 65 m above the PLEM will be used to control orientation of the PLEM. Once set down on seabed, the extendable legs on the PLEM shall be engaged. The Installation tolerances for the Mooring base are as follows:

- Position Tolerance ia 3 m from as installed position of Mooring Base
- Orientation Tolerance is $3^0$ from as installed orientation of Mooring Base

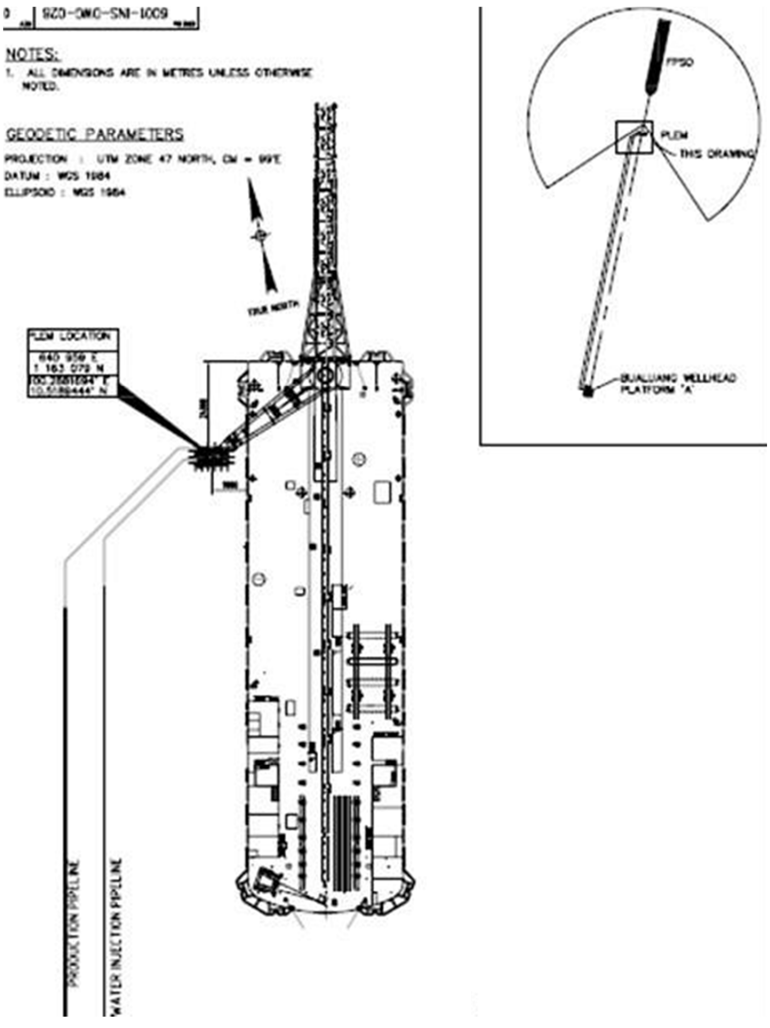


**Figure 6.3:** PLEM Installation using barge

### 6.1.4. Mooring Base Installation

The SPC will be fitted with the SPU onshore at the loadout site. During PLEM installation, the SPC will be lifted with the SPU connected to the lift rigging. The structure will be lifted off the Maritime Might moored on the Port side of the Lewek

Champion, slewed over the pipe tunnel to the starboard side deck. The SPU umbilical hoses will be fitted to the SPU before lowering into the water. The pump valves on the SPU will be open fully to allow venting of the pile cans as they are lowered into the water. Once submerged, the structure will be lowered to the seabed and set down using USBL beacons and ROV to monitor position and orientation. Once set down on seabed, the suction pump units will be engaged and the SPC set into the seabed. Installation tolerances for the Mooring base are as follows:

**Table 6.1**: Installation tolerances for Mooring base

| Description | Values |
|---|---|
| Position Tolerance | 1 m |
| Elevation Tolerance | +1.0 m / -0.0 m |
| Orientation Tolerance | ± 3 degrees |
| Levelness Tolerance Between centre of pile cans | ± 1.4” (35.65mm) |
| Target Penetration | 4.5 m below mudline |

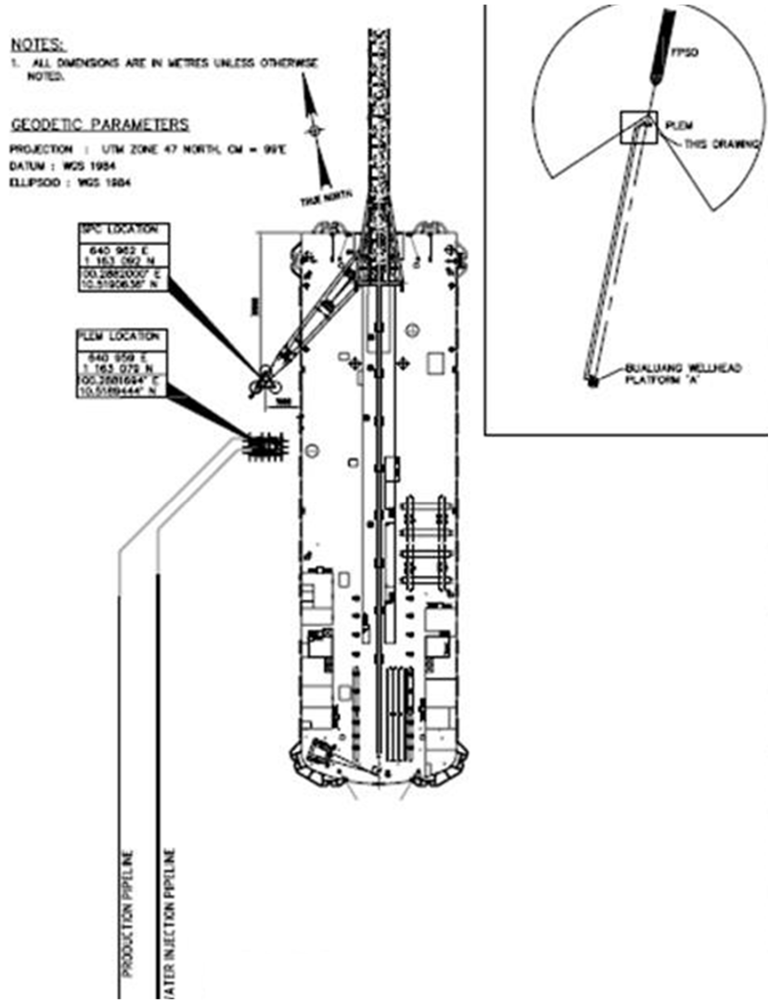


**Figure 6.4:** Mooring Base Installation using barge

## *6.2. Installation of PLEM and Tie-In of Expansion Spools*

Subsea jumper spool is a short length pipe which is function for connectiion of a subsea pipeline and a riser to subsea structure. Satellite wells positioned some distance from the central manifold may be Tied-in by use of rigid or flexible subsea jumper spools. The subsea jumper spools may also connect other subsea structures such as PLEM/PLETS and Riser Bases. The subsea jumper spools have a vertical or a horizontal Collet connector at each end. Installation of these spools is done by a simple crane operation assisted by ROV and guide wires when required. Figure shows the arrangement of PLEM and 2 expansion spools.

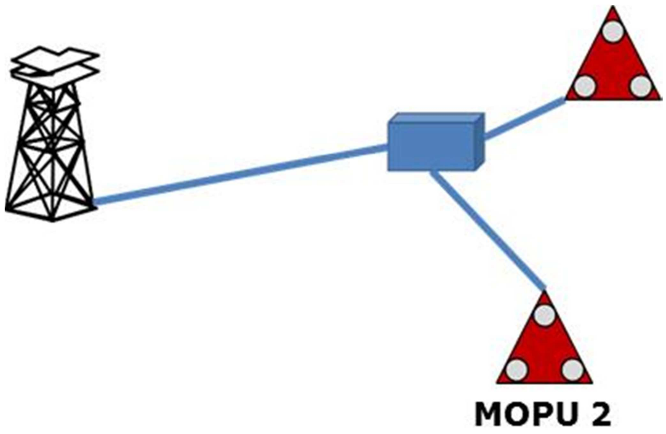


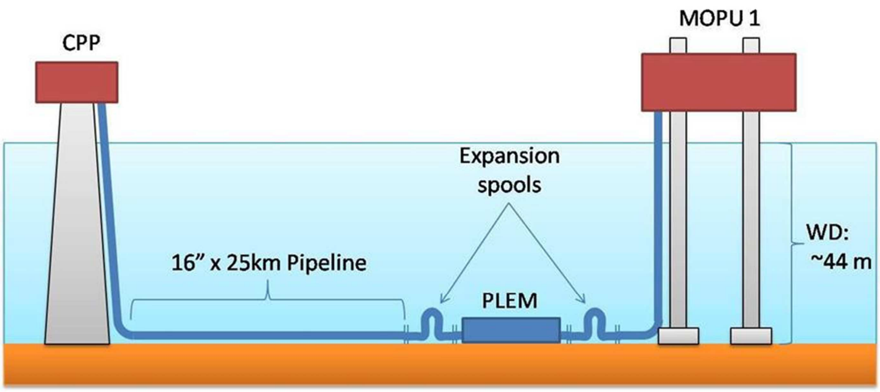


**Figure 6.5:** Arrangement of PLEM and two expansion spoools [Zamri]

### 6.2.1. Installation Barge

- DP DLB Lewek Champion
- 358 person accommodation
- 1 x 800MT main crane
- 2 x 30MT secondary crane
- Dynamic Positioning with 6 Azimuth thrusters (max thrust 378.7kN)


**Figure 6.6:** Installation barge used for PLEM installation [Zamri]

### 6.2.2. Design of PLEM

Design of PLEM as shown in Figure 6.7 and dimension of the PLEM as follows:

**Table 6.2**: Dimension of PLEM installation

| Description | Values |
|---|---|
| Designed Weight | ~ 70 MT |
| Dimension | 14m x 6m |
| Water Depth | 114ft (43.9m) |

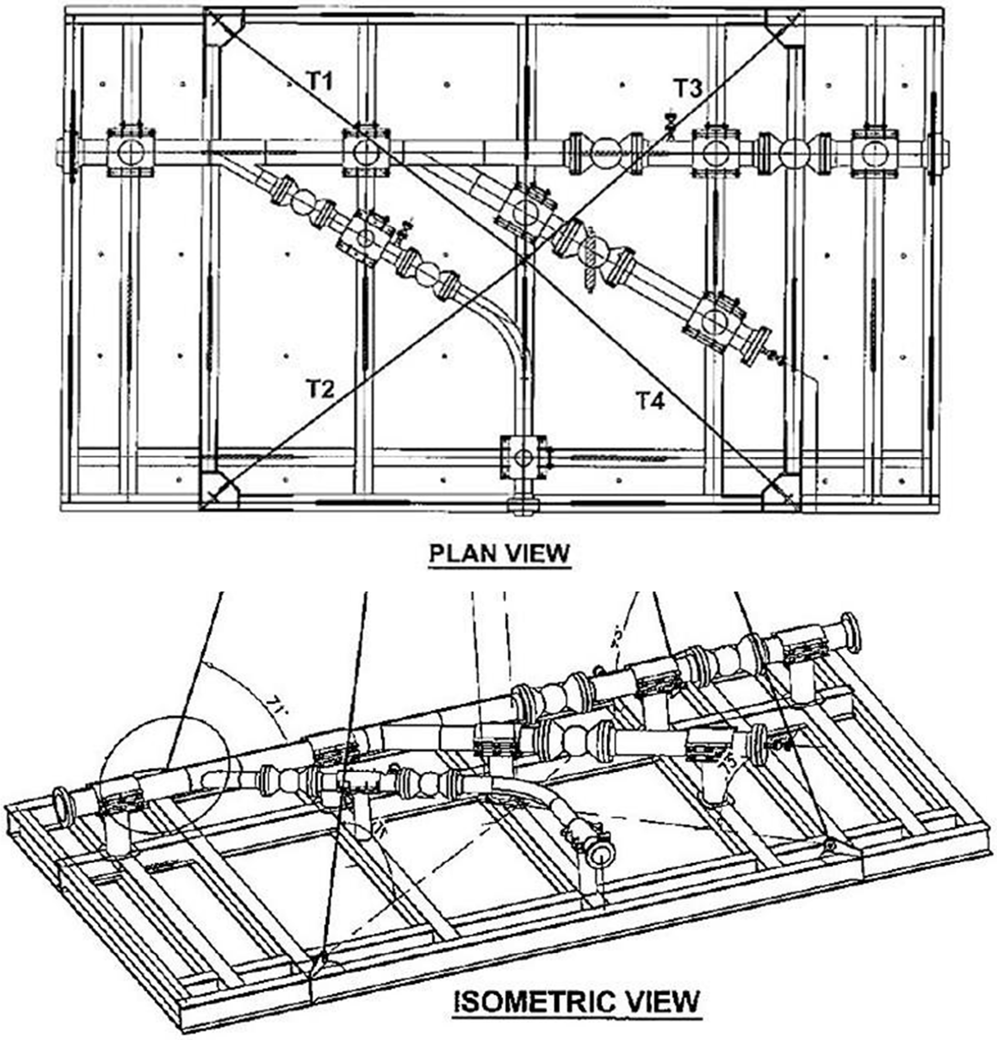


**Figure 6.7:** Plan and isometric views of PLEM design [Zamri]

### 6.2.3. Installation of PLEM

Installation of PLEM was using crane as shown below

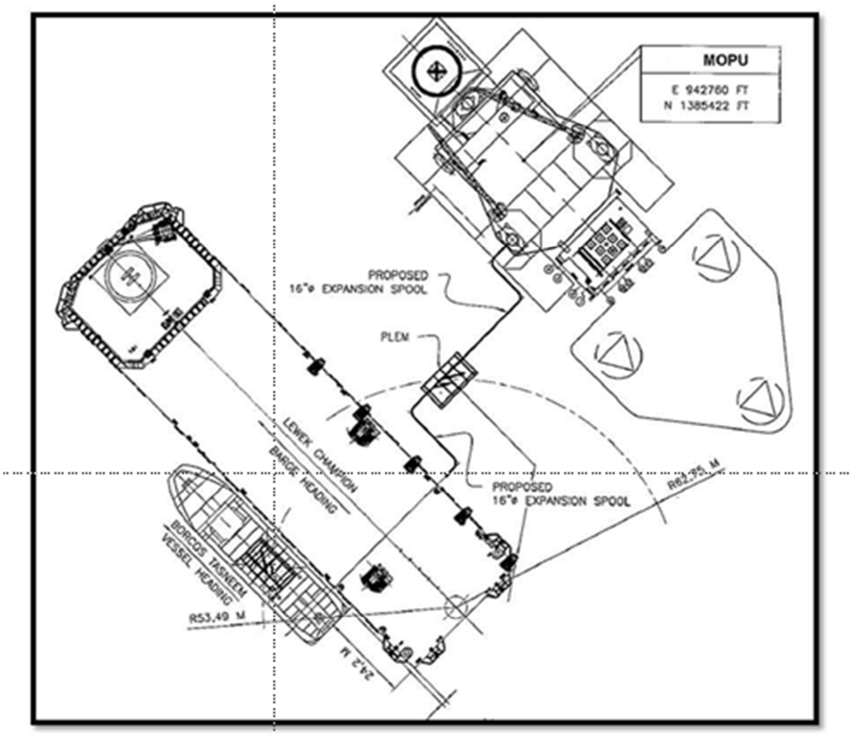


Barge setup for PLEM installation

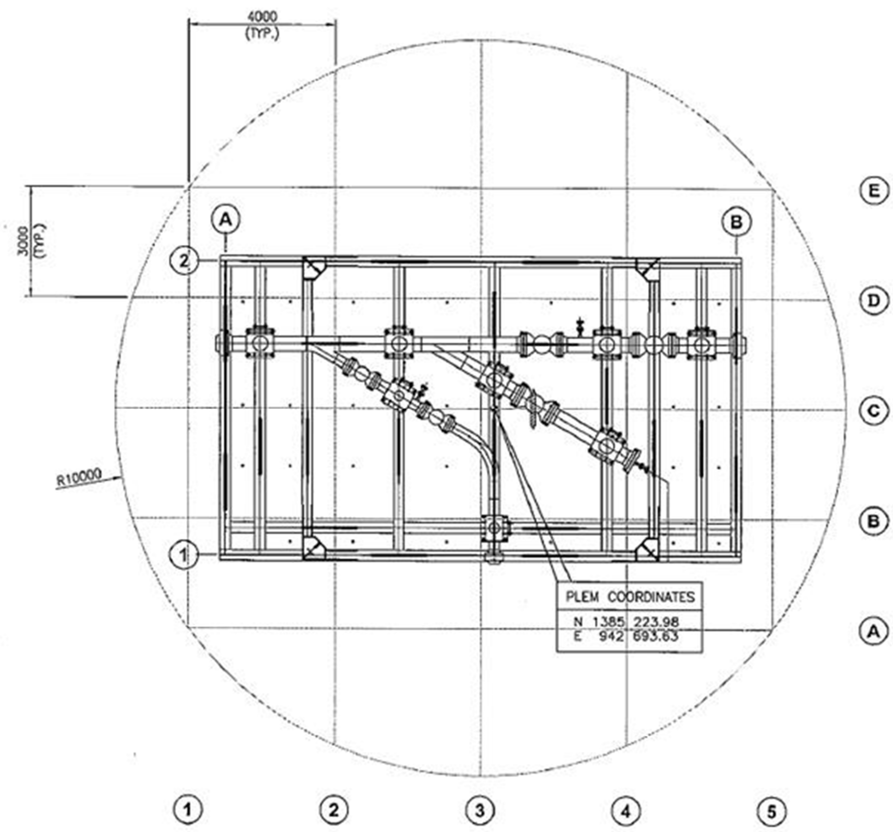


PLEM footprint and debris survey

**Figure 6.8:** Barge setup and PLEM footprint for installation [Zamri]

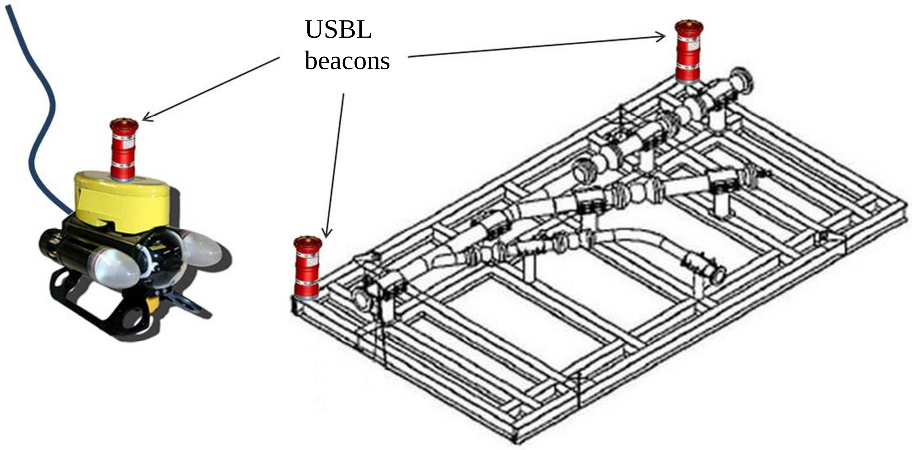


**Figure 6.9:** Pre-installation of PLEM [Zamri]

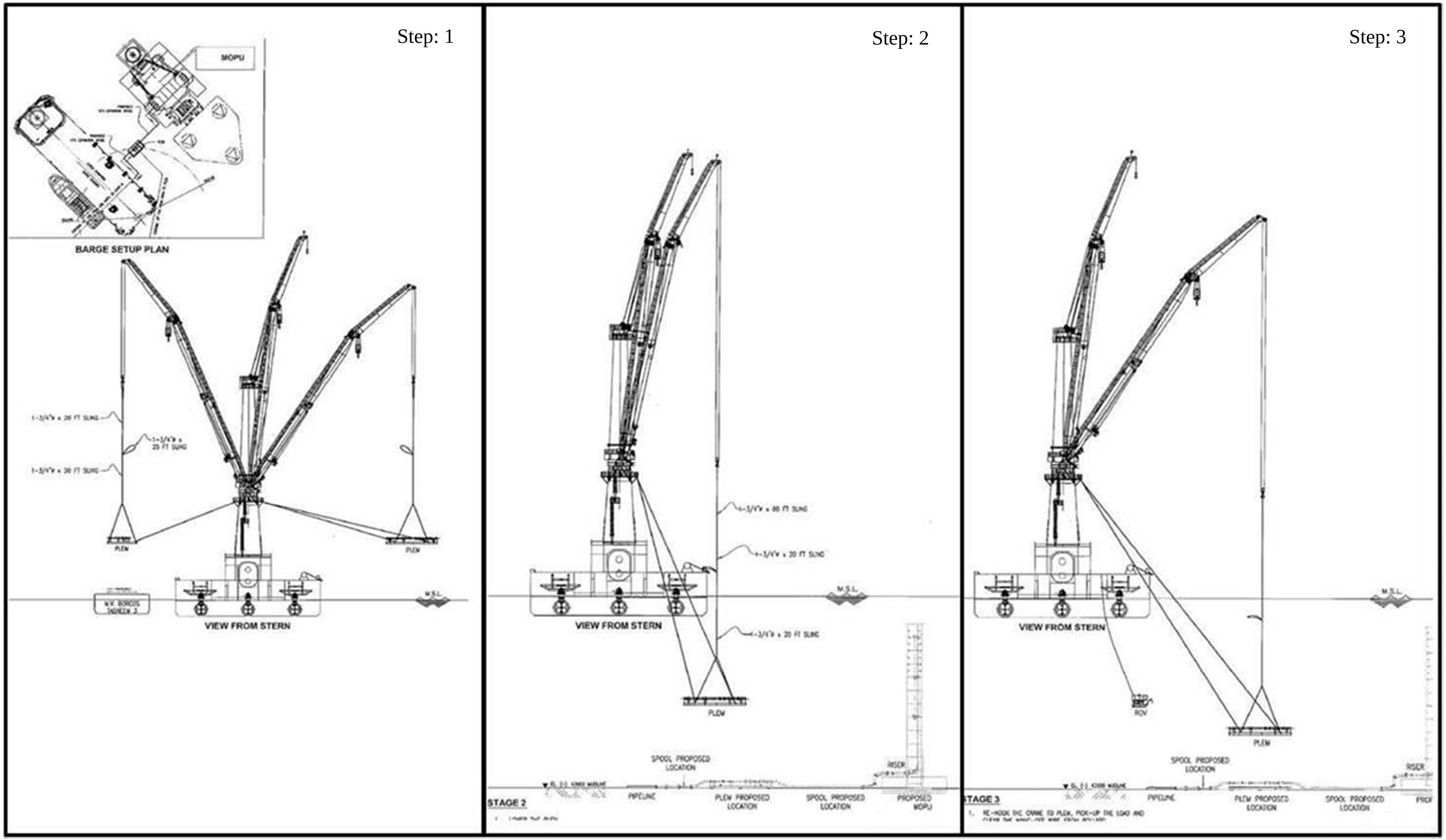
Step: 1
MOPU
BARGE SETUP PLAN
PLEM
PLEM
VIEW FROM STERN
M.S.L.
Step: 2
VIEW FROM STERN
M.S.L.
PLEM
SPOOL PROPOSED LOCATION
RISER
STAGE 2
PIPELINE
PLEM PROPOSED LOCATION
SPOOL PROPOSED LOCATION
PROPOSED MOPU
Step: 3
VIEW FROM STERN
M.S.L.
ROV
PLEM
SPOOL PROPOSED LOCATION
RISER
STAGE 3
PIPELINE
PLEM PROPOSED LOCATION
SPOOL PROPOSED LOCATION

**Figure 6.10:** Installation of PLEM from barge using crane [Zamri]

### 6.2.4. Expansion Spools

Design of Spools as shown in Figure 6.8 and dimension of the spools as follows:

- 16” diameter
- Full Well Stream (FWS)

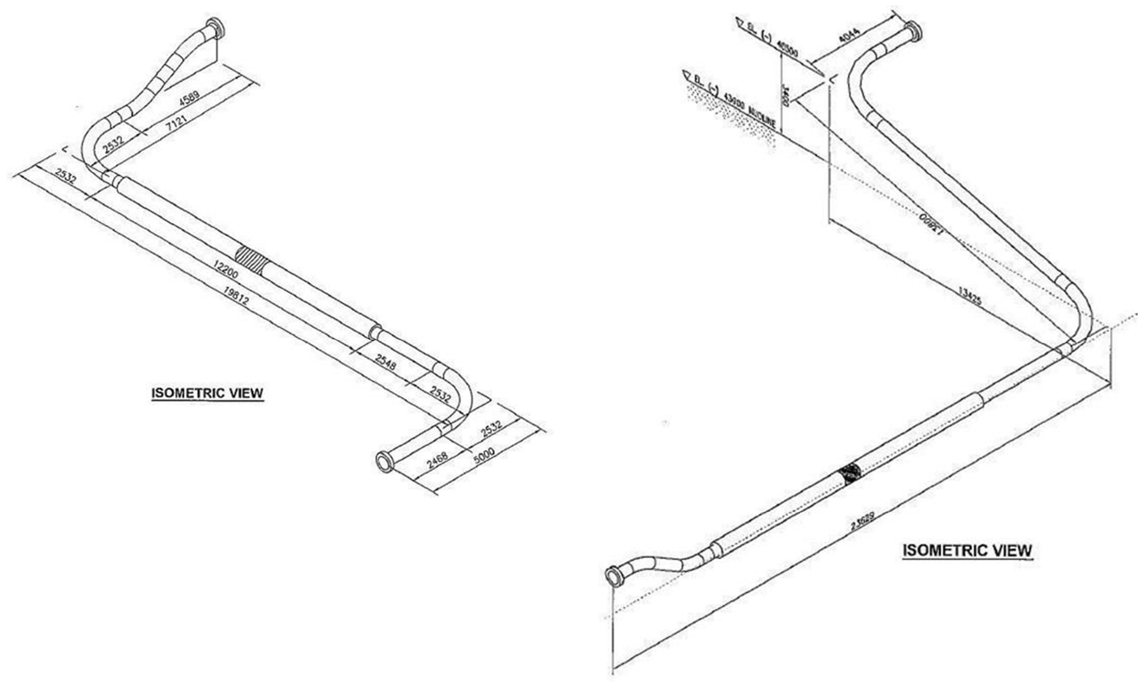


Expansion Spool at Pipeline / PLEM

Expansion Spool at PLEM / MOPU

**Figure 6.11:** Isometric view of Spools design [Zamri]

## 6.2.5. Installation of Spools

Installation of spools were using crane as shown below

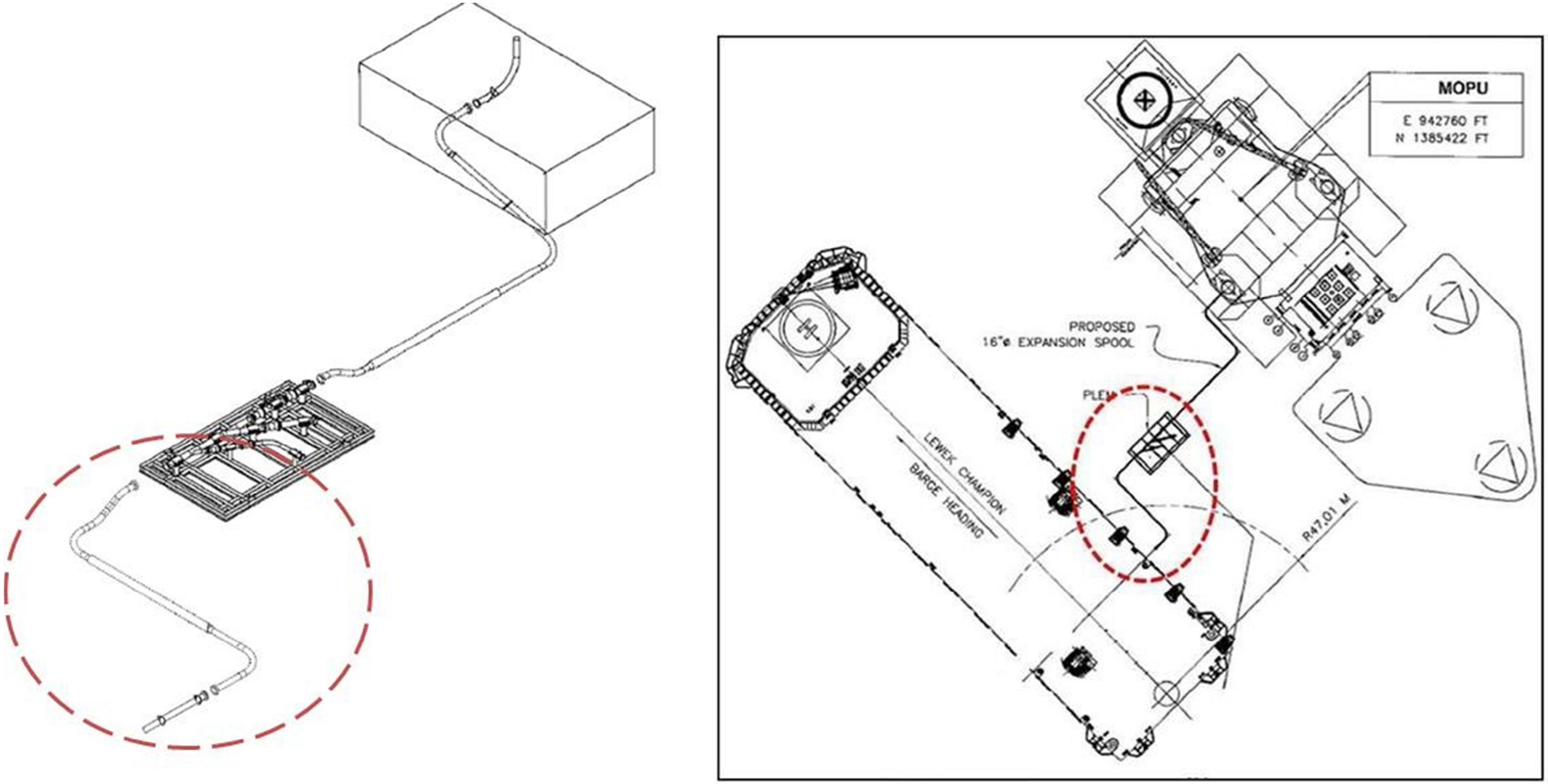


**Figure 6.12:** Barge Set-Up for Pipeline / PLEM Spool Installation [Zamri]

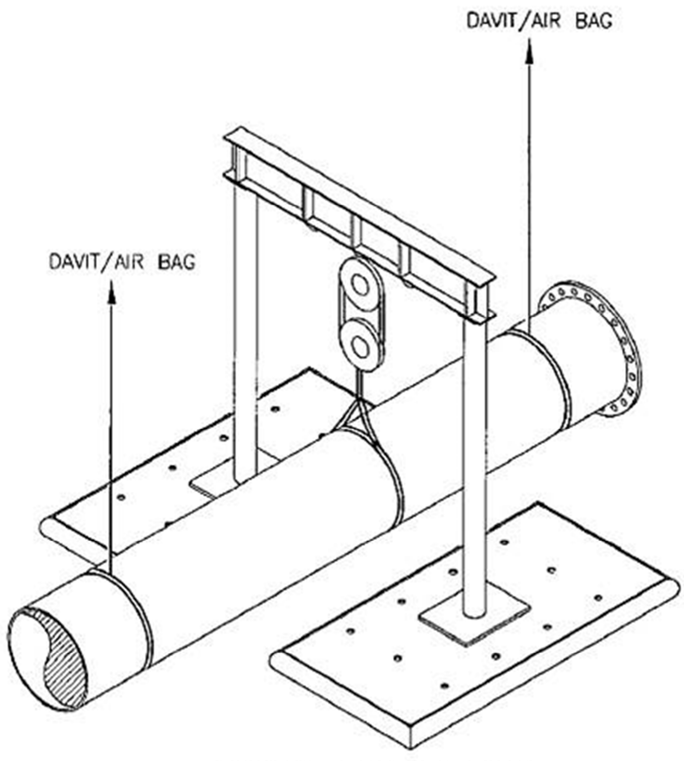


**Figure 6.13:** Pipeline on an A Frame from isometric view [Zamri]

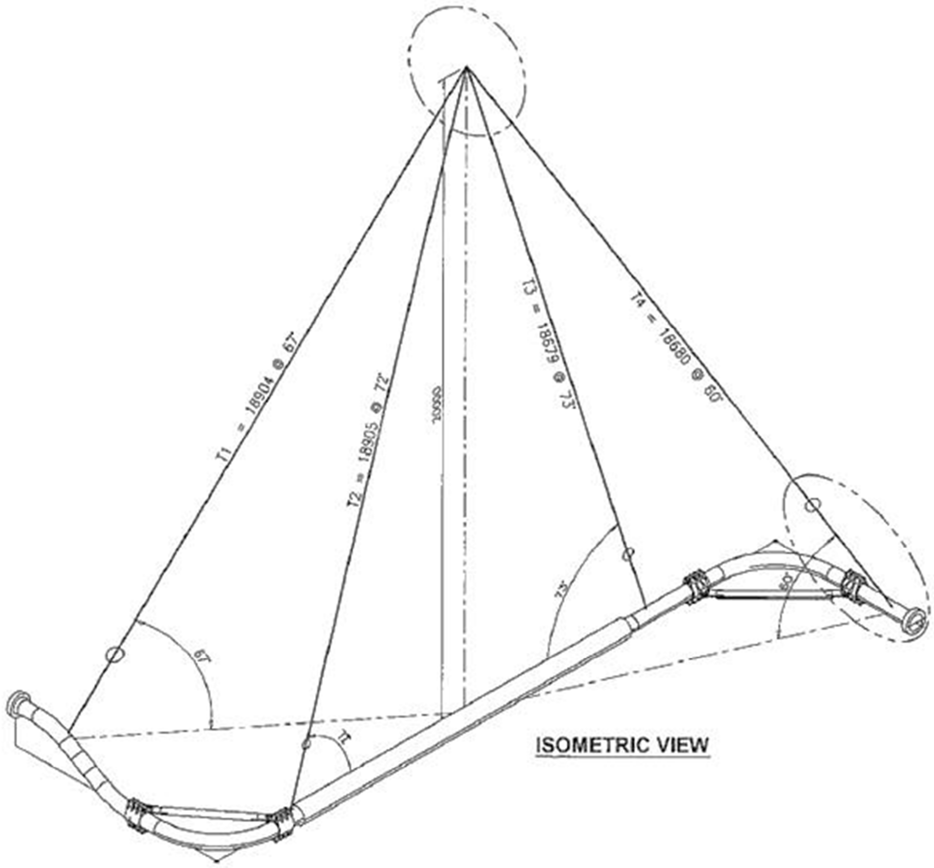


**Figure 6.14:** Lifting Riggings on Expansion Spool [Zamri]

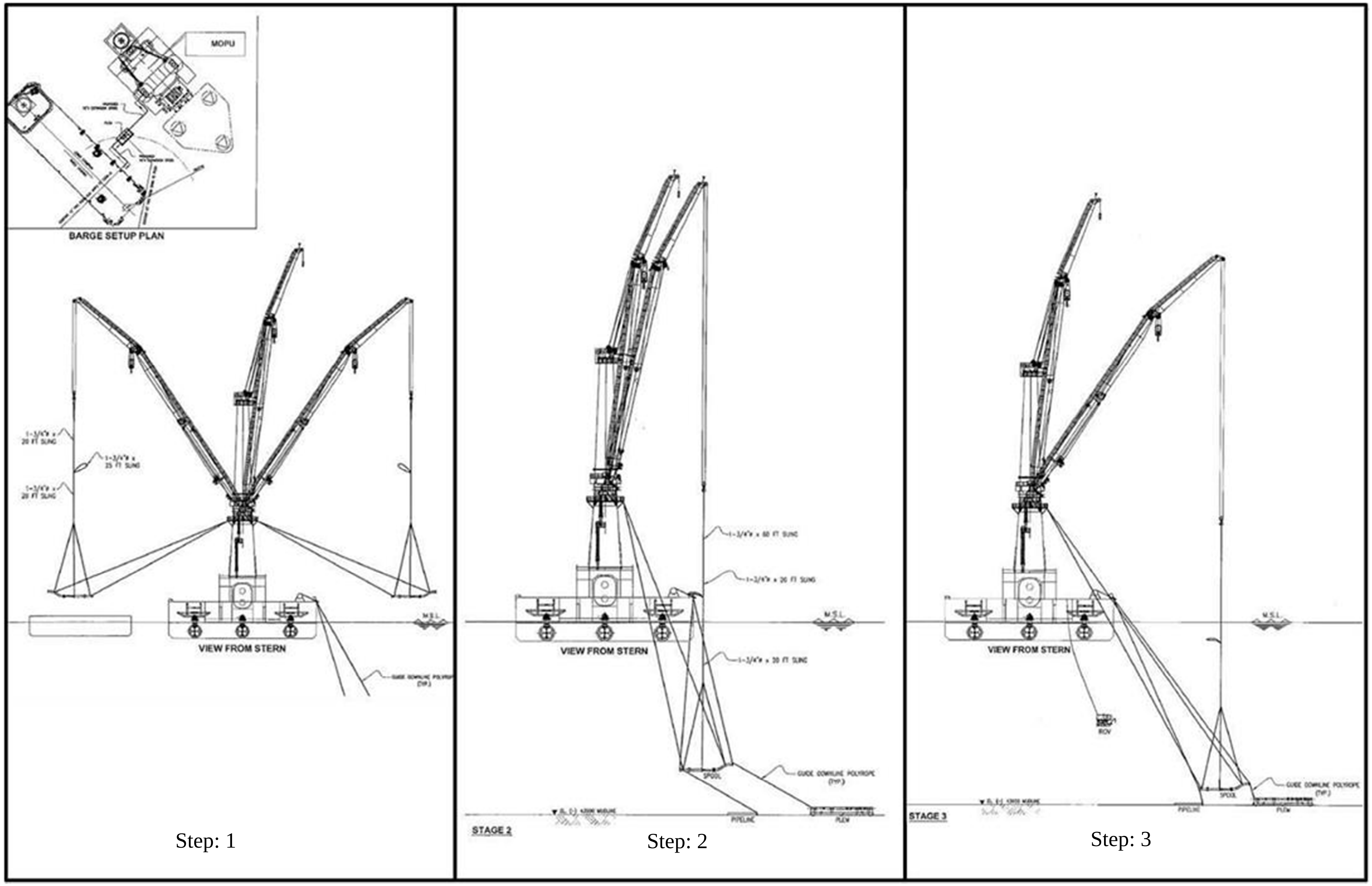


Step: 1 Step: 2 Step: 3

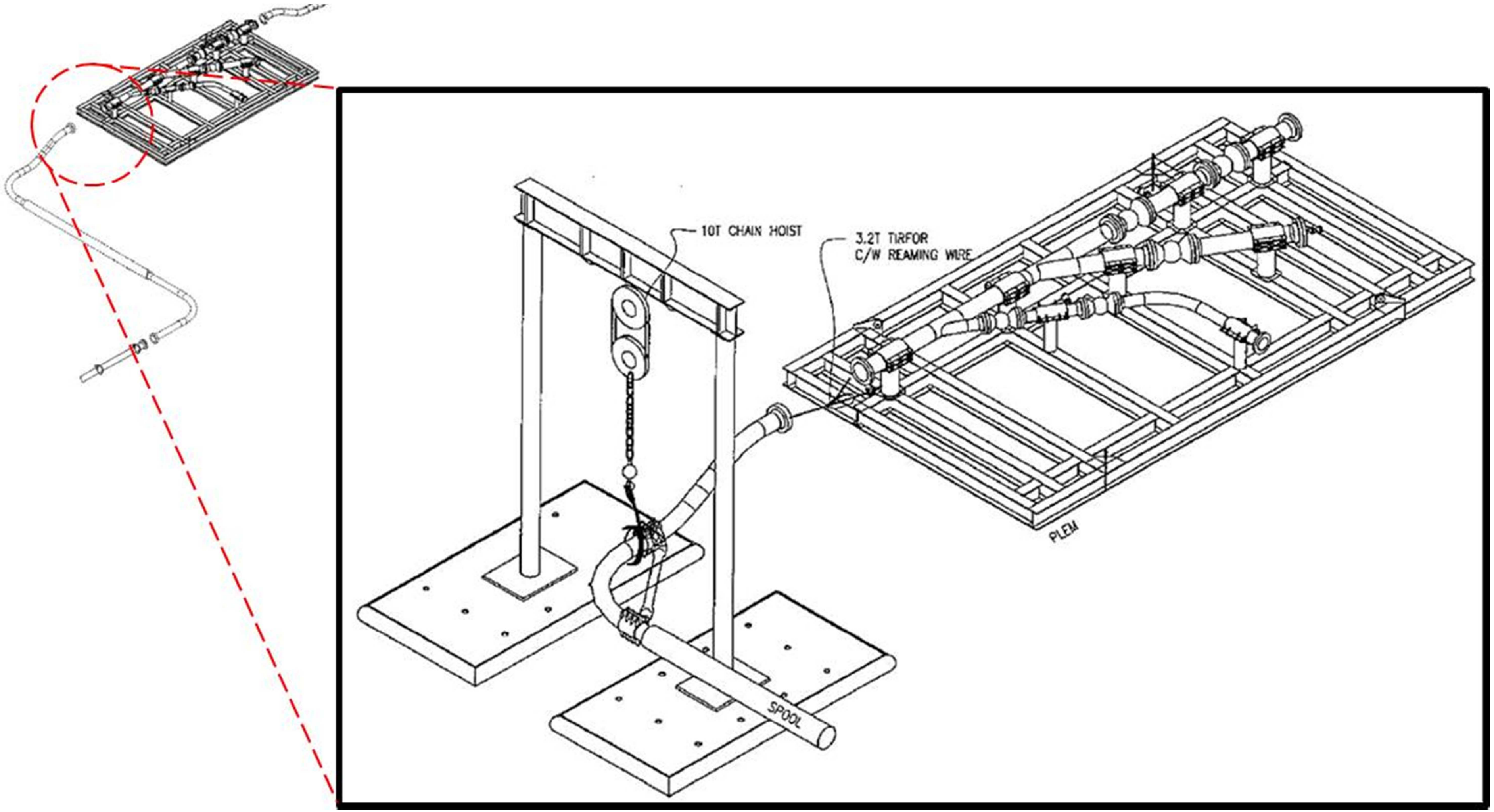


**Figure 6.15:** Expansion spool tie-in to PLEM [Zamri]

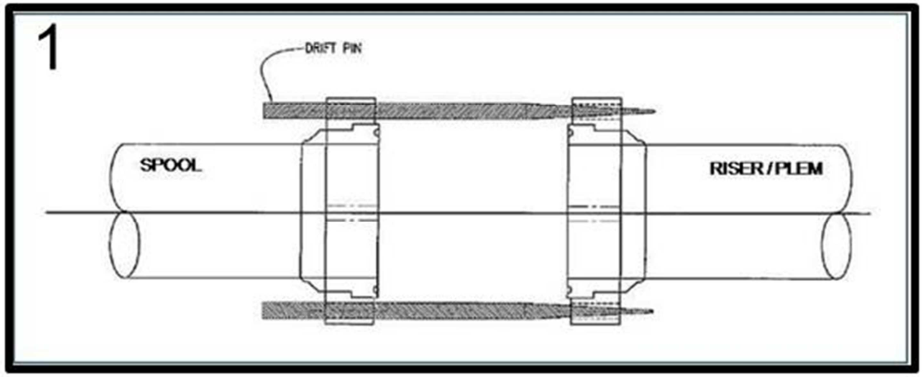
1
DRIFT PIN
SPOOL
RISER / PLEM

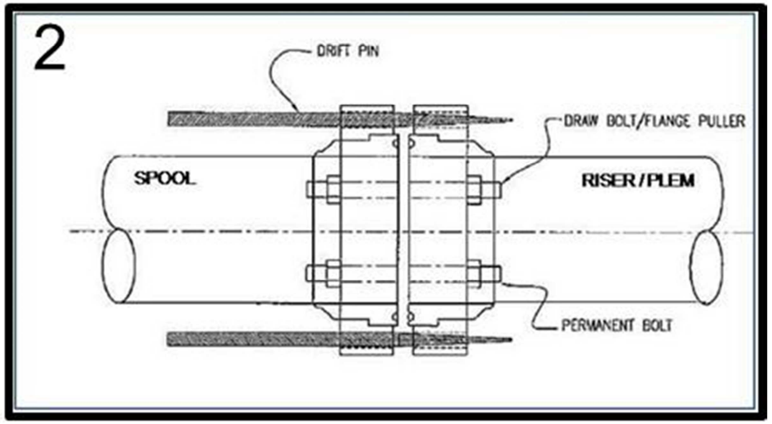
2
DRIFT PIN
DRAW BOLT/FLANGE PULLER
SPOOL
RISER / PLEM
PERMANENT BOLT

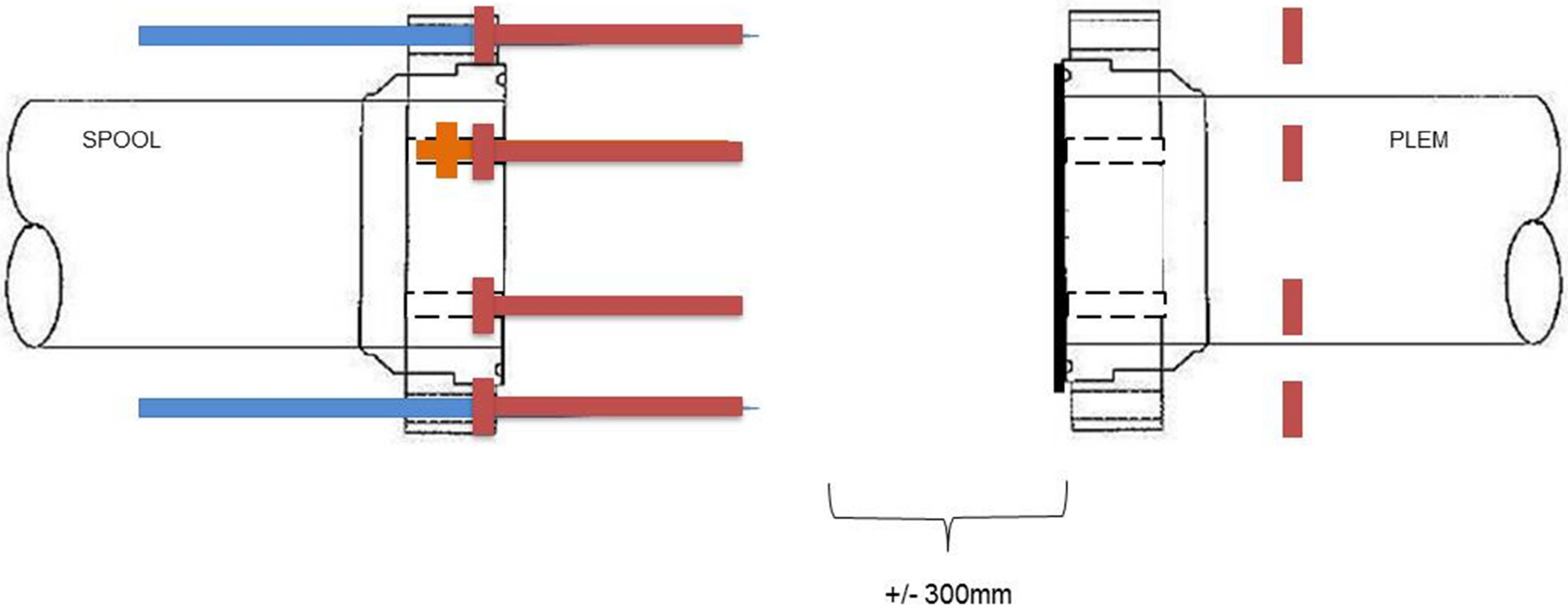
SPOOL
PLEM
+/- 300mm

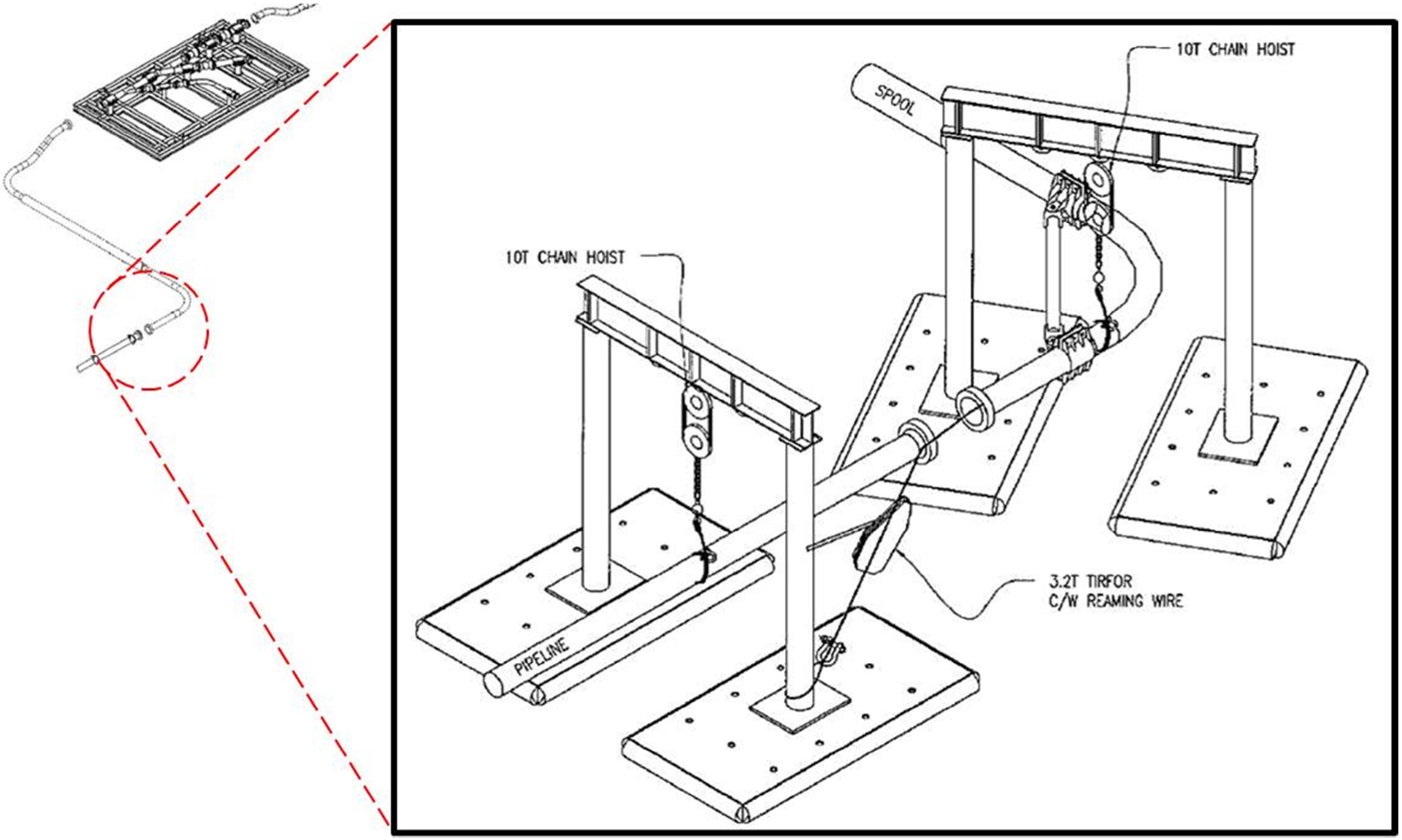


**Figure 6.16:** Expansion spool tie-in to pipeline [Zamri]

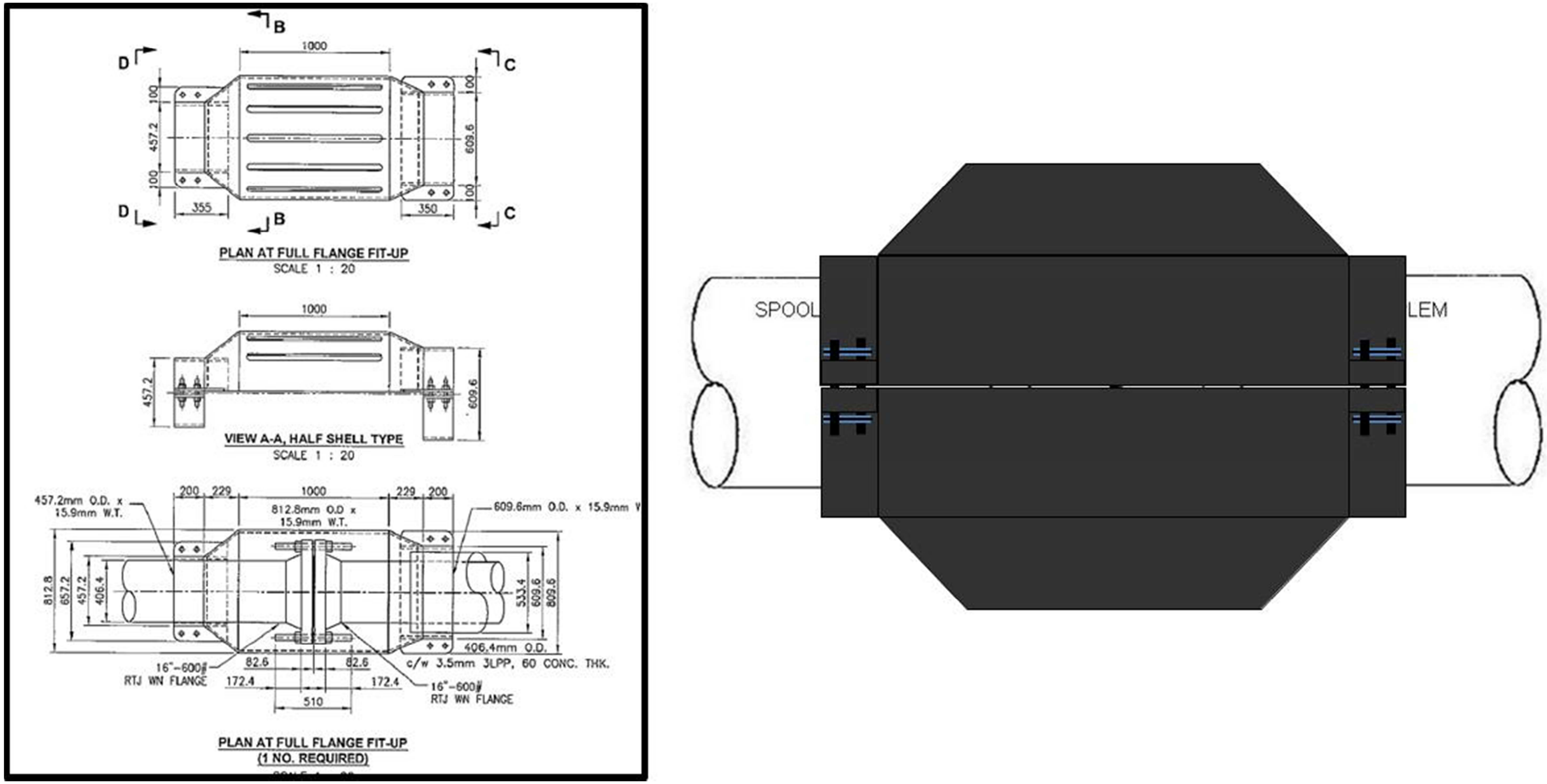


**Figure 6.17:** Flange Protector Drawings [Zamri]

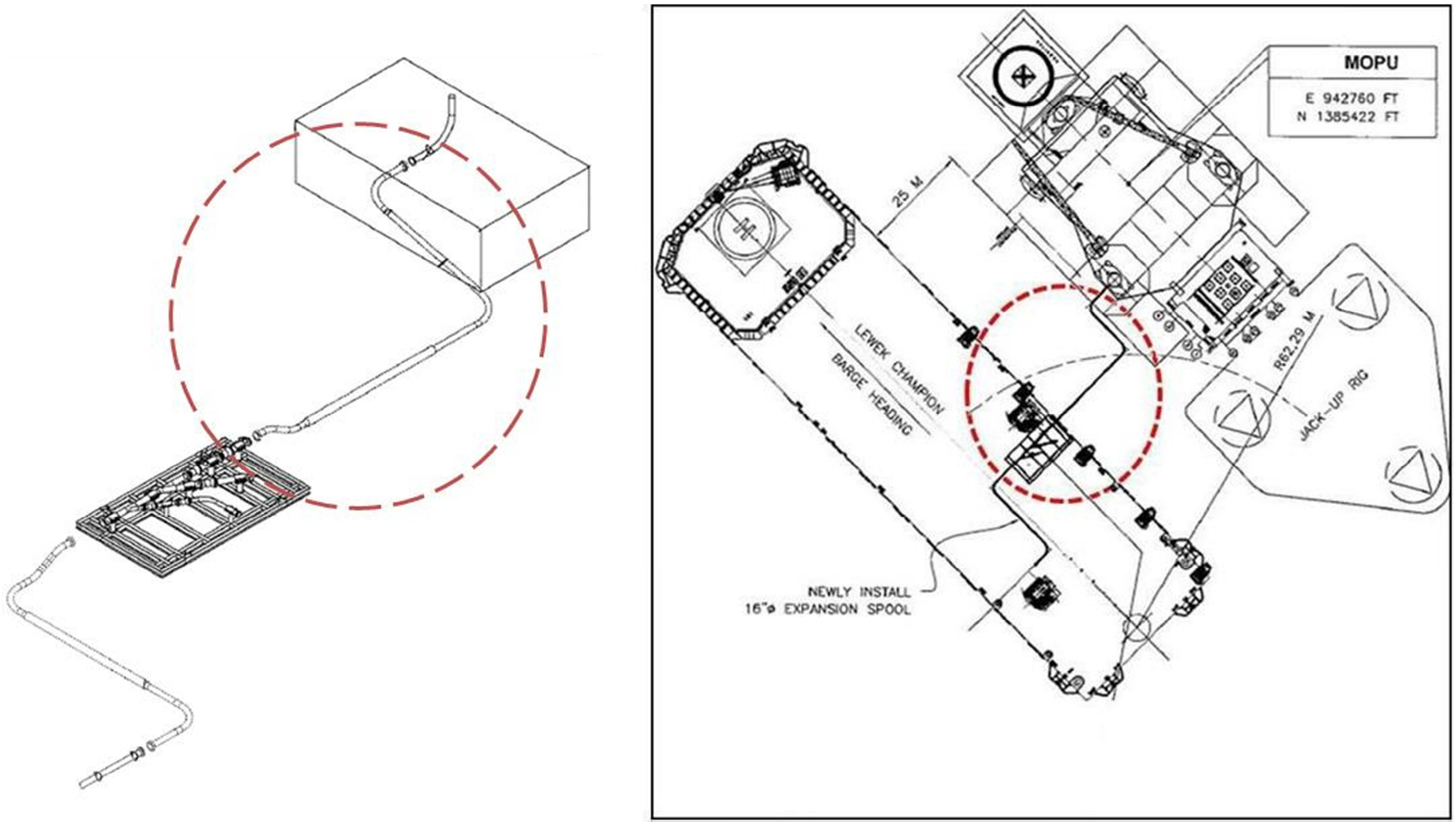


**Figure 6.18:** Barge Set-Up for PLEM / MOPU Spool Installation [Zamri]

**Figure 6.19:** Spools installation at site [Zamri]

### 6.2.6. Final Assembly

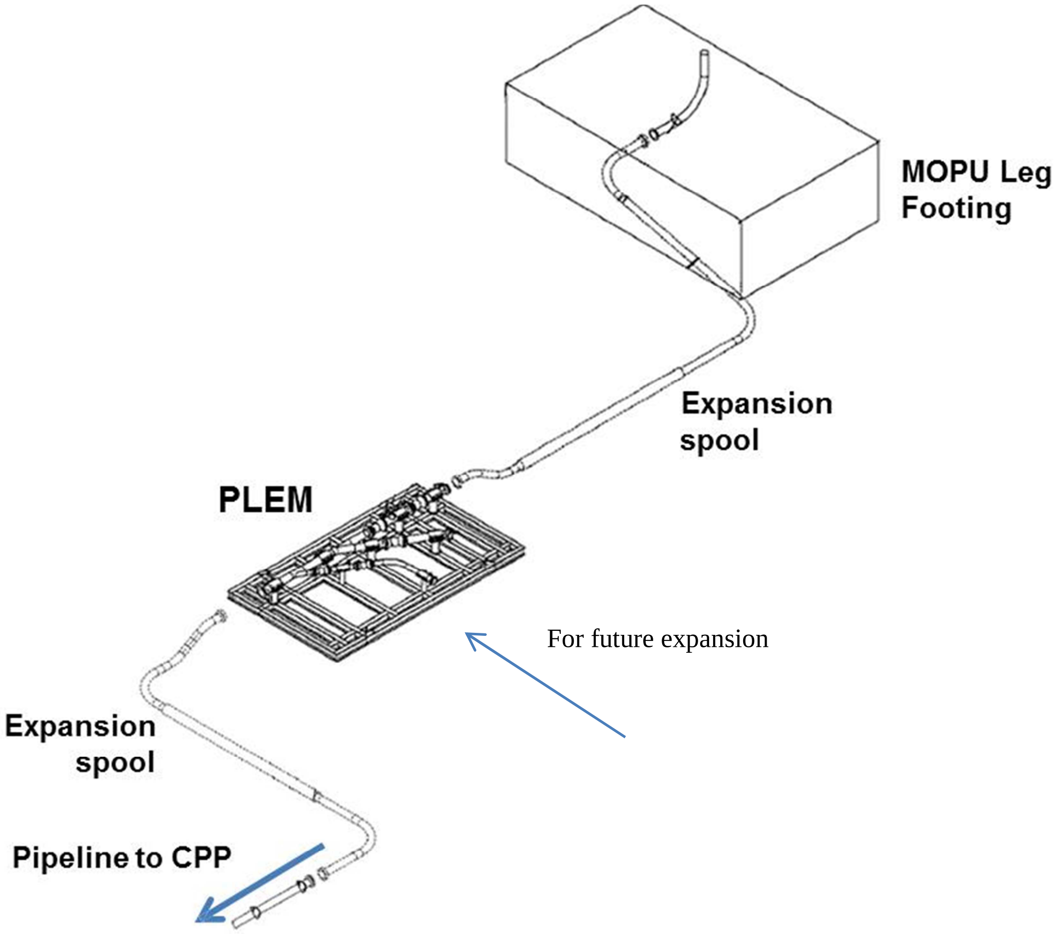


**Figure 6.20:** Final assembling of PLEM amd Spools at site [Zamri]

# Chapter.7

# 7.0 Deep-water PLEM Installation

## *7.1. Introduction*

The chapter discusses on deep water PLEM installation using the environmental data of offshore in Gulf of Mexico which comprises of water depth, hydrodynamic coefficient and DNV regulation. This chapter also covers vessel data, PLEM/PLET design parameter and installation parameter that have been consider in analysis. After all the basis design were finalized, modelling the installation were done by using Orcaflex software.

The PLEM and PLET systems are typically used in new construction where a pipeline terminates or needs to be jumper to another location, such as an FPSO, refinery and holding tank. PLETs, PLEMs, and tees can incorporate one or multiple tie-in points, vertical or horizontal, with other components such as isolation gate or ball valves, diverter valves, pig-launcher facilities, an array of sensors, or wyes.

In late 2014, the offshore market is suffering from a reduction in operator's limited capital investment due to low price of oil per barrel, which limits the field trial of unproven technologies in applying new methods. In this context, the subsea field development projects had becoming more strategic as the fields are in ultra-deep water condition (i.e. > 1500m). The installation of manifold in ultra-deep water is an outstanding issue (Penati, 2015). The exploration of deep or ultra-deep sea oil and gas fields has push into more economic superiority in term of SPS. The systems itself are high investment and high risk technology.

Frazer (2005) stated that over the last 10 years, the offshore industries in oil and gas exploitation has moved into deeper water. In 1990s, the water depth in Brazil and Norway were around 300m. Then, the current development of oil and gas exploitation in West Africa's water has reach 1500m water depth, while in Brazil and Gulf of Mexico (GoM) has reached 2000m water depth. The race towards deeper water depth has push the limitation for companies to spend less proportionally with current oil prices market, and achieve the same result that able to compete in the industries. Technology will play a very important role in counting these challenges and help accelerating the development.

The installation of PLEM/PLET as part of a deep water flow line system must closely integrate design. The installation procedures are to ensure the equipment running smoothly, predictably, and safely. The installation analysis for a pipeline system with a PLEM should check the following items as follows tensile of pipeline, bending & shear stress and hoop stress (Koto, 2017).

Critical factors for ultra-deep water subsea PLEM/PLET installation method are mainly influenced by the method limitation and economic cost. The conventional installation method, however, has its limitation such as the limited lifting capability of the drilling platforms and vessels. The use of wire rope in conventional methods reached its limit when use in deep water (i.e. > 1000m) where the weight of the wire itself is the same as the weight of the subsea hardware, thus axial resonance increase.

As the industries lean towards into deeper water depth, the suitable method or technique is required for ultra-deep water subsea installation such as in Gulf of Mexico. There has been many methods developed for installing in ultra-deep water, but the economic condition has push the boundary opted for method that is economic wise. In order to choose for the suitable method, several measures and parameters have to be looked into. In term of technical factors, the suitable method has to be properly presented and analyzed. In term of economic factors, the installation cost for the chosen method has to suit the economic demand.

## *7.2. Theoretical Principles*

### 7.2.1 Selection of lifting cable

For ultra-deep water installation, using conventional ways of lifting operation, the cable that is chosen must be compatible and able to perform the lifting criteria. The structures that are to be analyzed are a subsea PLET and PLEM. The lifting cable must have a payload capacity to sustain the subsea hardware.

### 7.2.1.1. Payload Capacity

Choosing a suitable lifting cable is an important task to minimize the costing of technology used. At different water depth, the lifting cable that is used must has payload capacity that can sustain the subsea hardware. To assess the payload capacity, the water depth and chosen cable has to be the main variable in order to calculate the reduce capacity. The submerged object will experiences a buoyancy force. The buoyancy force can be calculated as:

$$F_B = \nabla g \rho_{SW} \quad (7.1)$$

Where; $\nabla$ is the displaced volume of water (m$^3$), $g$ is the acceleration of gravity [m/s$^2$], $\rho_{SW}$ is the density of seawater [m$^3$] and $F_B$ is the buoyancy force [N].

The experiencing of buoyancy force is equal to the weight of the water displaced by the submerged weight. To find the submerged weight, the buoyancy is acting opposite of the gravity force. Therefore:

$$m_{sub} = \frac{F_G - F_B}{g} \ [kg] \quad (7.2)$$

$$F_G = mg \ [N]$$

Where; $F_G$ is the gravity force (N), $m$ is the weight of object in air per unit length [kg/m] and $m_{sub}$ is the submerged weight of object per unit length [kg/m].

### 7.2.1.2. Reduced Payload Capacity

Due to increasing of water depth, the payload capacity of the lifting line will be reduce to the self-weight of the lifting cable. The reduced payload can be calculated as follow:

$$Payloadcapacity = SWL - (m_{sub} x L) \ [kg] \quad (7.3)$$

Where; $SWL$ is the safety working load (kg) and $L$ is the length of lifting line [m].

To show the different of increasing water depth, the payload capacity can be calculated with increasing value of water depth up to desire.

### 7.2.1.3. Stretch Length of a Cable

In accordance to DNV-RP-H103 Section 5.2.1, a vertical cable will stretch due to its own weight and the weight of the lifted object at the end of the cable. The stretch length ($L_s$) can be calculated as follow:

$$L_s = L\left(1 + \frac{W + \frac{1}{2}wL}{EA}\right)\ [m] \qquad (7.4)$$

Where $L_s$ is the stretched length of cable (m), $L$ is the original length of cable [m], $W$ is the fully submerged weight of the lifted object [N], $w$ is the fully submerged weight per unit length of the cable [N/m], $E$ is the modulus elasticity of the cable [N/m$^2$] and $A$ is the nominal cross sectional area of a cable [m$^2$].

## 7.2.2. Installation Method Analysis for Fiber Rope Deployment System (FRDS)

### 7.2.2.1. Analysis Method

According to Cao (2016), the acted hydrodynamic force on the weight-balancing chain is complicated. For the convenience of the analysis few assumptions are made:

1. Throughout the installation process, the chain is considered as elastic
2. The displacement of the chain is parallel to wave direction and ocean current
3. The wind load can be ignored
4. The chain lateral displacement that is due to heave motion can be ignored

The analysis will be comprises of static and dynamic analysis as shown below:

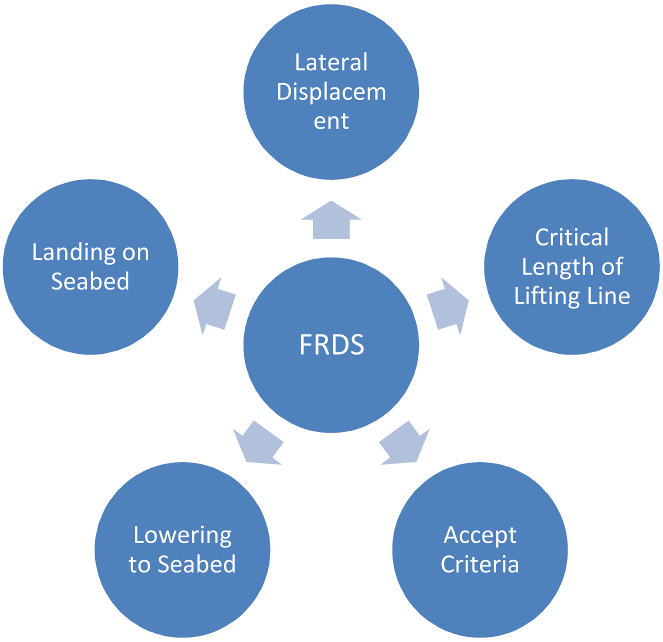


### 7.2.2.2. Lateral Displacement

According to DNV-RP-H103 Section 5.2.2, the lifted object will experience horizontal offset due to current. It is important to estimate the lateral displacement that is due to the current. The offset is required to estimate the payout length of deployment line required to reach the seafloor. It is also required to manage positioning before landing to the seabed. Figure 7.1 demonstrates the mechanical model of the lateral displacement.

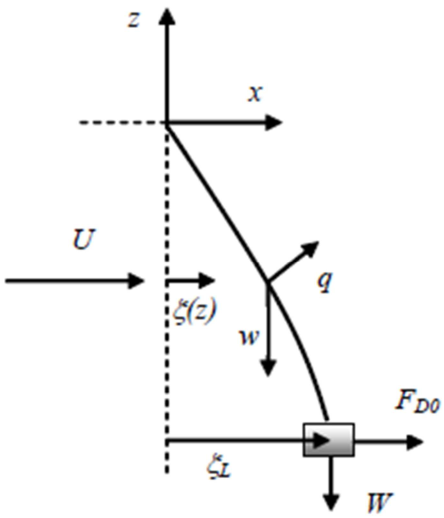


**Figure 7.1:** Theoretical Model for Lateral Displacement, DNV-RP-H103

For calculating the horizontal offset, in accordance of DNV-RP-H103 Section 5.2.2.2, the horizontal offset of the lifted objects with uniform current is:

$$\varepsilon_L = L\left(\frac{q}{w}k - \lambda\right)\ln\left(\frac{k}{k+1}\right) + \frac{qL}{w}\ [m] \tag{7.5}$$

$$k = \frac{W}{wL}$$

$$\lambda = \frac{F_{DO}}{wL}$$

$$q = \frac{1}{2}\rho_{sw} C_{Dn} D_c U^2\ [\frac{N}{m}]$$

Where; $q$ is the drag force on lifting line per unit length [N/m], $w$ is the submerged weight of lifting line [N/m], $W$ is the submerged weight of lifted object [N], $U$ is the current velocity [m/s], $\varepsilon_L$ is the horizontal offset of the lifted object [m], $k$ is the ratio between the weight of the lifted object and weight of the lifting line [-], $\lambda$ is the ratio between the drag on the lifted object and weight of the lifting line [-],$C_{Dn}$ is the drag coefficient for normal flow past lifting line [-], $D_c$ is the lifting line diameter [m], $\rho_{sw}$ is the density of seawater [kg/m$^3$].

The drag force can be calculated as

$$F_{DO} = \frac{1}{2}\rho_w C_{Dx} A_x U^2\ [N] \tag{7.6}$$

Where; $F_{DO}$ is the drag force on lifted object [N], $C_{Dx}$ is the drag coefficient for flow past lifted object, x-direction [-], $A_x$ is the projected area of lifted object, x-direction [m$^2$],

The submerged weight of lifted object can be expressed as

$$W = F_G - F_B\ [N] \tag{7.7}$$

$$F_G = Mxg\ \ [N] \tag{7.8}$$

$$F_B = \rho_{sw} x \nabla x g\ [N] \tag{7.9}$$

where; $F_G$ is the gravitational force [N], $F_B$ is the buoyancy force [N], $\nabla$ is the displaced volume of water [m$^3$] and $g$ is the acceleration of gravity [m/s$^2$].

From the Figure 7.1 above, it is seen the weight of lifting cable manipulate the value for the submerged weight and drag force of the lifting line. Therefore, different lifting line will produce different results.

### 7.2.2.3. Critical Length of Lifting Line

The lifting line system exhibits natural period in the function of line length regarding different installation scenario that effect the resonant motion. As the length of the lifting cable increases, the natural frequency of the lifting system decreases. The change of the length of lifting cable will cause resonance motion between the natural period and the crane tip motion.

#### *7.2.2.3.1. Natural Period of the Lifting System*

Natural period is the period of one complete oscillation of the lifting line. According to Boe (2010), the natural period of the lifting line is:

$$T_o = 2\pi\sqrt{\frac{M'+\frac{mL}{3}}{K_E}}\ [s] \qquad (7.10)$$

$$K_E = \frac{EA}{L}$$

Where; $M`$ is the weight of lifted object in air + hydrodynamic added mass z-direction [kg], $m$ is the weight of lifting line in air per unit length [kg/m], $L$ is the length of lifting line[m], $K_E$ is the stiffness of lifting system [N/m] and $EA$ is the axial stiffness of the lifting line [N].

#### *7.2.2.3.2. Crane Tip Motion Transfer Function*

For installation analysis, motion transfer function of the crane tip is determined by hydrodynamic software such as WAMIT or OrcaFlex. The data cannot be taken directly into consideration as it needed to be converted accordingly to any particular point desired. The heave motion of the vessel is important for the installation analysis. The vertical heave motion is made up by the heave, pitch and roll motion of the vessel. The line model in the OrcaFlex is connected to the midship for the pitch motion, therefore the pitch motion can be neglected. The combined heave motion transfer function at the crane tip can be calculated by:

$$Verticalcranetipmotion = RAO_{heave} + x * \sin(RAO_{roll}) \quad [\frac{m}{m}] \qquad (7.11)$$

Where $RAO_{heave}$ is the vertical displacement amplitude in heave [m/m], x is the distance from the amid ship point for roll motion to location of crane tip [m] and $RAO_{roll}$ is the roll angle amplitude [deg/m].

### 7.2.3. Accept Criteria

In order to conduct safe operation, the dynamic analysis need to be compared to a set of accept criteria. According to DNV-RP-H103 Section 4.4;

1. The static and dynamic loads should not exceed the capacity requirement
2. Snap loads due to slack slings should be avoided

The capacity of the lifting line should act as the governing capacity requirement. The accept criteria 1 states that the summation of the static and dynamic force in the lifting line should not exceed the safety working load of the line.

$$F_{stat} + F_{dyn} < SWL_{line} \ [kg] \qquad (7.12)$$

$$F_{stat} = M_{sub} + L * m_{sub} \ \ [kg] \qquad (7.13)$$

Where; $F_{stat}$ is the static force in the lifting line [kg], $F_{dyn}$ is the dynamic force in lifting line [kg], $SWL_{line}$ is the safe working load of the lifting line [kg], $M_{sub}$ is the submerged weight of the lifted object [kg], $m_{sub}$ is the submerged weight of lifting line [kg/m] and $L$ is the length of lifting line [m].

From above equations, the maximum allowable dynamic force for accept criteria No.1 can be expressed as:

$$F_{dyn,max} = SWL_{line} - F_{stat} \quad [kg] \qquad (7.14)$$

The accept criteria 2 states that in accordance to DNV-RP-H103 Section 4.4.3, if the dynamic force exceeds the static weight of the object, snap force may occur. To avoid snap loads in the lifting line, the criterion is as follow:

$$F_{dyn} < 0.9 * M_{sub} \ [kg] \quad (7.15)$$

From the Equation, the maximum allowable dynamic force for accept criteria No.2 can be expressed as:

$$F_{dyn.max} = 0.9 * M_{sub} \ [kg] \quad (7.16)$$

### 7.2.4. Lowering to Seabed

For different sea states and lifting line, the dynamic analysis has different output. According to DNV-RP-H103 Section 3.4.2.22, the perform analyses should cover from the following zero-up crossing wave period for a given significant wave height ($H_s$):

$$8.9 * \sqrt{\frac{H_S}{g}} \leq T_z \leq 13 \ [s] \quad (7.17)$$

Where; $H_s$ is the significant wave height [m], $g$ is the gravitational acceleration [m/s$^2$] and $T_z$ is the wave zero up-crossing period [s].

The wave peak period ($T_p$), may be taken from DNV-RP-C205 Section 3.5.5, applying a JONSWAP spectrum. The wave peak period is calculated from the OrcaFlex software where:

$$T_p = 1.4075 * T_z \quad (7.18)$$

Where; $T_p$ is the wave peak period.

The maximum dynamic force at different sea states is compared to the governing accepted criteria. It is found that the dynamic force:

$$Max\ dynamic\ force\ = \ max\ effective\ tension\ in\ lifting\ line - static\ tension\ in\ lifting\ line\ [t] \quad (7.19)$$

### 7.2.5. Landing on Seabed

According to DNV-RP-H103 Section 6.2.1.1, the aim of evaluating the landing on seabed is to assure that:

1. During the landing, the failure of the object foundation does not take place
2. Damage due to acceleration sensitive equipment does not occur

The motion of the lifted object close to the seabed can be analyze for all installation scenario. The characteristic static soil resistance can be ignored. The motion of the lifted object can be expressed as:

$$Motion\ of\ lifted\ object =$$
$$Max\ position\ during\ simulation - \ static\ problems\ [m] \quad (7.20)$$

## *7.3. Design of PLEM and PLET*

### 7.3.1. PLEM and PLET Design Parameter

According to Thorgessen (2014), the design of the subsea PLEM and PLET can be taken as follow:

**Table 7.1:** Design Parameter for PLET and PLEM

| Particular | PLET | PLEM |
|---|---|---|
| **Weight in air [t]** | 60.9 | 100.1 |
| **Length [m]** | 6 | 7 |
| **Breadth [m]** | 6 | 9 |
| **Height [m]** | 7 | 5 |

### 7.3.2. Current

According to Cao (2016), the current velocity profile for Gulf of Mexico is stated as below table. For the current velocity as in practice, it is differ as going deeper into the ocean. For this study purposes, it is focus on the difference in the lateral displacement offset due to current when performing the lowering operation. The current profile is assumed to be constant for the water depth from 0m to 3000m, with the value is set to 0.6m/s. (Thorgersen, 2014)

**Table 7.2:** Current Velocity for Different Water Depth (Cao, 2016)

| Water Depth | Current Velocity (m/s) |
|---|---|
| **0** | 1.05 |
| **250** | 0.93 |
| **580** | 0.70 |
| **750** | 0.61 |
| **1080** | 0.52 |
| **1250** | 0.49 |
| **1500** | 0.46 |

### 7.3.1.1. Water Depth

As per title of the paper, the depth that will be covered for this paper is ranging from 0m to 3000m with step of 500m. The paper is subjected to Gulf of Mexico, which ongoing project of Perdido having depth of 2800m and future project Stones with water depth of 3000m. Based on the information given, this book is intended to do analysis within that 500m steps from 0m with constant sea water density 1025kg/m$^3$.

### 7.3.1.2. Waves

Based on Chakrabarti (2005), for operation purposes the applicable wave spectrum is the Pierson-Moskowitz for the use in Gulf of Mexico. The vessel heading (θ) that is relative to the wave direction is shown in Figure 7.2 below.

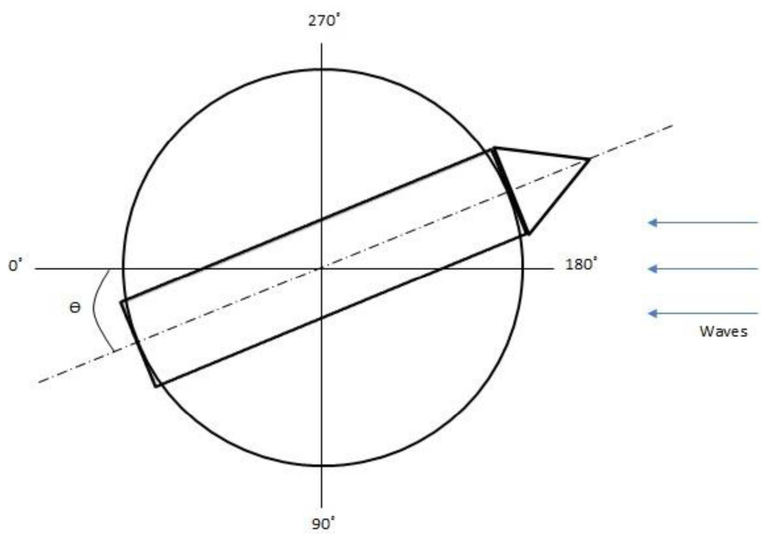

**Figure 7.2:** Wave Direction versus Vessel Heading (Thorgensen, 2014)

**Table 7.3:** Sea-States for Significant Wave Height and Zero Crossing Period

| Significant Wave Height (Hs) [m] | Zero Crossing Period (Tz) [s] | |
|---|---|---|
| | From | To |
| **1.0** | 2.8 | 13.0 |
| **1.5** | 3.5 | 13.0 |
| **2.0** | 4.0 | 13.0 |
| **2.5** | 4.5 | 13.0 |
| **3.0** | 5.0 | 13.0 |
| **3.5** | 5.3 | 13.0 |
| **4.0** | 5.7 | 13.0 |

### 7.3.3. Cable Data

For the comparison study for the lifting line, the chosen to be compare with the fiber rope is the conventional steel wire. A fiber rope and the steel wire both have same safe working load (SWL) of 125T.

The chosen cable both are industries proven, having past track records. The fiber rope that is chose for this study is a 12x12 strand, braid optimized for bending (BOB) rope developed by Cortland. The rope having 88mm of diameter was used on project Skandi Santos (Daniel, 2010).

From the product brochure, the rope minimum break load is 567T, and weight in air 693.1kg/100m.

The chosen steel wire is a non-rotating 35xK19s Compacted Steel produced by Kiswire. The diameter of the wire is 2 5/8” with minimum break load of 383.4T. The steel wire has weight in air of 2259kg/100m.

According to Thorgensen (2014), the cable stiffness for the fiber rope and steel wire is as follow.

**Table 7.4**: Lifting Cable Data

| | Fiber Rope | Steel Wire |
|---|---|---|
| **Minimum Breaking Load (t)** | 567 | 383.4 |

| | | |
|---|---|---|
| **Weight in air (kg/100m)** | 693.1 | 2259 |
| **Submerged Weight (kg/m)** | 0.87 | 19.92 |
| **Cable stiffness, EA (N)** | $148.3 \times 10^6$ | $511 \times 10^6$ |

### 7.3.4. Hydrodynamic Coefficient

#### 7.3.4.1. Added Mass Coefficient, $C_A$

The added mass coefficient is by referring from DNV-RP-H103. The value is to be interpolated between the ratios of $b/a$.

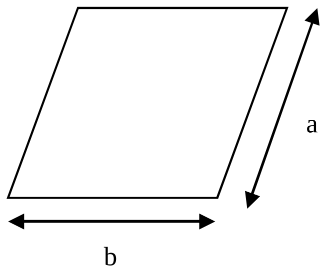


| Rectangular Plate | | $b/a$ | $C_A$ |
|---|---|---|---|
| | Vertical | 1.00 | 0.579 |
| | | 1.25 | 0.642 |
| | | 1.50 | 0.690 |
| | | 1.59 | 0.704 |
| | | 2.00 | 0.757 |
| | | 2.50 | 0.801 |
| | | 3.00 | 0.830 |
| | | 3.17 | 0.840 |
| | | 4.00 | 0.872 |
| | | 5.00 | 0.897 |
| | | 6.25 | 0.917 |
| | | 8.00 | 0.934 |
| | | 10.00 | 0.947 |
| | | ∞ | 1.000 |

**Figure 7.3:** Added Mass Coefficient (DNV-RP-H103)

**Table 7.5:** Added Mass Coefficient in Coordinates Direction

| Parameter | PLET | PLEM |
|---|---|---|
| Added mass coefficient x-direction , $C_{AX}$ | 0.621 | 0.731 |
| Added mass coefficient y-direction , $C_{AY}$ | 0.621 | 0.671 |
| Added mass coefficient z-direction , $C_{AZ}$ | 0.627 | 0.649 |

### 7.3.4.2. Drag Coefficient, $C_D$

The drag coefficient for objects are subjected to oscillatory flow, the value is hard to be determine without having experimental test or suitable computational fluid analysis tools. In accordance to DNV-RP-H103, Section 4.6.2.4, the typical subsea structure in oscillatory flow is having drag coefficient of 2.5.

**Table 7.6**: Drag Coefficient in Coordinate's Direction

| Parameter | PLET | PLEM |
|---|---|---|
| Drag Coefficientx,y,z direction , $C_{DX}$, $C_{DY}$, $C_{DZ}$ | 2.5 | 2.5 |

### 7.3.4.3. Hydrodynamics Added Mass, $A_{33}$

The hydrodynamics added mass is calculated referring to DNV-RP-H103 Section 4.6.3 the following equations. The reduction factor can be refer from the Appendix

$$A_{330} = \rho_{sw} * C_A * V_R [kg] \quad (7.21)$$

$$V_R = \frac{\pi}{4} a^2 b \; [m^3] \quad (7.22)$$

$$A_{33s} = \left[1 + \sqrt{\frac{1-\lambda^2}{2(1+\lambda^2)}}\right] * A_{330} \; [kg] \quad (7.23)$$

$$\lambda = \frac{\sqrt{A_p}}{h+\sqrt{A_p}} \quad (7.24)$$

$$A_{33} = A_{33s} * Added\ mass\ reduction\ factor\ [kg] \quad (7.25)$$

**Table 7.7**: Hydrodynamic Added Mass in Coordinate's Direction

| Parameter | PLET | PLEM |
|---|---|---|
| Hydrodynamic added mass x-direction, $A_{33X}$ [t] | 187.8 | 102.9 |
| Hydrodynamic added mass y-direction, $A_{33Y}$ [t] | 187.8 | 75.8 |
| Hydrodynamic added mass z-direction, $A_{33Z}$ [t] | 187.8 | 170 |

#### 7.3.4.4. Hydrodynamic Inertia Coefficient, $C_M$

The hydrodynamic inertia coefficient is the summation product of added mass coefficient with 1.

$$C_M = 1 + C_A \tag{7.26}$$

**Table 7.8**: Hydrodynamic Inertia Coefficient in Coordinate's Direction

| Parameter | PLET | PLEM |
|---|---|---|
| **Hydrodynamic inertia coefficient x-direction, $C_{MX}$** | 1.621 | 1.731 |
| **Hydrodynamic inertia coefficient y-direction, $C_{MY}$** | 1.621 | 1.671 |
| **Hydrodynamic inertia coefficient z-direction, $C_{MZ}$** | 1.627 | 1.641 |

### 7.3.5. Software Tools

The main tools used in finding the dynamic analysis for this book is by using OrcaFlex. The software OrcaFlex is developed by Orcina. Orcaflex is a software for the dynamic analysis of offshore marine systems, which held capabilities of wide technical usage and user friendliness. It has many applications in offshore engineering such as for risers, moorings, installation analysis and much more. For this book, which mainly focus on installation of subsea hardware, the use of OrcaFlex make the task easier than using complex software such as AnsysAqwa.

### 7.3.6. Input Parameters

#### 7.3.6.1. Vessel Data

The standard model in OrcaFlex is used as the main vessel properties for this installation analysis. Under "Model" section, choose "New Vessel". The parameters are as follow:

**Table 7.9**: Vessel Data

| Dimension | Values |
|---|---|
| Length [m] | 103 |

| | |
|---|---|
| Depth [m] | 13.32 |
| Beam [m] | 16 |
| Draught [m] | 6.66 |

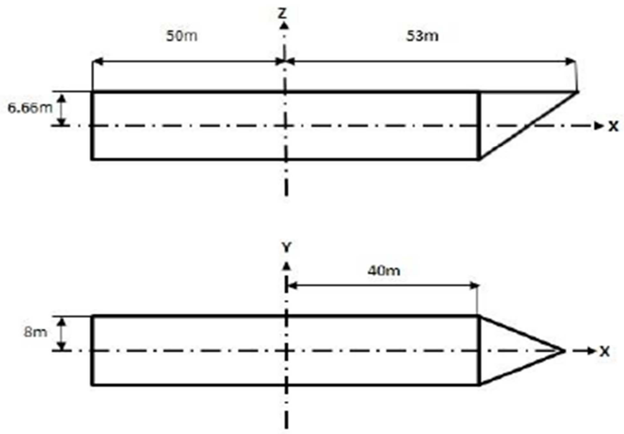


**Figure 7.4:** Configuration of Vessel in Orcaflex

The heading of orientation is set to 22.5 deg. The primary motion is set to "None" while the superimposed motion is set to "Displacement RAOs + Harmonic Motion". For the included effects, the "Added Mass and Damping" is checked. The static analysis is set to "6 DOF ".

### 7.3.6.2. PLEM/PLET Data

For the purpose of simplify matters, the shape of the PLEM and PLET is considered as box. Under "Model" section, choose the 6D Buoy. The 6D Buoy is connected using local coordinates. The input parameters for the 6D Buoy is by using coordinates system, where it is located in the volumetric center of the PLEM and PLET figures below:

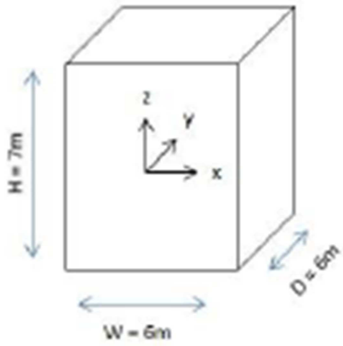


**Figure 7.5:** The Model of PLET in Orcaflex

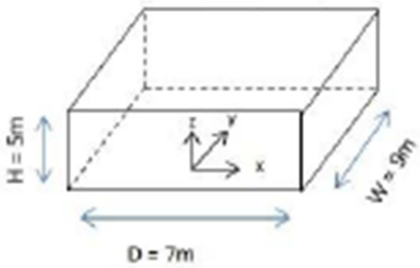


**Figure 7.6:** The Model of PLEM in Orcaflex

### 7.3.6.3. Line Data

The line function is to model the fiber rope as the lifting line for the installation analysis. Under “Model” section, select “New Line”. The line is the connection for the vessel model and PLEM/PLET model to simulate the lowering operation. The point for the line is connected as follow:

**Table 7.10**: Line Connection for PLET

| | Object Relative Position | | |
|---|---|---|---|
| **Connection** | X | Y | Z |
| **Vessel** | 0 | 8 | 6.66 |
| **PLET** | 0 | 0 | 3.5 |

**Table 7.11**: Line Connection for PLEM

| | Object Relative Position | | |
|---|---|---|---|

| Connection | X | Y | Z |
|---|---|---|---|
| Vessel | 0 | 8 | 6.66 |
| PLEM | 0 | 0 | 2.5 |

Under the "Structure" tab, the length of the line is set 2950m. Under the "Line Type", the geometry, limits can be input.

#### 7.3.6.4. Environmental Loading Conditions

The subjected vessel is set to be at Gulf of Mexico, where the waves are modelled based on Pierson- Moskowitz wave spectrum (Chakrabarti, 2005). OrcaFlex does not have wave based on Pierson-Moskowitz and has the JONSWAP wave spectrum. In accordance to DNV-RP-H103 section 2.2.6, the JONSWAP spectrum can be reduced into Pierson-Moskowitz for peak parameter of $\gamma = 1$. The experiment is modelled through different sea states, which are by changing the significant wave height and wave zero-up crossing period. The wave direction is set to 180˚.

The sea surface is set to z = 0m, while the seabed is set to $z = -3000m$. The simulation time is set to 1800s. The current speed also is set to 0.6m/s.

## *7.4. Simulation and Results*

### 7.4.1. Reduced Payload Capacity

As the length of lifting line increases, the payload capacity decreases due to the self-weight of the lifting cable. The steel wire and fiber rope have the same safe working load (SWL) of 125t. The lifting line need to withstand the weight of itself and the subsea PLEM/PLET by not exceeding the SWL. The calculated payload was conducted in different water depth are tabulated as shown in Table 7.12. From the table, the result shows significant different as the water depth increases. The steel wire payload reduced about half of its original payload while the fiber rope only loses significant small value.

**Table 7.12:** Reduce Payload Capacity for Steel Wire and Fiber Rope

| Water Depth [m] | Steel Wire [t] | Fiber Rope [t] |
|---|---|---|
| **0** | 125.0 | 125.0 |
| **500** | 115.0 | 124.6 |
| **1000** | 105.1 | 124.1 |
| **1500** | 95.1 | 123.7 |
| **2000** | 85.2 | 123.3 |
| **2500** | 75.2 | 122.8 |
| **3000** | 65.2 | 122.4 |

Figure 6.1 shows the reduced payload for the steel wire and fiber rope at different water depth. To able the steel wire to have payload ~125t, larger steel wire need to be use. This lead to challenges related to logistic, larger installation vessel to provide larger deployment winch and the load of the deck will increase. The use of fiber rope for ultra-deep water is seen as optimum as the payload capacity only reduced less than 3% while the steel wire lose about 47%.

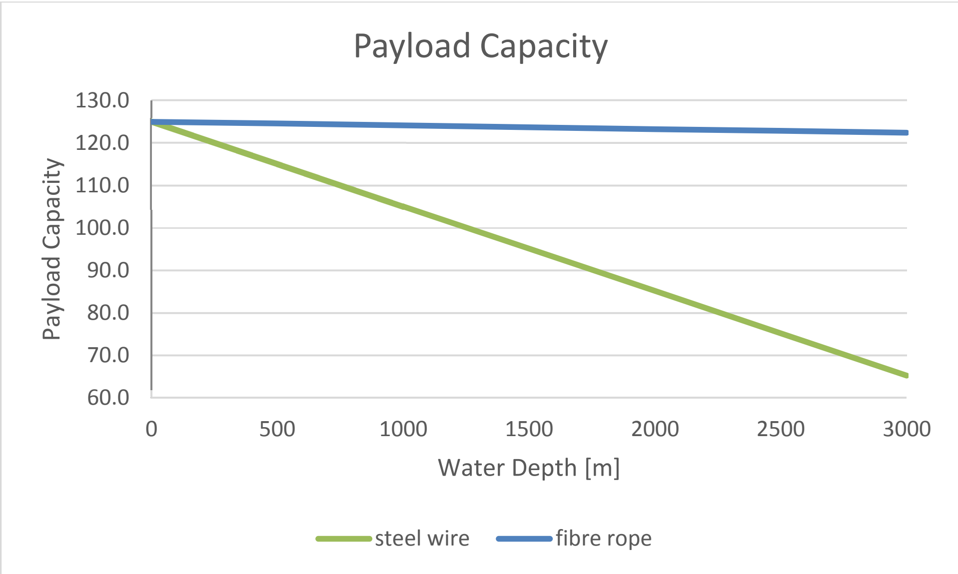


**Figure 7.7:** Payload Capacity at Different Water Depth.

## 7.4.2. Elongation of the Lifting Cable

Due to the weight of the cable and subsea PLEM/PLET, the fiber rope experiencing elongation. From the Table 7.13, the change in length of the cable is very small. The strain value also possesses small percentage of <1%.

**Table 7.13:** Elongation for Installing PLET and PLEM

| Criteria | PLET | PLEM |
|---|---|---|
| **L [m]** | 3000 | 3000 |
| **W [kN]** | 597.6 | 982 |
| **W [N/m]** | 8.53 | 8.53 |
| **EA [N]** | $148.3 \times 10^6$ | $148.3 \times 10^6$ |
| **Ls [m]** | 3012.3 | 3020.1 |
| **ΔL [m]** | 12.3 | 20.1 |
| **ε** | 0.004 | 0.007 |

## 7.4.3. Lateral Displacement

It is important to estimate the lateral displacement that is due to current for managing the position of the PLEM/PLET on the seafloor. The lateral displacement is for scenario of 3000m, and results are presented in Table 7.14 below:

**Table 7.14:** Lateral Displacement Due To Current

| Subsea Structure | Lateral Displacement [m] |
|---|---|
| **PLET** | 258 |
| **PLEM** | 208.8 |

Due to the ultra-deep water condition, the horizontal offset of the subsea structure is seems to be a problem related to positioning on the seafloor. This is because the weight of the lifting line is very small which affect the ratio between the lifted object and weight of the lifting line and also because the counteracting force caused by the weight of the lifting line. This situation increase the time required for positioning of the lifted object and duration of the operation.

## 7.4.4. Critical Length of Lifting Line

To assess the critical length of the lifting line, we need to identify the motion transfer function of the crane tip and natural period of the lifting line. Using the RAOs from the Appendix B, the result is presented in Figure 7.8. From the Figure 7.8, the vertical crane tip has wave peak periods of 6.5s.The large crane tip motion is because of vessel natural period in roll.

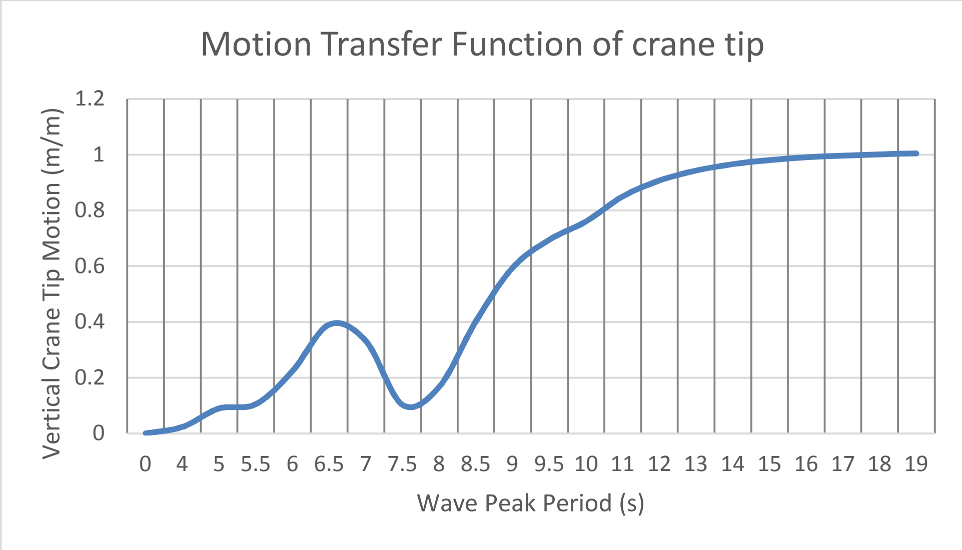


**Figure 7.8:** Motion Transfer Function of the Crane Tip

The natural period of the lifting line is assessed for different length of lifting line. The result is shown in Figure 7.9.

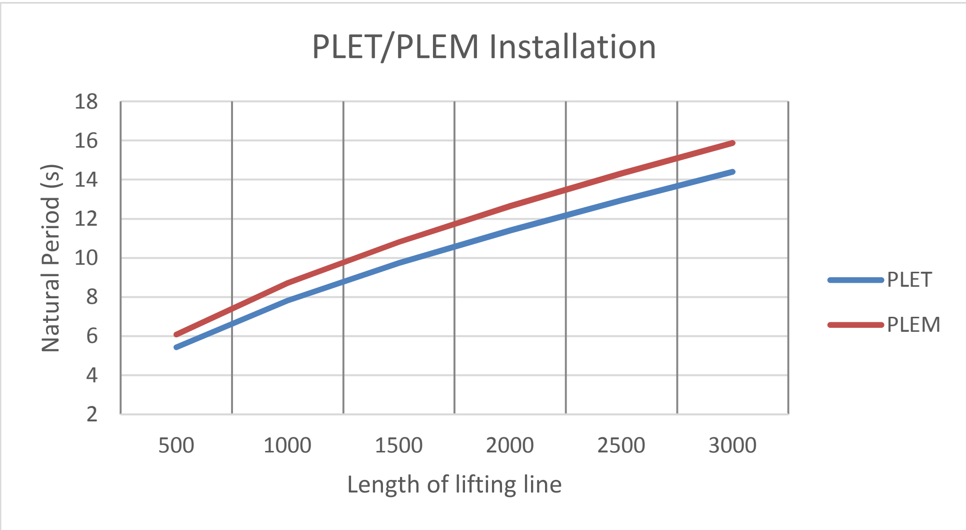


**Figure 7.9:** The Natural Period for PLET and PLEM Installation.

From the crossing of both data, the result is as shown in Table 7.15

**Table 7.15:** Length of Lifting Line Causing Resonant Motion

| Subsea Structure | Length of Lifting Line [m] |
|---|---|
| **PLET** | 705 |
| **PLEM** | 555 |

The value is the critical length of the lifting line before it experience resonant motion. Large motion of crane tip and the lifted object will result in large dynamic forces.

### 7.4.5. Accept Criteria

The accept criteria shows the maximum allowable dynamic force for lifting the subsea PLEM/PLET. Table 7.16 shows the maximum dynamic force for accept criteria 1 at different lifting line length.

**Table 7.16:** Maximum Dynamic Force for PLET and PLEM, Accept Criteria 1

| | PLET | | PLEM | |
|---|---|---|---|---|
| L | $F_{stat}$ [t] | $F_{dyn.max}$ [t] | $F_{stat}$ [t] | $F_{dyn,max}$ [t] |
| **500** | 61 | 63.6 | 101 | 24.5 |
| **1000** | 62 | 63.2 | 101 | 24.0 |
| **1500** | 62 | 62.8 | 101 | 23.6 |
| **2000** | 63 | 62.3 | 102 | 23.2 |
| **2500** | 63 | 61.9 | 102 | 22.7 |
| **3000** | 64 | 61.5 | 103 | 22.3 |

Table 7.17 shows the dynamic force for accept criteria 2. The maximum dynamic force is not difference from the length of the lifting line. The force is constant for all line length.

**Table 7.17:** Maximum Dynamic Force for PLET and PLEM, Accept Criteria 2

| | PLET | PLEM |
|---|---|---|
| **$M_{sub}$ [t]** | 60.9 | 100.1 |
| **$F_{dyn,max}$ [t]** | 54.8 | 90.1 |

It is seen from Table 7.16 and 7.17, the accept criteria 2 is used for PLET in governing the dynamic force in lowering to seabed. The accept criteria 1 is used in governing the PLEM dynamic force for lowering to seabed.

### 7.4.6. Lowering to Seabed

Referring the sea-states as in Table 7.2, using the OrcaFlex software, the dynamic force is analyzed with simulation time of 1800s. The maximum dynamic force at end of line connection (holding the PLEM/PLET) with different sea-states is shown in Appendix. The result for PLET is compared to accept criteria 2 maximum allowable dynamic force and shown in Figure 7.10.

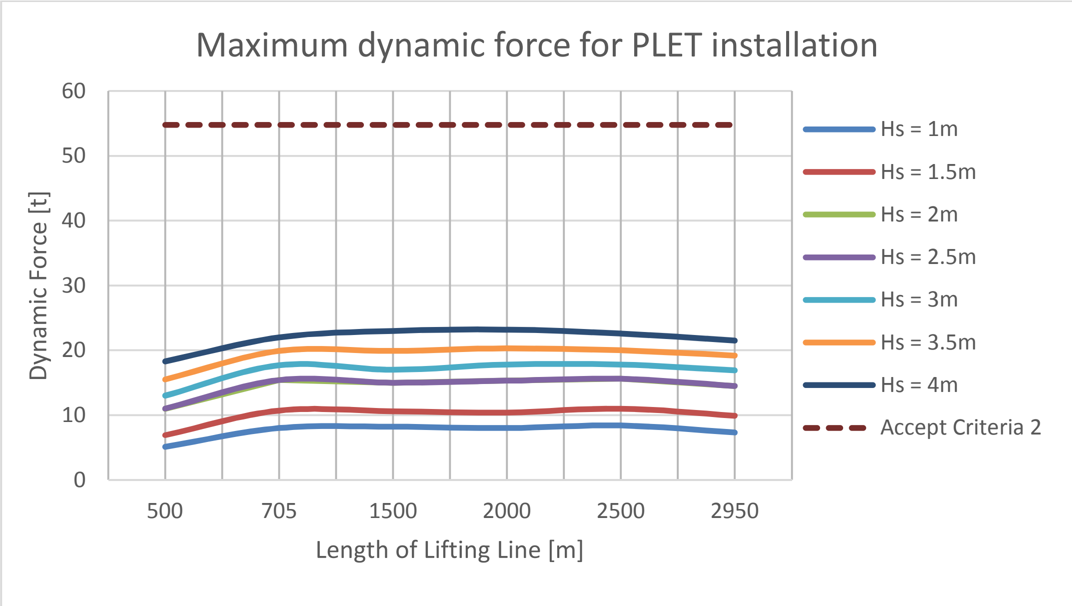


**Figure 7.10:** Dynamic Force for PLET Installation

For PLEM, the result is compared with accept criteria 1 maximum allowable dynamic force at different lifting line length. Figure 7.11 shows the result for PLEM installation. It is seen from Figure 7.11 that for subsea PLET installation, no limiting weather criteria is obtained and the force for different significant wave height has no impact on the maximum dynamic force on the lifting line.

For the installation of subsea PLEM, the limiting weather criteria are stricter for the fiber rope. It is limited to sea-states with significant wave height ≤ 2.5m.

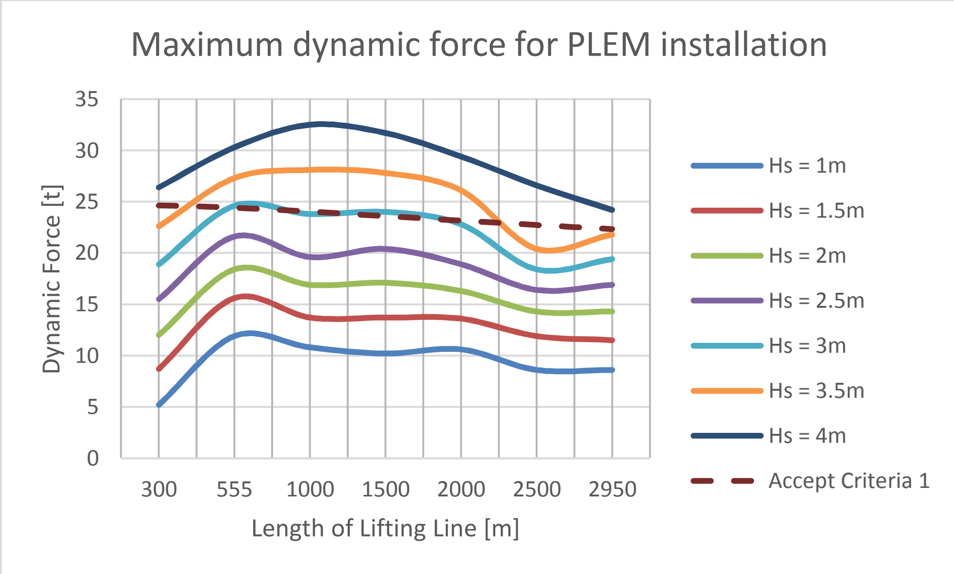


**Figure 7.11:** Dynamic Force for PLEM Installation

### 7.4.7. Landing on Seabed

After the lowering operation, the landing on seabed is important to assess the motion of the lifted object. The motion of the lifted object is with different sea-states and the result is from OrcaFlex and tabulated in Appendix. Figure 7.12 shows the result for motion of the PLET while Figure 7.12 shows the result for motion of the PLEM.

From the above figure, the motion of the lifted PLET is higher than the lifted PLEM. The motion is for adjustment when positioning the ROV upon landing on the seabed.

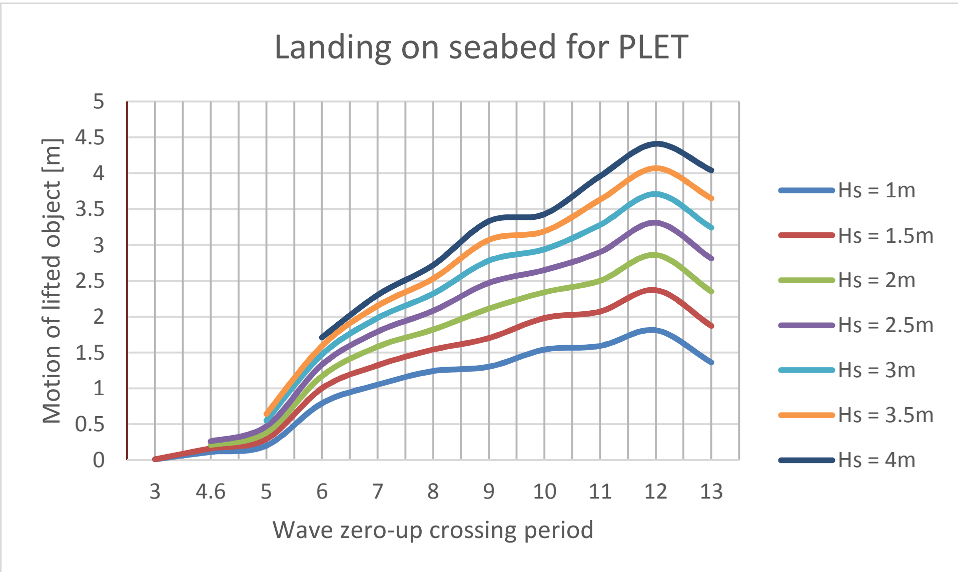


**Figure 7.12:** Motion of Lifted Object for PLET

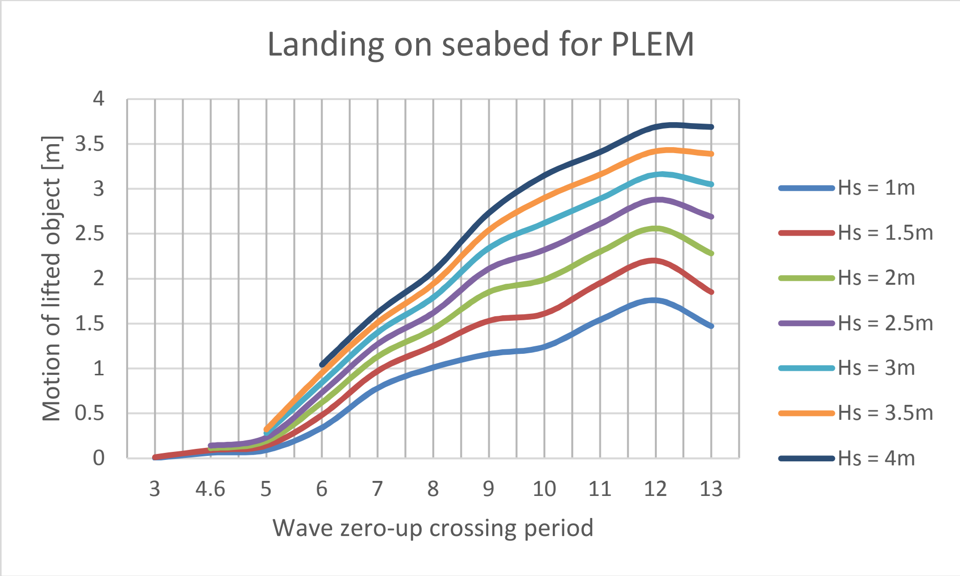


**Figure 7.13:** Motion of Lifted for PLEM.

# References


1. Adibah Fatihah.M.Y, Noor Zairie.M, Nur Ain.A.R, Nursahliza.M.Y, J.Koto, 2017, Review on Roncador Field Production and Gas Lift Pipeline, Journal of Subsea and Offshore -science and engineering-, Vol.6, pp.14-21.
2. Alan Wang, Shaohua Zhu, Xiaohuan Zhu, Jingkuo Xu, Min He, Changzhi Zhang (2013). Pendulous Installation Method and its Installation Analysis for a Deepwater Manifold in South China Sea. International Offshore and Polar Engineering Conference. June 30-July 5. Alaska, USA. 1-11
3. Alan Wang, Yun Yang, Shaohua Zhu, Huailiang Li, Jingkuo Xu and Min He (2012). Latest Progress in Deepwater Installation Technologies. International Offshore and Polar Engineering Conference. June 17-22. Rhodes, Greece. 1-12
4. American Institute of Steel Construction (AISC), Manual of Steel Construction: Allowable Stress Design, nineth ed., AISC, Chicago, 2002.
5. American Petroleum Institute (API), Recommended Practice for Planning, Designing and Constructing Fixed Offshore Platforms–Working Stress Design, API RP 2A-WSD (2007).
6. Boe T, Nestegard A (2010). Dynamic Force during Deepwater Lifting Operations. International Offshore and Polar Engineering Conference
7. Chakrabarti Subrata (2005). Handbook of Offshore Engineering ( Volume 1). Illinois, USA. Elsevier
8. Det Norske Veritas (2011). Modelling and Analysis of Marine Operation. [Brochure]. DNV
9. Det Norske Veritas (DNV), Cathodic Protection Design, DNV RP B401 (1993)
10. Det Norske Veritas (DNV), Foundations, DNV, Classification Notes No. 30.4 (1992)
11. Espen Sletteb, 2012, Tie-in Spools – A Verification Study, Master Thesis, Faculty of Science and Technology, University of Stavanger.
12. FMC Technologies
13. Frazer, I, Perinet, D, and Vennemann, O (2005). Technology Required for the Installation of Production Facilities in 10,000 ft of Water. Offshore Technology Conference, Paper OTC-17317, 1-8 pp.

14. G. Corbetta, BRUTUS: The Rigid Spoolpiece Installation System, OTC 11047, Offshore Technology Conference, Houston, Texas, 1999.
15. GE Oil & Gas, GE Oil & Gas internal documentation
16. Installation for the GFI Field Bualuang, Gulf of Thailand, Kingdom of Thailand, 2007
17. J. Koto (2017). Introduction to Subsea Pipeline End Structure, Ocean & Aerospace Research Institute, Indonesia, Edition 2
18. J. Koto and A.K. Junaidi, 2017, Subsea Pipeline Design & Analysis, Ocean & Aerospace Research Institute, Indonesia
19. J. Koto, 2016, Subsea Manifold and Its Application, Ocean & Aerospace Research Institute, Indonesia
20. J.K. Antani, W.T. Dick, D. Balch, T. Van Der Leij, Design, Fabrication and Installation of the Neptune Export Lateral PLEMs, OTC 19688, Offshore Technology Confer-ence, Houston, Texas, 2008.
21. Johansson Daniel (2010), Practical use of a Fiber Rope Lifting System on the Petrobras SESV "Skandi Santos", Subsea Lifting Conference.March 19-24. Stavenger, Norway. 12-32
22. K.H. Andersen, H.P. Jostad, Foundation Design of Skirted Foundations and Anchors in Clay, OTC 10824, Offshore Technology Conference, Houston, Texas, 1999.
23. L. Penati, M. Ducceschi, A. Favi, D. Rossin (2015). Installation Challenges for Ultra-Deep Waters. 12th Offshore Mediterranean Conference. March 25-27. Ravenna, Italy. 1-15
24. M. Faulk, FMC ManTIS (Manifolds & Tie-in Systems), SUT Subsea Awareness Course, Houston, 2008.
25. Muhammad Aiman Bin Amir Zakee, 2017, Installation Of Subsea PLEM/PLET In Ultra-Deep Water, Thesis, Naval Architecture & Offshore Engineering, Faculty of Mechanical Engineering, Universiti Teknologi Malaysia
26. N. Janbu, Grunnlag i geoteknikk, Tapir forlag, Trondheim, Norway (in Norwegian). (1970)
27. N. Janbu, L.O. Grande, K. Eggereide, Effective Stress Stability Analysis for Gravity Structures, BOSS'76, Trondheim, Vol. 1 (1976) 449–466.
28. Offshore Technology, Salamander Energy Bualuang Oil Project, Gulf of Thailand, Thailand

29. Oil State, Integrated Solutions. Proven Results.
30. Oilfield Wiki, PLEM Design Methodology
31. R.T. Gilchrist, Deep-water Pipeline End Manifold Design, Oil & Gas Journal, special issue (1998, November 2)
32. RESL Energy Engineering, Plem/Plet And Subsea Manifold Design.
33. Ron Nelson (1997). Heave Compensated Landing System – A Novel Tool for Subsea Intervention. Offshore Technology Conference. 5-8 May, Houston, Texas, USA. 1-10
34. Simen Thorgerssen (2014). Comparison Study of Deepwater Installation Methods. Master degree. University of Stavanger, Norway
35. Sverre Torben (2007). Fiber Rope Deployment System for Ultra Deep Water Installation. Offshore Technology Conference. 30April-3May. Houston, Texas, USA. 1-10
36. Sverre Torben, Per Ingeberg (2010). Field Pilot of Deep Water Installation in Two-Fall Using Fiber Rope. Rio Oil & Gas Expo and Conference. September 13-16. Rio de Janeiro. 1-10
37. T. Risoey, H. Mark, H. Johnsgard, J. Gramnaes (2007). The Pencil Buoy Method – A Subsurface Transportation and Installation Method. Offshore Technology Conference. April 30-May 3. Houston, Texas, USA. 1-7
38. Thorsen. S, 2012, Conceptual Design and Review of Open PLET System, Master Thesis, Faculty of Science and Technology, University of Stavanger.
39. Yong Bai and Qiang Bai, Subsea Engineering Handbook, 2010, Elsevier
40. Yuguang Cao, Xueyang Hu, Shihua Zhang, Songsen Xu, Jungin Lee, Jiancheng Yu (2016). Design of a novel installation device for a subsea production.Applied Ocean Research. 59. 24-37
41. Zamri B Ahmad, 2011, Installation of Pipeline End Manifold (PLEM) and Subsea Tie-In of Expansion Spools, Deepwater Subsea Tie-Back Workshop, 25-26 January.

# Appendixes

## A.1. Example.1

Figure.A-1 shows installation of subsea Pipeline End Termination (PLET) in 1200 meter water depth using a crane ship.

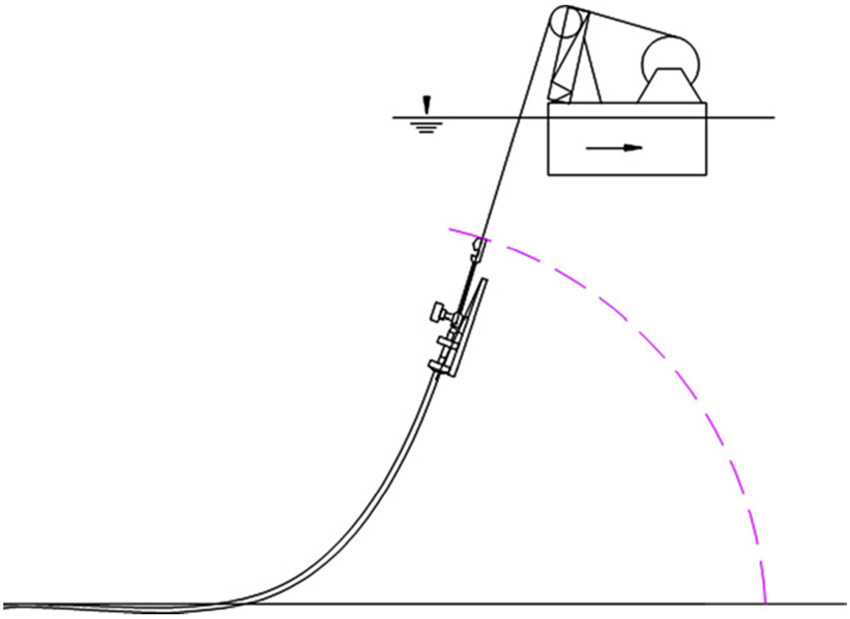

**Figure A-1:** PLET static forces analysis during installation

Based on the figure, determines as follows:

a. Moment due to pipe top tension
b. Moment due to the transverse weight
c. Moment due to the longitudinal weight
d. Total moment about the pivot

**Answer.**

Figure below shown distribution force acting on the PLET during installation.

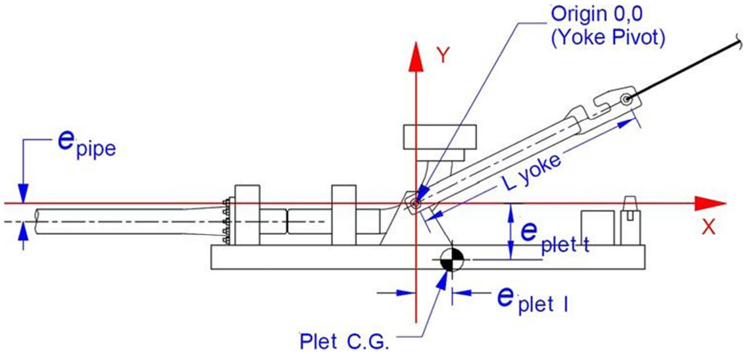

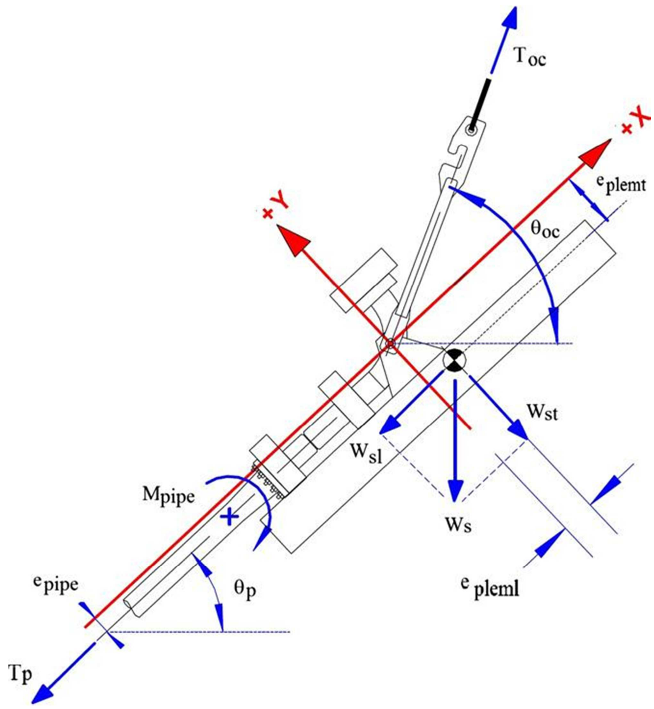


a. Moment due to pipe top tension ($M_{tp}$) can be calculated using the following equation

$$M_{tp} = -T_p \cdot e_{pipe}, \text{ where } T_p = {W_s}\Big/\left[\frac{\cos(\theta_p)}{\cos(\theta_{oc})} \cdot \sin(\theta_{oc}) - \sin(\theta_p)\right]$$

b. Moment due to the transverse weight ($M_{pleml}$) can be calculated using the following equation:

$$M_{pleml} = W_{st} \cdot e_{pleml} \text{ , where } W_{st} = W_s \cdot \cos(\theta_p)$$

c. Moment due to the longitudinal weight ($M_{plemt}$) can be calculated using the following equation.

$$M_{plemt} = W_{sl} \cdot e_{plemt} \text{ , where } W_{sl} = W_s \cdot \sin(\theta_p)$$

d. Total moment about the pivot ($M_{pipe}$)

$$M_{pipe} = M_{tp} + M_{pleml} + M_{plemt}$$

## *A.2. Exercise.1*

Table A-1 shows parameters of a subsea Pipeline End Termination (PLET) in deep water using a ship. Based on the table determine total moment acting to the PLET

**Table A-1:** Parameter of PLET.

| Parameters | Value |
|---|---|
| **PLEM** | |
| $W_s$ (kg) | 11339.809 |
| $L_{yoke}$ (m) | 1.8288 |
| $e_{pleml}$ (m) | 0.1524 |
| $e_{plemt}$ (m) | 0.3048 |
| **Pipe** | |
| $OD$ (m) | 0.168275 |
| $W.T$ (in) | 0.719 |
| $e_{pipe}$ (m) | 0.0762 |
| **Cable** | |
| $OD$ (m) | 0.073025 |
| $W_c$ (kg/m) | 18.60205 |
| **Water depth (m)** | 1219.2 |
| **seawater density (kg/m$^3$)** | 1025.181632 |

## *A.3. PLEM Data Analysis*

### Reduction Factor for Hydrodynamic Added Mass Coefficient

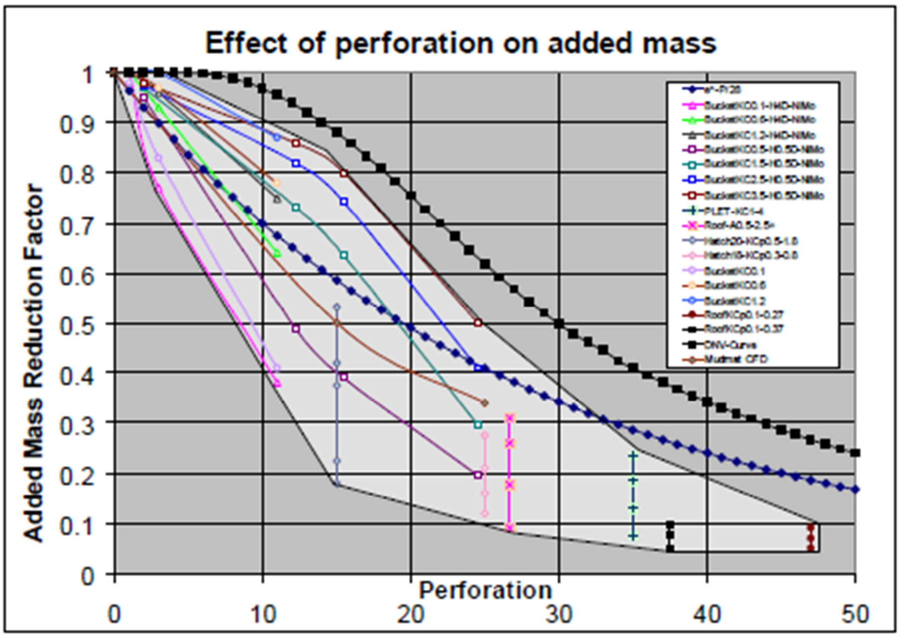
Effect of perforation on added mass
Added Mass Reduction Factor
1
0.9
0.8
0.7
0.6
0.5
0.4
0.3
0.2
0.1
0
Perforation
0
10
20
30
40
50
PLET-KC1-4
BucketKC0.1
BucketKC0.6
BucketKC1.2
DNV-Curve
Mudmat CFD

# RAOs Vessel Data

0° | 22,5° | 45° | 67,5° | 90° | 112,5° | 135° | 157,5° | 180°

Periods: 22

| Period (s) | Surge Ampl. (m/m) | Surge Phase (deg) | Sway Ampl. (m/m) | Sway Phase (deg) | Heave Ampl. (m/m) | Heave Phase (deg) | Roll Ampl. (deg/m) | Roll Phase (deg) | Pitch Ampl. (deg/m) | Pitch Phase (deg) | Yaw Ampl. (deg/m) | Yaw Phase (deg) |
|---|---|---|---|---|---|---|---|---|---|---|---|---|
| 0,00 | 0,000 | 0,0 | 0,000 | 360,0 | 0,000 | 360,0 | 0,000 | 0,0 | 0,000 | 0,0 | 0,000 | 360,0 |
| 4,00 | 0,0081 | 68,3 | 0,00082 | 206,8 | 0,014 | 282,6 | 0,065 | 106,7 | 0,056 | -97,1 | 0,035 | 247,0 |
| 5,00 | 0,012 | -88,5 | 0,016 | 264,8 | 0,065 | 133,4 | 0,175 | -63,7 | 0,265 | -220,4 | 0,032 | 214,2 |
| 5,50 | 0,017 | 66,2 | 0,018 | 126,2 | 0,091 | 190,1 | 0,099 | 63,4 | 0,678 | -177,4 | 0,122 | 182,6 |
| 6,00 | 0,033 | 99,9 | 0,044 | 89,6 | 0,166 | 237,5 | 0,410 | 80,6 | 0,887 | -165,6 | 0,087 | 134,3 |
| 6,50 | 0,029 | 104,8 | 0,044 | 65,1 | 0,306 | 239,5 | 0,607 | 79,1 | 0,660 | -135,3 | 0,140 | 40,8 |
| 7,00 | 0,024 | -55,5 | 0,030 | 12,7 | 0,244 | 211,8 | 0,625 | 73,2 | 1,079 | -93,8 | 0,270 | 18,2 |
| 7,50 | 0,108 | -70,6 | 0,046 | -49,3 | 0,042 | 169,3 | 0,433 | 68,2 | 1,558 | -89,5 | 0,372 | 11,3 |
| 8,00 | 0,203 | -75,4 | 0,078 | -69,1 | 0,149 | 22,9 | 0,129 | 135,0 | 1,804 | -89,7 | 0,441 | 8,2 |
| 8,50 | 0,295 | -78,6 | 0,113 | -74,2 | 0,299 | 15,6 | 0,747 | 176,2 | 1,892 | -90,6 | 0,479 | 6,7 |
| 9,00 | 0,378 | -80,8 | 0,150 | -77,2 | 0,422 | 12,4 | 1,233 | 145,5 | 1,880 | -91,2 | 0,498 | 6,1 |
| 9,50 | 0,449 | -82,3 | 0,182 | -80,6 | 0,525 | 10,3 | 1,222 | 124,5 | 1,814 | -91,6 | 0,504 | 5,6 |
| 10,00 | 0,510 | -83,4 | 0,208 | -82,7 | 0,608 | 8,8 | 1,093 | 114,0 | 1,725 | -91,7 | 0,500 | 4,9 |
| 11,00 | 0,607 | -84,8 | 0,248 | -84,8 | 0,730 | 6,5 | 0,864 | 104,9 | 1,526 | -91,6 | 0,470 | 4,0 |
| 12,00 | 0,678 | -85,7 | 0,277 | -85,9 | 0,809 | 4,9 | 0,704 | 101,1 | 1,338 | -91,3 | 0,429 | 3,3 |
| 13,00 | 0,730 | -86,3 | 0,299 | -86,6 | 0,861 | 3,9 | 0,588 | 99,1 | 1,172 | -91,0 | 0,387 | 2,7 |
| 14,00 | 0,768 | -86,9 | 0,315 | -87,1 | 0,897 | 3,2 | 0,498 | 97,8 | 1,030 | -90,8 | 0,347 | 2,3 |
| 15,00 | 0,797 | -87,3 | 0,328 | -87,5 | 0,921 | 2,7 | 0,428 | 96,8 | 0,910 | -90,7 | 0,312 | 2,0 |
| 16,00 | 0,819 | -87,6 | 0,337 | -87,8 | 0,939 | 2,3 | 0,372 | 96,2 | 0,808 | -90,5 | 0,280 | 1,8 |
| 17,00 | 0,836 | -87,9 | 0,344 | -88,1 | 0,952 | 2,0 | 0,326 | 95,6 | 0,721 | -90,4 | 0,252 | 1,6 |
| 18,00 | 0,849 | -88,1 | 0,350 | -88,3 | 0,961 | 1,7 | 0,289 | 95,2 | 0,646 | -90,4 | 0,228 | 1,4 |
| 19,00 | 0,860 | -88,3 | 0,355 | -88,5 | 0,969 | 1,5 | 0,257 | 94,8 | 0,582 | -90,3 | 0,207 | 1,3 |
| 20,00 | 0,869 | -88,5 | 0,358 | -88,6 | 0,975 | 1,4 | 0,231 | 94,5 | 0,527 | -90,3 | 0,188 | 1,1 |
| 21,00 | 0,877 | -88,6 | 0,362 | -88,8 | 0,979 | 1,3 | 0,208 | 94,2 | 0,480 | -90,3 | 0,172 | 1,0 |
| 22,00 | 0,883 | -88,7 | 0,365 | -88,9 | 0,982 | 1,1 | 0,189 | 94,0 | 0,438 | -90,2 | 0,158 | 0,95 |
| Infinity | 0,924 | 90,0 | 0,383 | 90,0 | 1,000 | 0,0 | 0,000 | 0,0 | 0,000 | 0,0 | 0,000 | 0,0 |

## Lowering to Seabed

The maximum dynamic force at end of line connection (holding the PLEM/PLET) with different sea-states.

PLET installation, maximum dynamic force in lifting line [t]

| L | Hs | | | | | | |
|---|---|---|---|---|---|---|---|
| | 1 | 1.5 | 2 | 2.5 | 3 | 3.5 | 4 |
| 500 | 5.1 | 6.9 | 11 | 11 | 13 | 15.5 | 18.3 |
| 705 | 8 | 10.7 | 15.4 | 15.4 | 17.7 | 19.9 | 22 |
| 1500 | 8.2 | 10.6 | 15 | 15 | 17 | 19.9 | 23 |
| 2000 | 8 | 10.4 | 15.3 | 15.3 | 17.8 | 20.3 | 23.2 |
| 2500 | 8.4 | 11 | 15.6 | 15.6 | 17.8 | 20 | 22.6 |
| 2950 | 7.3 | 9.9 | 14.5 | 14.5 | 16.9 | 19.2 | 21.5 |

PLEM installation, maximum dynamic force in lifting line [t]

| L | Hs | | | | | | |
|---|---|---|---|---|---|---|---|
| | 1 | 1.5 | 2 | 2.5 | 3 | 3.5 | 4 |
| 300 | 5.2 | 8.7 | 12 | 15.5 | 18.9 | 22.6 | 26.4 |
| 555 | 11.9 | 15.6 | 18.4 | 21.6 | 24.6 | 27.3 | 30.3 |
| 1000 | 10.8 | 13.7 | 16.9 | 19.6 | 23.8 | 28.1 | 32.5 |
| 1500 | 10.2 | 13.7 | 17.1 | 20.4 | 24 | 27.8 | 31.7 |
| 2000 | 10.6 | 13.6 | 16.3 | 18.9 | 22.8 | 26.1 | 29.4 |
| 2500 | 8.6 | 11.9 | 14.3 | 16.4 | 18.4 | 20.4 | 26.6 |
| 2950 | 8.6 | 11.5 | 14.3 | 16.9 | 19.4 | 21.8 | 24.2 |

## Landing on Seabed

| PLET | | | | | | | | | | | |
|---|---|---|---|---|---|---|---|---|---|---|---|
| Hs | Tz [s] | | | | | | | | | | |
| | 3 | 4.6 | 5 | 6 | 7 | 8 | 9 | 10 | 11 | 12 | 13 |
| 1 | 0.01 | 0.11 | 0.2 | 0.79 | 1.05 | 1.24 | 1.3 | 1.54 | 1.59 | 1.81 | 1.36 |
| 1.5 | 0.01 | 0.16 | 0.29 | 1 | 1.32 | 1.54 | 1.7 | 1.98 | 2.07 | 2.37 | 1.87 |
| 2 | | 0.21 | 0.38 | 1.17 | 1.58 | 1.82 | 2.11 | 2.34 | 2.5 | 2.86 | 2.35 |
| 2.5 | | 0.26 | 0.47 | 1.33 | 1.79 | 2.08 | 2.47 | 2.65 | 2.9 | 3.31 | 2.81 |
| 3 | | | 0.55 | 1.47 | 1.98 | 2.32 | 2.78 | 2.94 | 3.28 | 3.71 | 3.24 |
| 3.5 | | | 0.64 | 1.59 | 2.15 | 2.53 | 3.07 | 3.19 | 3.63 | 4.07 | 3.65 |
| 4 | | | | 1.71 | 2.3 | 2.72 | 3.33 | 3.43 | 3.96 | 4.41 | 4.04 |

| PLEM | | | | | | | | | | | |
|---|---|---|---|---|---|---|---|---|---|---|---|
| Hs | Tz [s] | | | | | | | | | | |
| | 3 | 4.6 | 5 | 6 | 7 | 8 | 9 | 10 | 11 | 12 | 13 |
| 1 | 0 | 0.06 | 0.09 | 0.34 | 0.78 | 1.01 | 1.16 | 1.24 | 1.54 | 1.76 | 1.47 |
| 1.5 | 0.01 | 0.09 | 0.14 | 0.48 | 0.97 | 1.25 | 1.53 | 1.61 | 1.95 | 2.2 | 1.85 |
| 2 | | 0.11 | 0.19 | 0.62 | 1.13 | 1.44 | 1.85 | 1.99 | 2.3 | 2.56 | 2.28 |
| 2.5 | | 0.14 | 0.23 | 0.73 | 1.27 | 1.62 | 2.11 | 2.32 | 2.61 | 2.88 | 2.69 |
| 3 | | | 0.28 | 0.84 | 1.4 | 1.79 | 2.34 | 2.62 | 2.89 | 3.16 | 3.05 |
| 3.5 | | | 0.32 | 0.95 | 1.51 | 1.94 | 2.54 | 2.9 | 3.16 | 3.42 | 3.39 |
| 4 | | | | 1.04 | 1.62 | 2.08 | 2.73 | 3.15 | 3.41 | 3.69 | 3.69 |

## Orcaflex Setup

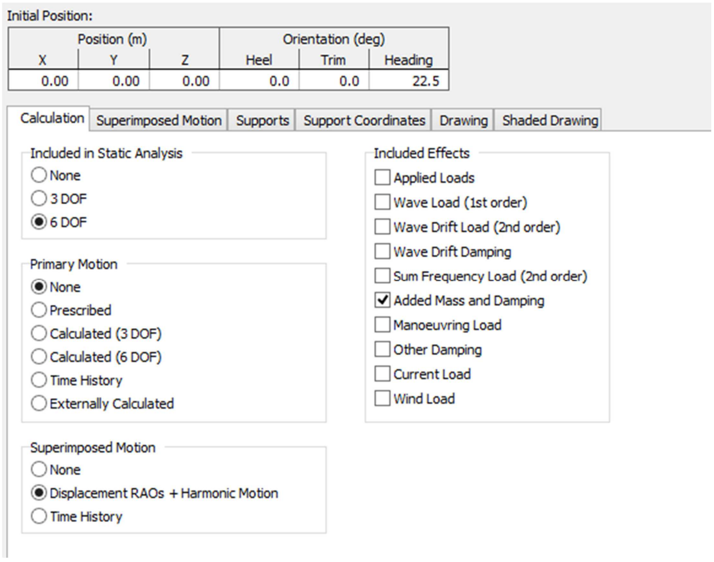


**Figure E.1:** Vessel Setup

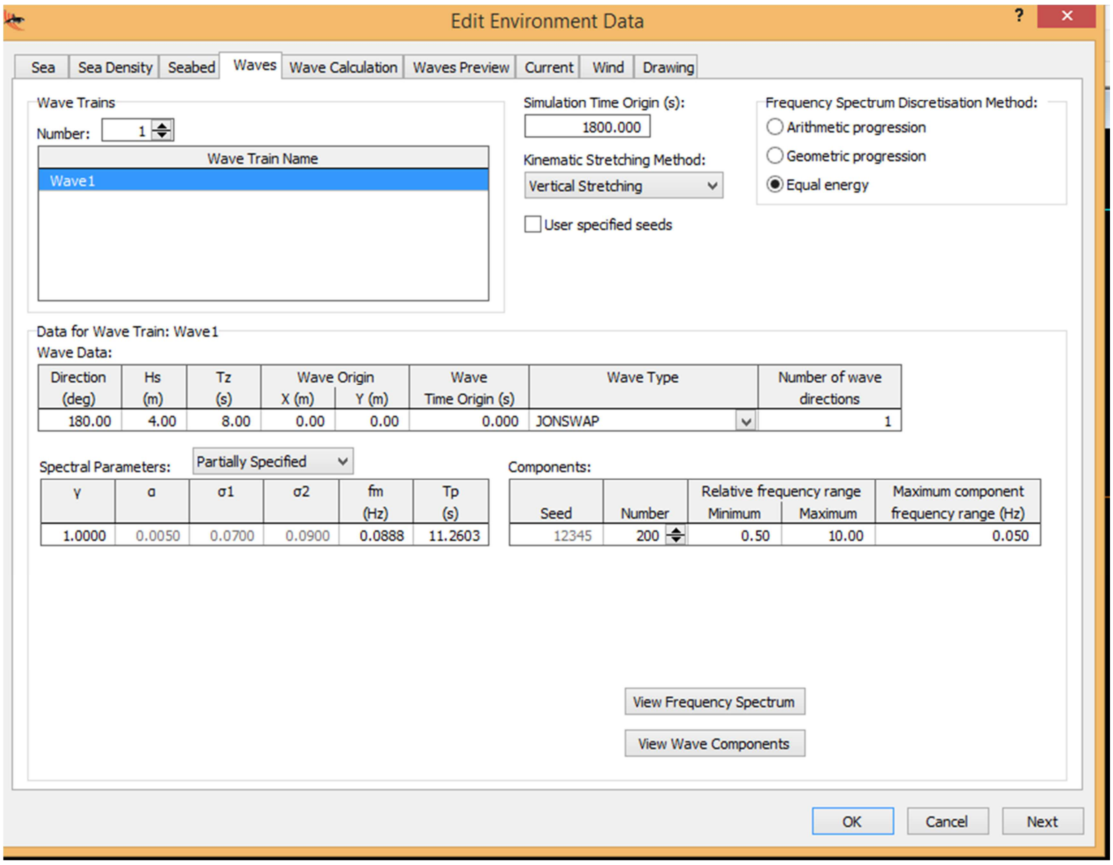


**Figure E.2:** Environment Loading Condition

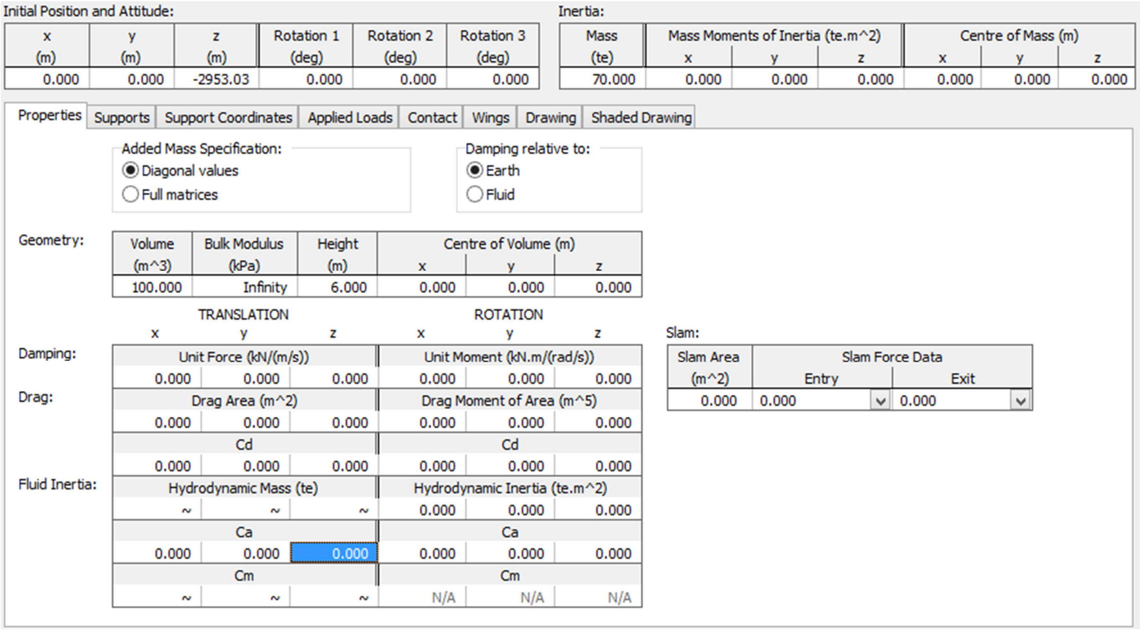


**Figure E.3:** Subsea PLEM/PLET Parameter

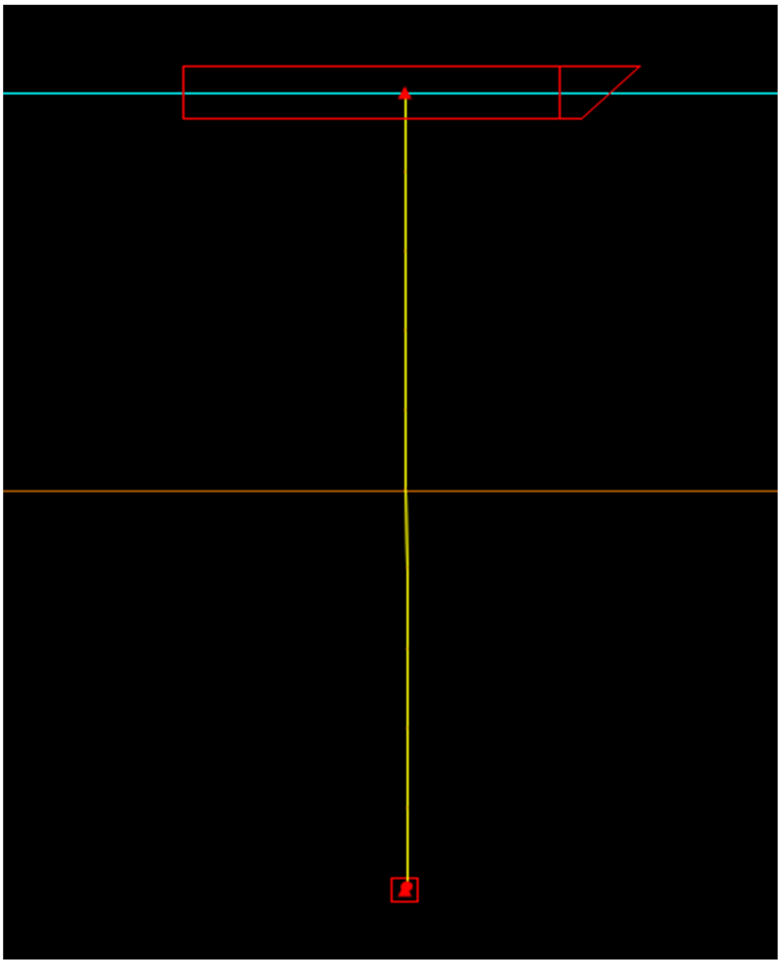

**Figure E.4:** Vessel, Line and Subsea PLEM/PLET Configuration

# Autobiographies

Jaswar Koto was born on October, 1970. He is a descendant of the Prophet Rasullullah S.A.W through Husein R.A. He is a President of Ocean and Aerospace Research Institute, Indonesia. Professor on offshore engineering and also President of International Society of Ocean, Mechanical & Aerospace for scientists and engineers.

He has been invited as a Visiting Professor more than 16 times, received several international awards and supervised PhD, Master and Bachelor Students.

He received his bachelor degree in 1994 from Institut Teknologi Sepuluh Nopember (ITS), Indonesia, Curtin University in 1996 and Notre Dame University in 1999. In 2003 he has completed PhD with receiving award in engineering form Aerospace and Marine Engineering, Osaka Prefecture University, Japan.

He has started his researches since 1994 on structure analysis of fluid flow in subsea pipelines, subsea pipeline corrosion due to Carbon Monoxide, design and hydrodynamic analysis of AUV in Australia. Then, he joined Research and Development Institute, Sumitomo Heavy Industries -Marine Engineering-, Japan. In 2005, he joined ExxonMobil projects. Since 2010, he has a contract with Department of Aeronautical, Automotive, and Ocean Engineering, Faculty of Mechanical Engineering. He is also appointed as head of High Performance Computing, CICT, Universiti Teknologi Malaysia

## Published by

Ocean & Aerospace Research Institute, Indonesia
Pekanbaru-Riau, INDONESIA
http://isomase.org/OCAri/Home.php

## Edited by

Mechanical-Offshore Engineering,
Universiti Teknologi Malaysia,
MALAYSIA
http://hpc.utm.my/

## Supported by

International Society of Ocean, Mechanical &
Aerospace - scientists & engineers –
D/A: Resty Menara Hotel
Jalan Sisingamangaraja No. 89 (28282),
Pekanbaru-Riau INDONESIA
http://www.isomase.org/

Deep Water & Offshore
Indonesian Oil and Gas Community,
INDONESIA

PLEM 2017060102